

Copyright

by

Tania Marlene Garrón

2017

**The Dissertation Committee for Tania Marlene Garrón Certifies that this is the
approved version of the following dissertation:**

**HUMAN DPP4/CD26 TRANSGENIC MICE AS SURROGATE
MODELS FOR MERS**

Committee:

Chien-Te Kent Tseng, Ph.D., Supervisor

Yingzi Cong, Ph.D.

Julian Leibowitz, M.D., Ph.D.

Chad Mire, Ph.D.

Slobodan Paessler, D.V.M., Ph.D.

Dean, Graduate School of Biomedical Sciences

**HUMAN DPP4/CD26 TRANSGENIC MICE AS SURROGATE
MODELS FOR MERS**

by

Tania Marlene Garrón, B.S.

Dissertation

Presented to the Faculty of the Graduate School of

The University of Texas Medical Branch

in Partial Fulfillment

of the Requirements

for the Degree of

Doctor of Philosophy

The University of Texas Medical Branch

August, 2017

Dedication

To my parents, Dora and Absalón, my brother Gonzalo, and my wonderful daughter Karen. For all your love, encouragement, and constant support.

Acknowledgements

I would like to thank Dr. Tseng for his guidance and supervision; my committee members Drs. Yingzi Cong, Julian Leibowitz, Chad Mire, and Slobodan Paessler for their time and valuable input. I also would like to thank Dr. Rohit Jangra for his valuable help provided by proof-reading this Dissertation.

The results of this Project are part of a team effort which has generated two publications where Dr. Anurodh Agrawal, Dr. Xinrong Tao and I are first co-authors with equal contribution. I would like to acknowledge the work of Dr. Anurodh Agrawal in the Transgene construction as well as the RT-qPCR results. Dr. Maki Wakamiya was responsible for generating the transgenic mice at the UTMB-Transgenic Mouse Core Facility. Also, either Dr. Wakamiya or Dr. Agrawal was in charge of the Western Blot tests for genotyping. From the very beginning, I was in charge of the maintenance of the transgenic mice colony in ABSL-2, and later as the colony started to grow, I received the help of Dr. Anurodh Agrawal. Dr. Teh-sheng Chan provided valuable advice for the maintenance of our colony. Dr. Bi-Hung Peng collaborated with us with the histological results. While Dr. Xinrong Tao was in charge of the IHC staining, I was in charge of the determination of the S-protein specific IgG antibodies by ELISA. Dr. Tao also worked side by side collaborating with me in both BSL-3 and ABSL-3 facilities. On the one hand, the work we performed in BSL-3 included the generation of the stock virus, the testing of all different tissues collected by using Vero E-6 infectivity Assay, the testing of blood samples to determine Neutralizing antibodies by Microneutralization Assay. On the other hand, in ABSL-3 we were in charge of all the animal experiments throughout the whole Project.

**HUMAN DPP4/CD26 TRANSGENIC MICE AS SURROGATE
MODELS FOR MERS**

Publication No. _____

Tania Marlene Garrón, Ph.D.

The University of Texas Medical Branch, 2017

Supervisor: Chien-Te Kent Tseng, Ph.D.

ABSTRACT

Continued occurrences of the Middle East Respiratory Syndrome caused by a coronavirus (MERS-CoV) and its proven transmissibility among humans constitute an ongoing public health threat. Animal models, especially small animal models that simulate human disease are needed for studies of pathogenesis and development of vaccines and antivirals for prevention and treatment of MERS-CoV infection and disease. Mice and other commonly used laboratory small animal species (i.e., hamsters and ferrets) are not susceptible to MERS-CoV because they lack the expression of human dipeptidyl peptidase 4 (hDPP4), the functional viral entry receptor. To overcome this deficiency, we developed several lineages of transgenic (Tg) mice expressing hDPP4 globally by using the pCAGGS.MCS under the control of the CAG promoter, which is a composite promoter consisting of the cytomegalovirus (CMV)/immediate-early enhancer and the chicken β -actin promoter, containing rabbit globin splicing and polyadenylation sites, as surrogate models for MERS-CoV infections. We showed that one lineage (line 52) of Tg mice globally expressing hDPP4 is highly susceptible to intranasal (i.n.) challenge with a high-dose (i.e., 10^6 50% tissue culture infectious dose [TCID₅₀]) of MERS-CoV, resulting in acute death, by day 6, profound weight loss (> 20%) starting at day 2, acute and intense viral infection in lungs with prominent inflammatory infiltrates and prominent viral infection at day 4 in the brain with little to no cellular infiltrates. Additionally, studies identified the 50% lethal dose (LD₅₀) and the 50% infectious dose (ID₅₀) of MERS-CoV to be ~5 and 0.4 TCID₅₀ of MERS-CoV, respectively. This Tg mouse model has been used successfully as a robust preclinical model for testing the efficacy of medical countermeasures for MERS.

TABLE OF CONTENTS

List of Figures	x
List of Illustrations	xi
List of Tables.....	xi
List of Abbreviations.....	xi
ABSTRACT	vi
CHAPTER I: INTRODUCTION	1
Middle East Respiratory Syndrome Coronavirus (MERS-CoV)	1
Taxonomy and nomenclature	1
Genomic organization	2
Spike protein	4
Viral Replication Cycle.....	5
Middle East Severe Acute Respiratory Syndrome (MERS)	6
Number of cases and geographical distribution	6
Clinical Symptoms	7
Transmission	7
Autopsy of a single patient with MERS-CoV infection.....	8
Clinical history of the patient	8
Findings.....	9
Host-virus interactions	10
DPP4 and its role as the functional receptor for MERS-CoV	12
Animal models for MERS-CoV infection.....	14
Rhesus macaques.....	14
Common Marmosets	15
New Zealand white rabbits.....	16
Ad5-Human DPP4 transduced mice	16
MERS-CoV-RBD (S377-588-Fc) as a subunit vaccine and HR2 fusion inhibitor peptides against MERS-CoV infection.....	17
S377-588-Fc as a subunit vaccine for MERS-CoV infection	17
HR-2 fusion inhibitor peptides against MERS-CoV infection.....	18

Objective of this Dissertation Project.....	18
Hypothesis	19
CHAPTER II: MATERIALS AND METHODS	20
Mice, virus, and cells.....	20
Viral infections	21
Construction and characterization of a hCD26 expressing plasmid in vitro.....	21
Generation, detection, and breeding of transgenic mice	22
Virus isolations.....	23
RNA extraction and real-time RT-qPCR	23
Serological assays	24
Vero E6 cell-based microneutralization assay	24
ELISA TEST	25
Histology and IHC testing.....	26
Animal studies.....	26
Susceptibility, morbidity and mortality study	26
Determination of LD ₅₀ and ID ₅₀ studies.....	27
Immune responses, and immunity of hCD26/DPP4 transgenic mice to MERS-CoV infection studies.....	28
Kinetics and tissue distribution studies - viral infection in hCD26/DPP4 Tg ⁺ mice challenged with 10 LD ₅₀ of MERS-CoV.....	8
Efficacy of the S377-588-Fc as a subunit vaccine	28
Preventive and the therapeutic efficacy of a fusion inhibitor peptide.....	29
CHAPTER III: GENERATION OF A TRANSGENIC MOUSE MODEL OF MIDDLE EAST RESPIRATORY SYNDROME	30
Introduction	31
Results	31
Characterization of the hCD26 transgene construct in tissue culture	33
Generation and characterization of hCD26 transgenic mice.....	33

Transgenic mice expressing hCD26 are permissive to MERS-CoV infection that results in disease and mortality	36
Line 52 transgenic mice expressing hCD26 developed disseminated infection	37
Histopathology in MERS-CoV-infected hCD26 Tg ⁺ mice	40
Discussion	41

CHAPTER IV: CHARACTERIZATION AND DEMONSTRATION OF THE VALUE OF A LETHAL MOUSE MODEL OF MIDDLE EAST RESPIRATORY SYNDROME CORONAVIRUS INFECTION AND DISEASE

Introduction	46
Results	46
Determination of LD ₅₀ and ID ₅₀	46
Infection-induced immune response and immunity to re-challenge with MERS-CoV	48
Kinetics and tissue distribution of viral infection in hCD26/DPP4 Tg ⁺ mice challenged with 10 LD ₅₀ of MERS-CoV	50
Histopathology of hCD26/DPP4 transgenic mice infected with 10 LD ₅₀ of MERS-CoV	52
Use of hCD26/DPP4 transgenic mice as a preclinical model for the Development of vaccines and treatments for MERS	55
Evaluation of the efficacy of S377-588-Fc as a subunit vaccine	55
Evaluation of the efficacy of the HR2M6 virus fusion inhibitor for prophylactic and therapeutic treatment	56
Discussion	58

CHAPTER V: FINAL DISCUSSION

Human MERS-CoV infections	61
Animal models for MERS-CoV infection and Disease	62
Non-human primates (NHP)	64
New Zealand White rabbits	66

Dromedary camels.....	67
Alpaca.....	69
Mice models of MERS-CoV infection.....	71
1. hDPP4 transduced mouse model.....	72
2. hDPP4 transgenic mice (Agrawal, Garron et al. 2015, Tao, Garron et al. 2015).....	72
3. Regeneron Knock-in (KI) model.....	73
4. Codon-optimized hDPP4 transgenic mice	74
5. Transgenic mouse model (Li Kun’s group-IOWA).....	74
6. Genomic engineered mice model (288/330 ^{+/+})	76
7. DPP4 KI model (Li Kun’s group-IOWA).....	77
Conclusions	79
List of references	81
Vita.....	95

LIST OF FIGURES

Figure 1. Transfection with the hCD26 transgene construct, pCAGGS.hCD26, effectively converts nonsusceptible mouse fibroblastic 17CL-1 cells to become fully supportive of productive MERS-CoV infection	32
Figure 2. Expression of hCD26 in transgene-positive (Tg ⁺) mice	35
Figure 3. Transgenic mice expressing hCD26 are permissive to MERS-CoV infection, leading to morbidity and mortality	39
Figure 4. Histopathological changes in the lungs and brains of hCD26 Tg ⁺ mice challenged with MERS-CoV	40
Figure 5. Kinetics and tissue distribution of MERS-CoV infection in hCD26/DPP4 transgenic mice.....	51
Figure 6. Photomicrographs (taken using low [left panels] - and high [right panels]-power magnification) of lungs of hCD26/DPP4 Tg ⁺ mice challenged with 10 LD ₅₀ of MERS-CoV.....	53
Figure 7. Photomicrographs (taken using high-power magnification) of brain stem and cortex of hCD26/DPP4 Tg ⁺ mice challenged with 10 LD ₅₀ of MERS-CoV.....	54
Figure 8. Immunization of hCD26/DDp4 Tg ⁺ mice with a receptor binding domain (RBD) and challenge with 100 LD ₅₀ of MERS-CoV.....	56

Figure 9. Prophylactic and therapeutic evaluations of the activity of the HR2M6 fusion inhibitor against MERS-CoV infection and disease in hCD26/DPP4 transgenic mice.....	57
---	----

LIST OF ILLUSTRATIONS

Illustration 1. Genome organization of MERS-CoV	3
Illustration 2. Schematic representation of MERS-CoV Spike (S)	5
Illustration 3. Schematic representation of CD26/DPP4.....	12

LIST OF TABLES

Table 1. Founders of hCD26 transgenic lineages.....	36
Table 2. Determining the 50% lethal dose and 50% infectious dose of MERS-CoV in hCD26/DPP4 transgenic mice.....	47
Table 3. Determining the 50% infectious dose of MERS-CoV in hCD26/DPP4 transgenic mice.....	48
Table 4. MERS-CoV serum antibody titers in survivors of the initial challenge and their response to rechallenge	49
Table 5. Advantages and disadvantages of naturally permissive animal models.....	79
Table 6. Advantages and disadvantages of mice (non-naturally permissive animal models).....	80

LIST OF ABBREVIATIONS

6-HB	6- α -helix bundle
AAALAC	Association for Assessment and Accreditation of Laboratory Animal Care
ABSL-3	Animal BSL-3
BSL-3	Biosafety Level 3
CD26	Cluster of differentiation 26
CMV	cytomegalovirus
CNS	Central nervous system
CoVs	Coronavirus
CPE	cytopathic effect
DMV	double-membrane vesicles

dpi	days postinfection
"DPP4 "	Dipeptidyl peptidase 4
E protein	Envelope protein
ELISA	enzyme-linked immunosorbent assay
EMC-2012	Erasmus Medical Center-2012
GI	gastrointestinal
GIP	glucose-dependent insulinotropic polypeptide
GLP-1	glucagon-like peptide 1
hACE-2	human Angiotensin convertase-2
hCD26	human Cluster of differentiation 26
hDPP4	human Dipeptidyl peptidase 4
HR1	Heptad Repeat 1
HR2	Heptad Repeat 2
HRP	horseradish peroxidase
i.m.	intramuscular
i.n.	intranasal
i.t.	intratracheal
ID ₅₀	50% infectious dose
IFN	Interferon
IgG	Immunoglobulin
IHC	Immunohistochemistry
LD ₅₀	50% lethal dose
M protein	Membrane protein
MERS	Middle East Respiratory Syndrome
MERS-CoV	Middle East Respiratory Syndrome Coronavirus
mRNA	messenger Ribonucleic Nucleic Acid
N protein	Nucleocapsid protein
NIH	National Institutes of Health
NOU	notification-of-usage
nsps	nonstructural proteins
o.c.	ocular

OPD	o-phenylenediamine dihydrochloride
ORFs	open reading frames
PHA	phytohemagglutinin
p.i.	postinfection
pp1a	Polyprotein 1a
pp1ab	Polyprotein 1ab
RT-qPCR	Reverse Transcription - quantitative Polymerase Chain Reaction
RFP	Red Fluorescent Protein
rMERS-CoV	recombinant MERS-CoV
RNA	Ribonucleic acid
S protein	Spike protein
S1	Subunit 1 of MERS-CoV Spike protein
S2	Subunit 2 of MERS-CoV Spike protein
TCID ₅₀	50% tissue culture infectious doses
Tg ⁻	transgene-negative
Tg ⁺	transgene-positive
TMPRSS2	Transmembrane protease, serine 2
TMRCA	Time to the Most Recent Common Ancestor
βCoV	Betacoronavirus

CHAPTER I: INTRODUCTION

Middle East Respiratory Syndrome Coronavirus (MERS-CoV)

Taxonomy and nomenclature

Middle East Respiratory Syndrome - Coronavirus (MERS-CoV), the causative agent of Middle East Respiratory Syndrome (MERS) is an enveloped, single-stranded, and positive-sense RNA virus with its genome size of approximately 30 kb (van Boheemen, de Graaf et al. 2012). MERS-CoV is a member of the order Nidovirales, family *Coronaviridae*, and genus *Betacoronavirus* (β CoV), lineage C. Before the discovery of MERS-CoV, there were only two lineage C β CoVs, which were isolated from bats. These bat CoVs are phylogenetically closely related to MERS-CoV and are known as *Tylonycteris* bat CoV HKU4 (Ty-BatCoV-HKU4) and *Pipistrellus* bat CoV HKU5 (Pi-BatCoV-HKU5) and were discovered in Hong Kong in 2006 in *Tylonycteris pachypus* and *Pipistrellus abramus* species of bats, respectively (Woo, Lau et al. 2006, Woo, Wang et al. 2007, Woo, Lau et al. 2009). MERS-CoV is the first human CoV assigned to lineage C of the β CoV genus. This designation was made based on the International Committee on Taxonomy of Viruses (ICTV) criteria for CoV species identification. Before named as MERS-CoV, it was also known by other names such as “novel coronavirus,” “human coronavirus EMC,” “human betacoronavirus 2c EMC,” “human betacoronavirus 2c England-Qatar,” “human betacoronavirus 2c Jordan-N3,” and “betacoronavirus England 1,”. All these names represented the places where the complete viral genome was first sequenced (Erasmus Medical Center, Rotterdam, the Netherlands) or where the first laboratory-confirmed cases were identified or managed (Jordan, Qatar, and England) (Bermingham, Chand et al. 2012,

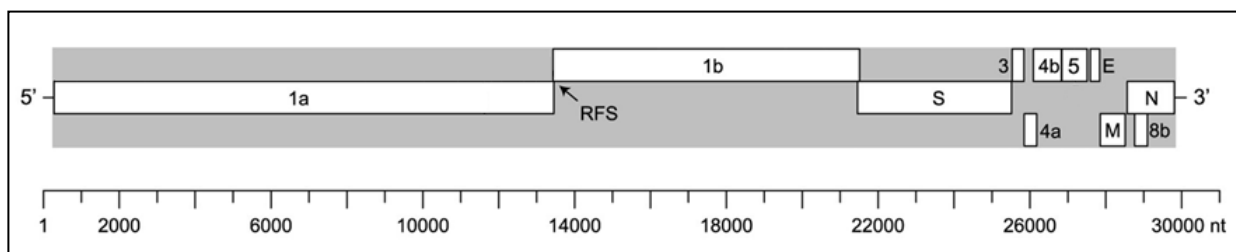
Zaki, van Boheemen et al. 2012, Cotten, Lam et al. 2013, de Groot, Baker et al. 2013, Pollack, Pringle et al. 2013).

Genomic organization

MERS-CoV has an RNA genome size of approximately 30 kb that is 5'-methyl-capped, polyadenylated and polycistronic (van Boheemen, de Graaf et al. 2012, Woo, Lau et al. 2012, Cotten, Lam et al. 2013). As shown in **Illustration 1**, the viral genes are arranged in 5'-replicase-structural-proteins (spike-envelope-membrane-nucleocapsid)-poly(A)-3' order (van Boheemen, de Graaf et al. 2012, Woo, Lau et al. 2012, Cotten, Lam et al. 2013, Frey, Redden et al. 2014) and the genome encodes for 10 complete, functional open reading frames (ORFs) (van Boheemen, de Graaf et al. 2012, Woo, Lau et al. 2012, Cotten, Lam et al. 2013). The partially overlapping 5'-terminal ORF1a/b located within the 5' two-thirds of the genome encodes for the large replicase polyproteins pp1a and pp1ab. The proteolytic cleavage of pp1a and pp1ab produces 16 putative nonstructural proteins (nsps), including nsp1 that has shown to inhibit host gene expression by means of targeting nuclear-transcribed mRNAs but not those mRNAs of cytoplasmic origin, nsp2 which may be responsible for disrupting the intracellular signaling, nsp-3 which has a structure similar to the papain-like protease of SARS-CoV, showing functions such as proteolytic processing of the viral replicase polyprotein, it has also been shown to have an IFN antagonist activity in vitro; nsp4 may contribute to the formation of the viral replication complex; nsp5 known also as 3C-like protease, chymotrypsin-like or main protein, is involved in proteolytic processing of the replicative polyprotein playing a role in the formation of the key functional enzymes such as helicase and replicase; nsp6, is a membrane integral component of the viral replication complex involved in double-membrane vesicles (DMV) formation; nsp7 and nsp8 in other

CoVs are part of a multimeric RNA polymerase complex; nsp9 also has been shown to have an important RNA/DNA binding activity (observed in SARS-CoV); nsp10 is required by nsp16 to complement its activity; the role of nsp11 also for other CoV is still unknown; nsp12 is the RNA-dependent RNA polymerase, its main role is in the replication and transcription to generate genomic and sub-genomic RNA with both polarities; nsp-3 is a helicase; nsp14 have shown to act as a proofreading exoribonuclease and also possess as methyl transferase activity for viral mRNA capping, both of these activities are important in the replication and transcription process; nsp15 has an endonuclease activity which is important for immune evasion and essential in the CoV replication cycle; finally nsp16 is a 2'-O-Methyl transferase which critical for role in capping of viral mRNA and in preventing the recognition by host sensor molecules (Cornillez-Ty, Liao et al. 2009, van Boheemen, de Graaf et al. 2012, Woo, Lau et al. 2012, Cotten, Lam et al. 2013, Frey, Redden et al. 2014, Yang, Chen et al. 2014, Lokugamage, Narayanan et al. 2015).

The membrane-anchored trimeric Spike (S) protein is a major immunogenic antigen involved in virus attachment and entry into host cells. S protein has also shown to play an essential role in determining virus virulence, protective immunity, tissue tropism, and host range (Qian, Dominguez et al. 2013). The other structural proteins, envelope (E), membrane (M), and nucleocapsid (N), are involved in the assembly of the virion. M protein, nsp3, and accessory proteins 4a, 4b, and 5 have been shown to possess *in vitro* interferon antagonist activities which may impact *in vivo* viral replication and pathogenesis (Niemeyer, Zillinger



et al. 2013, Yang, Zhang et al. 2013, Matthews, Coleman et al. 2014, Siu, Yeung et al. 2014, Yang, Chen et al. 2014).

March of 2012 was estimated to be the time to the most recent common ancestor (TMRCA) of MERS-CoV with a 95% confidence interval from December 2011 to June 2012 (Cotten, Watson et al. 2013, Cotten, Watson et al. 2014). The genomes of the MERS-CoV strains obtained from patients diagnosed between October 2012 and June 2013 compared with the genome of one of the first human MERS-CoV strains showed various nucleotide changes in the last third of their genomes. These variations represent potential amino acid changes in the S protein and the accessory proteins (Cotten, Watson et al. 2013). Particularly, codon 1020 at the Heptad Repeat 1 (HR1) domain of the S gene was identified to be under strong selection among different geographical lineages (Cotten, Watson et al. 2013, Cotten, Watson et al. 2014).

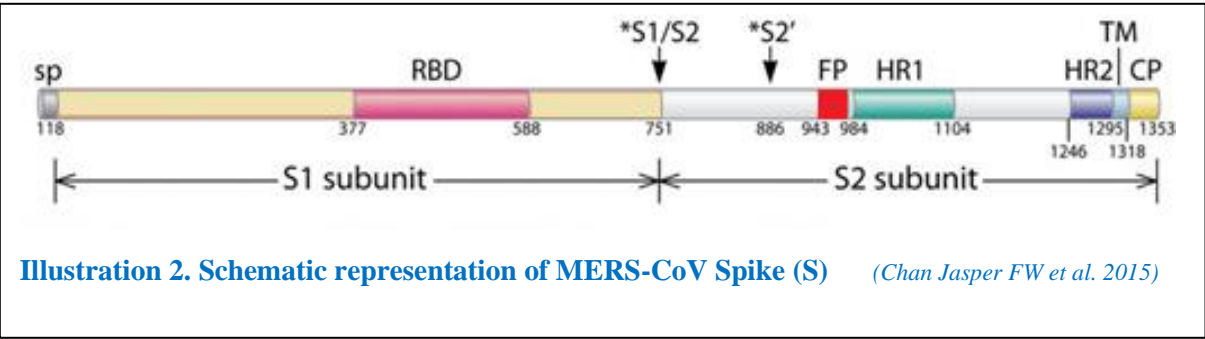
Spike Protein

The Spike (S) protein of MERS-CoV is a class I fusion protein that possesses 1353 amino-acids and is divided into two subunits, S1 and S2. The S protein is responsible for virus binding to the target cell (Gierer, Bertram et al. 2013, Lu, Hu et al. 2013) as well as the fusion of viral and host cell membranes (Gao, Lu et al. 2013) and is also a major target of neutralizing antibodies (Du, Kou et al. 2013, Gierer, Bertram et al. 2013, Mou, Raj et al. 2013). The S1 subunit contains the Receptor Binding Domain (RBD) and the N domain (Chen, Rajashankar et al. 2013). The S2 subunit is composed of the fusion peptide, the Heptad Repeat-1 (HR1) & HR2 domains, a transmembrane domain and a cytoplasmic domain (**Illustration 2**). All these S2 subunit components are important for facilitating the fusion of viral membrane with the cell membranes. Therefore, S protein is required by the

virus for binding to the receptor of the target cells and for catalyzing virus–cell membrane fusion. The process of fusion occurs only after S protein is cleaved sequentially, first during the excretion or budding process of the virions from the organelles of virus producing cells and second after the binding of virus to target-cell receptors (Gao, Lu et al. 2013, Lu, Liu et al. 2014).

Viral Replication Cycle

After binding of the S1 subunit, particularly the RBD region of the S protein to the cellular receptor, a conformational change is triggered in the S2 subunit, which leads to the insertion of the fusion peptide into the target cell membrane. The conformational changes lead to the formation of a 6-helix bundle (6-HB) fusion core that is made up of the HR1 and HR2 domains, which brings the viral and the target cell membranes together, to finally be



fused together (Gao, Lu et al. 2013, Lu, Liu et al. 2014). MERS-CoV can utilize either the cathepsin-mediated endosomal pathway or the TMPRSS2-mediated plasma membrane pathway to enter the host cell. However, in some cell lines, MERS-CoV can use both pathways (Gierer, Bertram et al. 2013, Shirato, Kawase et al. 2013).

Following the cell entry process, inner components of the virus, including genomic RNA are released in the cytoplasm. Later the ORF1a/b will encode the viral polyproteins pp1a and pp1ab. Double membrane vesicles and convoluted membranes are also formed in the perinuclear region of the infected cells during the life cycle of the MERS-CoV. These

vesicles can be distinguished by electron microscopy in the infected cells (de Wilde, Raj et al. 2013). Polyproteins pp1a and pp1ab are cotranslationally cleaved into 16 nsp by two proteases, the papain-like protease and the 3C-like protease encoded by ORF1a/b (van Boheemen, de Graaf et al. 2012, Lu, Liu et al. 2013, Lei, Mesters et al. 2014). Then, a replication-transcription complex is formed by these nsps, which allows the transcription of the full-length positive genomic RNA into a full-length negative-strand template that can be used for the synthesis of the new genomic RNAs and subgenomic negative-strands of RNA. These subgenomic RNAs serve as templates for synthesis of mRNAs that ultimately will be translated into structural and accessory proteins (de Wilde, Raj et al. 2013).

When the required numbers of genomic RNA and structural proteins are produced, assembly of the N protein and the genomic RNA leads to the formation of the helical nucleocapsid in the cytoplasm. The nucleocapsid acquires its envelope by budding through the intracellular membranes of the Golgi apparatus and endoplasmic reticulum. M, E and S proteins are transported to the budding compartment where M protein interacts with the nucleocapsid to create the complexes with the E and S protein to prompt viral budding. Finally, the assembled virions are released to the extracellular compartment, therefore completing the replication cycle of the virus.

Middle East Severe Acute Respiratory Syndrome (MERS)

Number of cases and geographical distribution

MERS-CoV is the etiological agent of the Middle East respiratory syndrome (MERS). The disease was first reported in September of 2012 and MERS-CoV was first isolated from the respiratory tract secretions of a man that died from viral pneumonia in Saudi Arabia. (Zaki, van Boheemen et al. 2012). Most of the MERS-CoV cases have

occurred in the Middle East. The cases reported outside of the Middle East are among people who have recently traveled to the Middle East or who have been in close contact with an individual who has recently been to the Middle East. As a result of frequent international travel, a total of four continents: Asia, Europe, Africa, and North America have been affected by this deadly disease (ECDC 2015). Since September 2012, the World Health Organization has been notified of 1,917 cases of MERS with 677 deaths (WHO 2017).

Clinical Symptoms

Early reports of MERS were mainly focused on severe cases that usually presented as acute pneumonia with rapid respiratory deterioration. Various patients also had underlying comorbid medical disorders, including hypertension, diabetes, chronic renal disease, and chronic cardiac disease (Assiri, Al-Tawfiq et al. 2013). The common symptoms of MERS include fever, headache, chills, myalgia, rigors, sore throat, nonproductive cough, and shortness of breath. Other symptoms of respiratory tract infections may also be observed such as rhinorrhea, sputum production, wheezing, and chest pain. Rapid clinical deterioration with the development of respiratory failure usually occurs within a few days after these initial symptoms (Al-Tawfiq, Hinedi et al. 2014). The radiographic abnormalities in the chest of severe cases often show progress from a mild focal lesion to multifocal lesions, particularly in the lower lobes in a unilateral or bilateral fashion (Assiri, Al-Tawfiq et al. 2013).

Transmission

MERS-CoV is believed to be transmitted to humans from bats (van Boheemen, de Graaf et al. 2012, Zaki, van Boheemen et al. 2012, Ithete, Stoffberg et al. 2013, Corman, Ithete et al. 2014, Yang, Liu et al. 2015) via dromedary camels (Azhar, El-Kafrawy et al.

2014, Briese, Mishra et al. 2014, Hemida, Chu et al. 2014). However, the possibility of direct transmission from bats to humans cannot be totally ruled out. The full genomic sequence of an African bat virus (Neo-CoV) showed 85.6% nucleotide identity with those of MERS-CoVs isolated from humans and dromedary camels. It was also demonstrated that the bat virus roots the phylogenetic tree of MERS-CoV, eventually evolving into camel- and/or human-permissive strains (Corman, Ithete et al. 2014). The first conclusive evidence that camels are source of MERS-CoV was obtained when full genomic sequences of the two isolates of MERS-CoV derived from a patient and his sick camel in Jeddah, Saudi Arabia were shown to be identical (Azhar, El-Kafrawy et al. 2014). Another study also showed that prevalence of seroconversion in camels is very high, 100% of the analyzed sera from camels from the Middle East (Oman) and 14% from Spanish camels had specific antibodies against MERS-CoV S protein (Reusken, Haagmans et al. 2013). Recently, it was also demonstrated that two mutations of the S protein of bat CoV HKU4 could enable entry of this virus into human cells. These mutations are naturally present in MERS-CoV S protein, potentially explaining why MERS-CoV can infect human cells. These mutations likely play a critical role in the bat-to-human transmission of MERS-CoV, either directly or through intermediate hosts (Yang, Liu et al. 2015). The proven human-to-human transmissibility (Assiri, McGeer et al. 2013, Health Protection Agency 2013), along with a high mutation rate of Coronaviruses in general raise concern that increased transmission rate of this deadly virus in humans is likely to occur.

Autopsy of a single patient with MERS-CoV infection

It took more than 3 years after the emergence of MERS for the first report of an autopsy of a human fatal case to be reported (Ng, Al Hosani et al. 2016). Therefore, most of

the animal models during that period of time were developed without knowledge of the pathological lesions and viral pathogenesis in human.

Clinical History of the patient

The patient was a 45 years old Filipino man who was recently exposed to sick contacts. He was working and living in Abu Dhabi, United Arab Emirates. He went to the Emergency Department on April 2, 2014, and reported fever, rhinorrhea, and cough that had started 4 days before. At the hospital, they performed chest X-ray and found a small opacity on the left side. The diagnosis was acute bronchitis, and he was prescribed prednisolone and paracetamol. Nevertheless, he returned after 4 days with a persistent cough and shortness of breath. His chest X-ray showed an even bigger opacity; he was diagnosed with pneumonia and discharged again with a prescription of antibiotics. However, he was admitted into the Emergency Department later that day with worsening symptoms. The next day, he was transferred to the ICU (intensive care unit) because of respiratory distress and tachypnea, and chest X-ray showed multiple opacities. He also developed kidney failure and was put on dialysis. The RT-qPCR from his nasopharyngeal swab was positive for MERS-CoV. His condition continued to deteriorate until he died on April 10. A total of 14 days passed from the onset of the disease until his death (Ng, Al Hosani et al. 2016).

Findings

The body of the patient was kept refrigerated at 4°C, and the autopsy was performed 10 days after death. Some of the findings included pleural effusion, pericardial effusion, edematous and consolidated lungs. Histopathological results indicated diffuse alveolar damage. Immunohistochemistry (IHC) results showed the presence of viral antigen in type 2 pneumocytes and syncytial epithelial cells. Pneumocyte infection suggests that direct

cytopathic effects contribute to MERS-CoV respiratory symptoms. Moreover, MERS-CoV antigen was found in the submucosal glands also. The infected submucosal glands may shed virus in respiratory secretions that could lead to human-to-human transmission (Ng, Al Hosani et al. 2016).

A common clinical finding in severe cases of patients infected with MERS-CoV is the development of renal failure. In some cases, MERS-CoV RNA has been detected in urine. However, no extra pulmonary MERS-CoV dissemination was found in this autopsy suggesting that direct renal infection was not responsible for the renal failure observed in this patient. It was probably due to cytokine dysregulation or hypoperfusion.

Host-virus interactions.

Like many other viruses, CoVs have evolved to evade the innate immune response by developing strategies that prevent induction of IFN (Katze, He et al. 2002) which is one crucial component of this initial response. The double-stranded RNA (dsRNA) of MERS-CoV is recognized by the innate immune system through activation of pattern recognition receptors (PRRs), cytosolic ones such as RIG-1 and MDA-5 (Takeuchi and Akira 2008) and membranous such as TLR3 (Perlman and Netland 2009, Blander and Sander 2012). This recognition process triggers the activation of Interferon Regulatory Factors 3 and 7 (IRF3, IRF7) which ultimately leads to the induction of type-1 interferon (IFN α and IFN β) (Yoneyama, Kikuchi et al. 2004). Type-1 IFNs are responsible for the activation of immune anti-viral effectors such as Natural Killer (NK) cells (Welsh and Waggoner 2013), T CD8+ cells and macrophages, permitting viral clearance (Taniguchi and Takaoka 2001). IFN α is known to promote antigen presentation in response to viruses, therefore if there is absence

of IFN α the development of a robust antiviral adaptive Th-1 immune response (mediated by IL-12 and IFN γ that decreases viral clearance) will be impaired.

Some reports regarding host-virus interaction have shown that IFN α plays a major role in orchestrating an early immune response against virus infection such in the case of SARS-CoV (Zhu 2004, Frieman, Heise et al. 2008, Perlman and Netland 2009). It has also been shown that SARS-CoV proteins contribute to diminishing type-1 IFN signaling to evade innate immunity (Frieman, Heise et al. 2008, Perlman and Netland 2009). Consistent with those findings, an *in vitro* study described a beneficial effect of IFN α treatment on MERS-CoV replication (de Wilde, Raj et al. 2013).

Faure et al. also characterized the immune response in two cases of patients infected with MERS-CoV, each of them showing a significantly different outcome. The first died after one 3 weeks in the ICU, while the second patient was still recovering by the time they published their findings. They highlighted the key role that “IFN α plays in the innate immune response to orchestrate an early adaptive Th-1 response, mediated by IL-12 and IFN γ , against MERS-CoV infection” (Faure, Poissy et al. 2014). They showed that the patient with poor outcome presented a significant decrease in receptors and regulators such as RIG-1, MDA5, and IRF3-7, involved in recognition of MERS-CoV. The reduction in IRF3 and 7 was linked mainly with a significant decrease in IFN α expression. Also, in contrast to the patient with a better outcome, the patient with poor outcome did not promote type-1 Interferon (IFN), in particular, IFN α , in response MERS-CoV infection. Also, levels of both, IL-12 and IFN γ were decreased (Faure, Poissy et al. 2014).

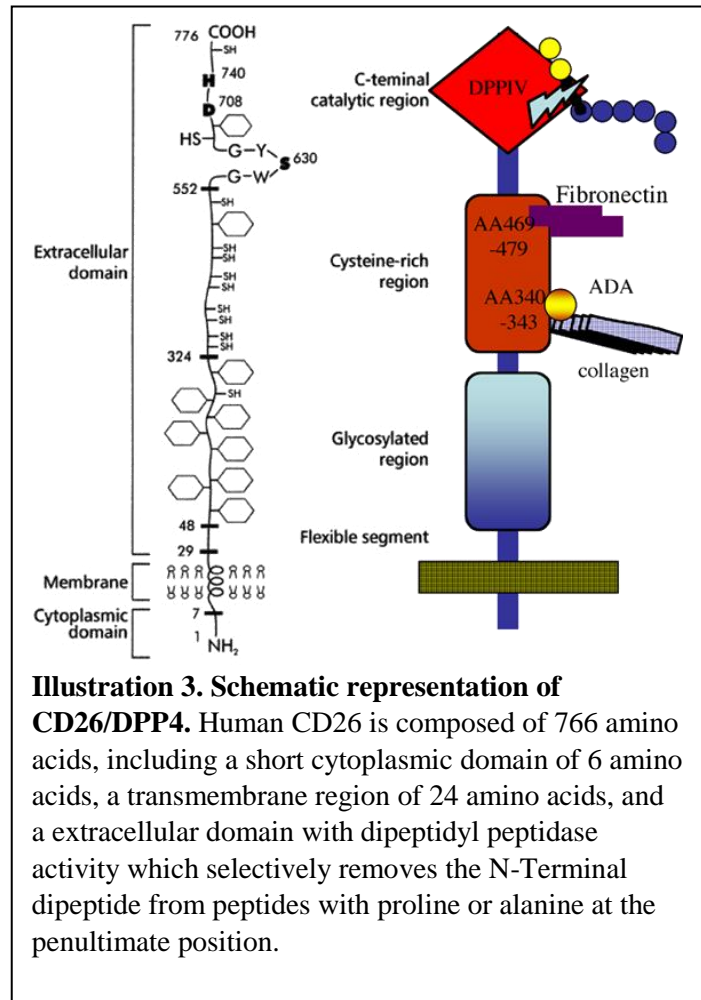
Additionally, it has been demonstrated that M protein, nsp3, and accessory proteins 4a, 4b, and 5 of MERS-CoV possess *in vitro* IFN-antagonist activities, which may impact in

vivo viral replication and pathogenesis (Niemeyer, Zillinger et al. 2013, Yang, Zhang et al. 2013, Matthews, Coleman et al. 2014, Siu, Yeung et al. 2014, Yang, Chen et al. 2014).

DPP4 and its role as the functional receptor for MERS-CoV.

In 2013, Dipeptidyl peptidase 4 (DPP4), which is also known as Cluster of differentiation 26 (CD26) was identified as the functional receptor for the MERS-CoV. DPP4 is required for binding and entry of the virus into the host cells. DPP4 is a type II transmembrane glycoprotein (Raj, Mou et al. 2013), and a cell-surface protease that removes the N-terminal dipeptide from peptides that have either the amino acid proline or alanine in the second position. Besides its catalytic activity, DPP4 interacts with several proteins such as adenosine deaminase (ADA), fibronectin, collagen, CXCR4, the HIV gp120 protein, and the tyrosine phosphatase CD45 (Lambeir, Durinx et al. 2003).

DPP4 is expressed on epithelial and endothelial cells in various tissues. Double IHC staining for MERS-CoV and DPP4, the MERS-CoV receptor, was observed in pneumocytes and syncytial cells, the main targets for MERS-CoV infection (Ng, Al Hosani et al. 2016).



DPP4 is expressed on T lymphocytes, where it is up-regulated after T cell activation. DPP4 is secreted in soluble form in plasma and other body fluids (Lambeir, Durinx et al. 2003). DPP4 also plays a role in glucose homeostasis. DPP4 inhibitors improve glucose tolerance in animal models of type 2 diabetes as well as in diabetic patients. The exopeptidase activity of DPP4 and its interactions with various molecules enables it to act as a co-stimulatory molecule to modulate chemotaxis and influence T cell activity. In addition, DPP4 has also been shown to be involved in malignant transformation and tumor invasion, and in HIV-1 entry (Lambeir, Durinx et al. 2003).

Evolutionarily, DPP4 is conserved; however, there are differences between various animal species and human in the amino acid sequences of the extracellular domain, which interacts with MERS-CoV. Mainly, 14 amino acids seem to be critical determinants of MERS-CoV S protein binding to DPP4 (Wang, Shi et al. 2013). MERS-CoV S protein is not able to bind to mouse, hamster, and ferret DPP4. The DPP4 of these species have significant differences in these 14 amino acids as compared with human DPP4 (hDPP4), consequently making these species resistant to MERS-CoV infection (de Wit, Prescott et al. 2013, Lu, Hu et al. 2013, Raj, Smits et al. 2014, van Doremalen, Miazgowicz et al. 2014). On the other hand, species such as rhesus macaques, common marmosets, and camels that have few or no differences in these 14 amino acid sequences appear to be susceptible to MERS-CoV infection (Munster, de Wit et al. 2013, Falzarano, de Wit et al. 2014, van Doremalen, Miazgowicz et al. 2014).

Animal models for MERS-CoV infection

Rhesus macaques

Rhesus macaques were the first animal model for MERS-CoV infection and disease. They were infected through a combined intratracheal (i.t.), i.n., ocular (o.c.), and oral inoculation with 7×10^6 50% tissue culture infectious doses (TCID₅₀) of MERS-CoV (de Wit, Rasmussen et al. 2013, Falzarano, de Wit et al. 2013, Munster, de Wit et al. 2013) or via i.t. inoculation with 6.5×10^7 TCID₅₀ of MERS-CoV (Yao, Bao et al. 2014). In both cases, rhesus macaques developed a mild respiratory illness 1 or 2 days after infection, which was resolved as early as 4 dpi (de Wit, Rasmussen et al. 2013). The clinical signs included fever, rapid abnormal breathing, and coughing (de Wit, Rasmussen et al. 2013, Falzarano, de Wit et al. 2013, Munster, de Wit et al. 2013, Yao, Bao et al. 2014). Gross lesions consisting of bright to dark red discolored foci in lungs were observed (Munster, de Wit et al. 2013, Yao, Bao et al. 2014). Histologic pulmonary lesions included interstitial (Yao, Bao et al. 2014) or broncho-interstitial pneumonia (de Wit, Rasmussen et al. 2013, Falzarano, de Wit et al. 2013). MERS-CoV RNA was detected in several upper and lower respiratory tract tissues via nasal and oropharyngeal swabs, and bronchoalveolar lavages (de Wit, Rasmussen et al. 2013). Viral RNA was not detected in blood or any visceral organs, including the kidney (de Wit, Rasmussen et al. 2013, Yao, Bao et al. 2014). Infectious virus was isolated only from the lower respiratory tract tissues (lungs). Viral antigen was detected by IHC in type I and type II pneumocytes and alveolar macrophages (de Wit, Rasmussen et al. 2013).

Common Marmosets

In Common Marmosets, MERS-CoV is able to cause moderate to severe, potentially lethal (22.2 % lethality) respiratory disease (Falzarano, de Wit et al. 2014). Common Marmosets were infected through a combined i.t., i.n., o.c., and oral inoculation with 5.2×10^6 TCID₅₀ of MERS-CoV. The clinical signs included tachypnea, difficulty breathing, cyanosis and hemorrhagic oral discharge with the need of early euthanasia for two out of nine marmosets at day 4 post-infection. The clinical signs were first noted at 1 dpi; the peak was reached at day 4 to 6 p.i. and resolved by 13 dpi (Falzarano, de Wit et al. 2014). Radiography showed pulmonary interstitial infiltration as early as 1 dpi, which resolved by day 13 post-infection (Falzarano, de Wit et al. 2014). The lungs showed gross lesions with edema and dark red discolored areas. Histologic lesions included bronchointerstitial pneumonia. Viral RNA was detected in nasal and oropharyngeal swabs, respiratory tract, gastrointestinal tract, heart, liver, spleen, kidney, adrenal gland, brain and blood indicating a disseminated viral infection. Infectious virus was isolated from the upper and lower respiratory tract. MERS-CoV antigen was detected by IHC in Type I and type II pneumocytes, and macrophages. Moreover, *in situ* hybridization indicated that type I pneumocytes and alveolar macrophages were the main sites of virus replication (Falzarano, de Wit et al. 2014).

Another group confirmed these clinical, virologic, and pathologic results in Marmosets even though the animals were inoculated via i.t. route only with 5×10^6 TCID₅₀ of MERS-CoV (Chan, Yao et al. 2015). On the contrary, Johnson et al. reported sublethal, mild-to-moderate respiratory disease when they infected Marmosets with the same amount of MERS-CoV (5×10^6 TCID₅₀) via i.t. inoculation. They were also not able to

recover infectious virus or detect viral RNA by RT-qPCR or viral antigens by IHC (Johnson, Via et al. 2015).

New Zealand white rabbits

To infect the upper as well as the lower respiratory tract, New Zealand white rabbits were infected both, intranasally with 1×10^6 TCID₅₀ and intratracheally with 4×10^6 TCID₅₀ of MERS-CoV (Haagmans, van den Brand et al. 2015). While no clinical signs and gross pathological lesions were observed, microscopic histopathological lesions were seen in both upper and lower respiratory tract at day 3 and 4 p.i.. MERS-CoV RNA was detected in several upper and lower respiratory tract tissues. Moreover, infectious virus was detected in nasal swabs up to 7 dpi (Haagmans, van den Brand et al. 2015). The authors suggest that rabbits could be used to study MERS-CoV transmission since this model shed virus from the URT; however, asymptomatic infection rules them out as a suitable model for the study of disease progression (Haagmans, van den Brand et al. 2015).

Ad5-Human DPP4 transduced mice

Due to the lack of binding of the MERS-CoV S protein to the murine DPP4, Wild-type mice are not susceptible to MERS-CoV infection (Coleman, Matthews et al. 2014). Glycosylation of the murine DPP4 can block infection (Peck, Cockrell et al. 2015). To make mice susceptible to MERS-CoV infection, mice that express the human DPP4 (hDPP4) gene were developed. Zhao's group inoculated a replication deficient adenovirus vector intranasally to induce transient expression of hDPP4 in the lungs of BALB/c, C57BL/6 and various knockout mice strains (Zhao, Li et al. 2014). Subsequently, these mice were challenged intranasally with 10^5 PFU of MERS-CoV. In the wild-type mice, clinical signs were minimal and were characterized by none to mild weight loss in young and older mice,

respectively. Mild gross pulmonary lesions corresponding to peribronchiolar and perivascular inflammation with subsequent development of interstitial pneumonia was observed. MERS-CoV replicated in the lungs and was cleared within 6 to 8 days in young mice and 10 to 14 days in older mice. The virus was not identified in other tissues outside the respiratory tract. In hDPP4-transduced Type I Interferon (IFN) knockout mice, the clinical signs, gross, and microscopic pathological lesions were more severe than those observed in transduced wild-type mice (Zhao, Li et al. 2014).

MERS-CoV-RBD (S377-588-Fc) as a subunit vaccine and HR2 fusion inhibitor peptides against MERS-CoV infection

1. S377-588-Fc as a subunit vaccine for MERS-CoV infection

There is an urgent need for effective vaccines for MERS-CoV infection. Some vaccine candidates that are being developed have been shown to be immunogenic in preclinical testing (Almazan, DeDiego et al. 2013, Du, Zhao et al. 2013, Song, Fux et al. 2013, Kim, Okada et al. 2014, Ma, Li et al. 2014, Ma, Wang et al. 2014). Some studies have focused on identifying sequences of the MERS-CoV-RBD region that can induce neutralizing antibody production in mice or rabbits and have shown their promise as subunit vaccines (Mou, Raj et al. 2013, Ma, Li et al. 2014, Ma, Wang et al. 2014). The RBD region that contains residues 377-588 has been identified as a critical neutralizing antibody inducing domain (Du, Kou et al. 2013, Ma, Wang et al. 2014, Zhang, Tang et al. 2015). Moreover, fusion of this domain with human Fc (S377-588-Fc) induced even higher neutralizing antibody response in immunized animals (Du, Kou et al. 2013, Ma, Wang et al. 2014). Further studies have shown that MF59 is probably the ideal adjuvant for the S377-588-Fc subunit vaccine (Zhang, Channappanavar et al. 2016).

2. HR2 fusion inhibitor peptides against MERS-CoV infection

Binding of the RBD with the DPP4 receptor on the target cell is followed by proteolytic cleavage, which exposes the fusion peptide located in the S2 subunit of the S protein. This allows it to be inserted into the plasma or endosomal membranes of the target cell. Thereafter, the HR2 binds to the HR1 in the S2 subunit to form a 6-HB fusion core, which brings the two membranes closer to fuse with each other (Lu, Liu et al. 2014). Peptides derived from the HR2 domain (such as HR2P) can interact with the HR1 region in the S protein to form a highly stable 6-HB complex not allowing the formation of the 6-HB fusion core which is the result of the interaction of both, viral HR1 and viral HR2, which are necessary for the fusion of the viral and target cell membrane. (Lu, Liu et al. 2014). Similar strategies have been used to block Human Immunodeficiency Virus (HIV) and Severe Respiratory Syndrome (SARS-CoV) infections (Jiang, Lin et al. 1993, Wild, Shugars et al. 1994, Liu, Xiao et al. 2004). Moreover, analogs of HR2 region such as HR2P-M2, which have been modified by the addition of hydrophilic residues, are significantly more soluble, stable and have higher antiviral activity against MERS-CoV (Channappanavar, Lu et al. 2015).

Objective of this Dissertation Project

The emergence of SARS-CoV in late 2002 through early 2003 caused more than 8,000 severe respiratory illnesses in humans with a ~10% mortality rate. This had a devastating social, economic, and public health impact worldwide (WHO 2003, Sorensen, Sorensen et al. 2006). Thereafter, MERS-CoV emerged as the causative agent of MERS in humans in the Middle East in 2012 (Zaki, van Boheemen et al. 2012, Assiri, McGeer et al. 2013). Unlike the relatively short SARS outbreak (of a few months), MERS-CoV is still

ongoing and is causing severe disease currently in the Middle East. Since September 2012, the World Health Organization has recorded 1,917 cases of MERS resulting in 677 deaths (35%) (WHO 2017). Proven human-to-human transmission, despite a much lower transmission rate than that of SARS-CoV, and the absence of effective medical countermeasures (not approved vaccines and treatments) to date makes the ongoing MERS outbreak a significant public health concern.

While considerable progress has been made in our understanding of MERS-CoV, significant gaps in our knowledge exist. These deficiencies, at least partly, stem from lack of a suitable small animal model for studies of pathogenesis and immunity as well as for the development of vaccines and antivirals. Standard small animal models are not susceptible to MERS-CoV infection due to lack of a functional dipeptidyl peptidase-4 (DPP4) viral entry receptor (Raj, Mou et al. 2013). Although a mouse model of lung infection in which an adenovirus was used to transiently express hDPP4 has been developed (Zhao, Li et al. 2014), inconsistent DPP4 expression and the lack of clinical illness in this model underlines the needs for a better model system. A classic transgenic mouse model has the potential to move forward our understanding of MERS-CoV infection and disease research. Building on our prior success in the establishment and characterization of robust transgenic mouse models for SARS-CoV (19), we propose to establish transgenic mice permissive to MERS-CoV infection and disease. We will develop transgenic mouse lineages with global expression of hDPP4 and will characterize MERS as a respiratory disease in this model. Additionally, we will examine the subsequent impact on host-virus interactions, including but not limited to, tissue distribution and levels of viral replication, along with morbidity and mortality, if any. Successful establishment of this model will provide valuable tools for bridging the

knowledge gap in MERS-CoV infection and pathogenesis. Such a model will also enable larger scale of antiviral screens, which are not possible with NHPs, for developing effective therapeutic measures.

Hypothesis

Transgenic mice expressing human DPP4/CD26 receptor will be useful as surrogate models for studying MERS pathogenesis and help the development of medical countermeasures for MERS.

CHAPTER II: MATERIALS AND METHODS

Mice, virus, and cells.

The EMC-2012 strain of MERS-CoV, kindly provided by Heinz Feldmann (NIH, Hamilton, MT) and Ron A. Fouchier (Erasmus Medical Center, Rotterdam, Netherlands), was used throughout this study. Vero E6 cells (American Type Culture Collection) were used to expand the virus stocks and titrate the yields of progeny viruses. The MERS-CoV-EMC/2012 strain that we received was designated passage zero (P0) and further expanded with three passages in Vero E6 cells for generating cell-free P1, P2, and P3 stocks; P3 was used as the working stock for experiments described in this study. The titers of individual stocks, determined by using Vero E6-based infectivity assays, were expressed as TCID₅₀ per milliliter. Aliquots of virus stock with an average of 10⁷ TCID₅₀/ml were stored at -80°C.

In addition, a strain of recombinant MERS-CoV expressing red fluorescent protein (rMERS-CoV/RFP), kindly provided by Ralph Baric, University of North Carolina at Chapel Hill (Scobey, Yount et al. 2013), was similarly expanded and used in some experiments to visualize the infection.

To determine if the hCD26 transgene can confer susceptibility to MERS-CoV infection and can lead to productive MERS-CoV infection, mouse fibroblastic 17 CL-1 cells were subject to a stable cotransfection with the hCD26 expression plasmid, pCAGGS-CD26, and a plasmid encoding puromycin resistance. After selection with puromycin (2 g/ml), the transfectants were assessed for level of transgene expression at the protein level by both immunofluorescence (IF) staining and Western blotting analyses.

Two mice lineages B6C3F1/J and C57BL/6J (Jackson Lab) were used to generate the transgenic mice.

Viral infections

All *in vitro* and animal studies involving infectious MERS-CoV were conducted within approved biosafety level 3 (BSL-3) and animal BSL-3 (ABSL-3) laboratories at the National Galveston Laboratory, strictly following approved notification-of-usage (NOU) and animal protocols and the guidelines and regulations of the National Institutes of Health (NIH) and Association for Assessment and Accreditation of Laboratory Animal Care (AAALAC)

Construction and characterization of the hCD26 expressing plasmid *in vitro*.

The transgene cassette expressing hCD26 (also known as DPP4) was constructed using pCAGGS.MCS, a eukaryotic expression vector, as previously described for the expression of human Angiotensin convertase 2 (hACE-2) receptor of SARS-CoV (Tseng, Huang et al. 2007). Briefly, cDNA of hCD26 generated from the mRNA of human phytohemagglutinin (PHA)-activated T cells (Tanaka, Camerini et al. 1992) was obtained from C. Morimoto, University of Tokyo, Tokyo, Japan and was cloned into pCAGGS.MCS under the control of the CAG promoter, which is a composite promoter consisting of the

cytomegalovirus (CMV)/immediate-early enhancer and the chicken β -actin promoter, containing rabbit globin splicing and polyadenylation sites. We chose the CAG promoter due to its ability to drive high levels of gene expression. In addition, unlike the first-generation CMV promoter, CAG promoter activity does not decline over generations of transgenic mouse breeding (Niwa, Yamamura et al. 1991).

To verify the transgene construct pCAGGS-hCD26 (**Fig. 1A**), we transfected 17CL-1 mouse fibroblast cells and assessed hCD26 protein expression by Western blot using a goat polyclonal antibody against hCD26 known to have ~5% cross-reactivity to mouse CD26 (R&D Systems). Established hCD26-expressing mouse 17CL-1 cells along with cells transfected with empty vector were tested for MERS-CoV susceptibility by monitoring yields of progeny virus as well as the development of cytopathic effect (CPE).

Generation, detection, and breeding of transgenic mice.

The transgene (~5.6 kb) comprising CAGG enhancer/promoter, intron sequence, human CD26 cDNA, and rabbit beta globin poly(A) signal was released from pCAGGS.hCD26 using SalI and AvrII restriction enzymes and injected into B6C3F1/J \times C57BL/6J or C57BL/6J zygotes. G0 founder mice were tested for transgene integration using quantitative PCR (RT-qPCR) and/or Southern blot analysis. Briefly, genomic DNA isolated from tail biopsy specimens was subjected to RT-qPCR using hCD26-specific primers (forward, 5'-CCAAAGACTGTACGGGTCC-3'; reverse, 5'-TCAACATAGAAGCAGGAGCAG-3') and fluorescence probe (5'-/56-FAM/AAGGCAGGAGCTGTGAATCCAAC/36-TAMSp/-3') on a C1000 Touch thermocycler linked to a CFX96 real-time detection system (Bio-Rad). In some cases, Southern blot analysis was used to identify transgene-positive founder mice. For this,

genomic DNA was digested by BamHI, separated on agarose gels, and transferred to Hybond-XL (GE Healthcare Life Sciences). The blots were hybridized with ³²P-labeled probes prepared by random priming. A 0.4-kb SalI-NcoI fragment of the CMV enhancer and a 0.7-kb BglII fragment (DPP4 3' untranslated region [3'UTR]), isolated from pCAGGS.hCD26, were used as probes. The Gsc2 5' probe was used to normalize the amount of DNA on the blots (Wakamiya, Lindsay et al. 1998). The transgenic mouse experiments were carried out in the barrier facility at the University of Texas Medical Branch transgenic mouse core facility. All animal work conformed to NIH and AAALAC regulations and guidelines.

Virus isolations

Collected tissue specimens of lungs, brain, heart, liver, kidney, spleen, and intestine were weighed and homogenized in phosphate-buffered saline (PBS) containing 10% fetal calf serum (FCS) with a TissueLyser (Qiagen, Retsch, Haan, Germany). After clarification of the cellular and tissue debris by centrifugation, the titers of the resulting suspensions of infected tissues were determined in the standard Vero E6 cell-based infectivity assays for quantifying yields of infectious virus. The virus titers of individual samples were expressed as log₁₀ TCID₅₀ per gram of tissue.

RNA extraction and real-time RT-qPCR.

Tissues collected at indicated times were placed in individual vials containing RNAlater solution (Qiagen), and stored at 4°C until used for extracting total RNA. Briefly, tissues were homogenized in 1 ml of TRIzol reagent (Life Technologies) with a TissueLyser. After clarifying by centrifugation at 12,000 × g for 5 min, the resulting suspensions were tested for total RNA and for quantification of MERS-CoV-specific RNA that targeted the

upstream E (upE) gene and mouse GAPDH or beta (β)-actin gene (internal controls). For the detection of viral gene expression in different tissues, 0.5 μ g of RNA extracted from individual tissues was used in a one-step real-time reverse transcription-PCR (RT-qPCR) with a set of primers and probes specific for the upE gene of MERS-CoV performed with a Superscript III One-Step RT-qPCR kit (Invitrogen) according to the manufacturer's instructions. The primers and probes used for analysis of the upE gene of MERS-CoV were as follows: forward, 5'-GCCTCTACACGGGACCCATA-3'; reverse, 5'-GCAACGCGCGATTCAGTT-3'; fluorescence probe, 5'-6-carboxyfluorescein (FAM)/CTCTTCACATAATCGCCCCGAGCTCG/36-5'-carboxytetramethylrhodamine (TAMRA)/-3'. The relative amount of targeted mRNA was determined by normalizing with an endogenous control GAPDH or (β -actin) gene and expressed as fold change by the standard threshold cycle ($\Delta\Delta$ CT) method (Tseng, Tseng et al. 2005).

Serological assays.

MERS-CoV-specific neutralizing antibody and S1 protein-specific Immunoglobulin (IgG) antibody responses were quantified by a classical infection reduction assay and a standard enzyme-linked immunosorbent assay (ELISA), respectively, as described previously (Tseng, Sbrana et al. 2012, Du, Kou et al. 2013).

Vero E6 cell-based microneutralization assay

Starting at a dilution of 1:10, 60- μ l volumes of serial 2-fold dilutions of heat-inactivated serum specimens collected via retro-orbital bleeding from surviving Tg⁺ mice at 21 days post-infection were transferred into duplicate wells of 96-well plates containing 120 TCID₅₀ of MERS-CoV in 60 μ l of M-2 medium/per well. The antibody-virus mixtures were incubated at 37°C for 1 h before transfer of 100 μ l of the mixtures (containing 100 TCID₅₀

of MERS-CoV) into confluent Vero E6 cell monolayers in 96-well plates. Six wells of Vero E6 cells cultured with equal volumes of M-2 medium with or without virus were included in these assays as positive and negative controls, respectively. When the wells of Vero E6 cells infected with virus alone developed advanced cytopathic effects (CPE), the neutralizing capacity of individual serum specimens was determined on the basis of the presence or absence of CPE. Reciprocals of the last dilutions of serum specimens capable of completely preventing the formation of CPE were used as the neutralizing antibody titers and expressed as 100% neutralizing titers (NT₁₀₀).

ELISA Test

For quantifying the total MERS-CoV S1-specific IgG antibodies, 96-well ELISA plates were pre-coated with recombinant His-tagged S protein (1 µg/ml), as described previously (Ma, Wang et al. 2014, Zhang, Channappanavar et al. 2016). After blocking with Tris-buffered saline (TBS) containing 10% FBS and 0.05% Tween 20 for 1 h at room temperature, 50-µl volumes of serial 10-fold dilutions of mouse serum specimens, starting at a dilution of 1:100, were added to the plates (Corning; catalog no. 3690), incubated for 1 h at 37°C, and thoroughly washed with TBS before addition of horseradish peroxidase (HRP)-conjugated anti-mouse IgG (Southern Biotech; catalog no. 1030-05) (1:4,000) for 1 h at 37°C. Thoroughly washed plates were incubated in the dark with o-phenylenediamine dihydrochloride (OPD) (Sigma; catalog no. P9187) for 15 min, and the reactions were stopped with 1N H₂SO₄ and read in an ELISA plate reader (Molecular Devices) for measurement of optical density (OD) at 450 nm. The highest dilutions of serum specimens with MERS-CoV S1-specific antibody with a mean OD reading of greater than or equal to 2

standard deviations (SD) greater than the mean for specimens of naive mice were used to define titers.

Histology and immunohistochemistry (IHC)

Tissues obtained from necropsy samples were fixed in 10% buffered formalin for 72 h, transferred to 70% ethanol, and later paraffin embedded. Histopathologic evaluation was performed on deparaffinized sections stained by routine hematoxylin-eosin (H&E) staining. IHC for MERS-CoV was performed using a previously described colorimetric indirect immunoalkaline phosphatase method (Tseng, Huang et al. 2007) with a rabbit anti-MERS-CoV polyclonal antibody, provided by Heinz Feldmann. The goat anti-hCD26 antibody (R&D Systems, catalog no. AF1180) was used to assess the distribution of hCD26 expression in transgenic mice by IHC. Normal mouse and goat sera were used as negative antibody controls. Biotinylated swine anti-rabbit immunoglobulin (Dako, catalog no. E0353) or rabbit anti-goat immunoglobulin (KPL, catalog no. 16-13-06) were used as secondary antibodies. The antigen was then visualized by incubation with streptavidin-alkaline phosphatase and naphthol-fast red substrate (Dako) and counterstained with Mayer's hematoxylin (Fisher Scientific).

Animal studies

Susceptibility, morbidity and mortality study

A pilot study indicated that hCD26 Tg⁺ mice of different genetic background were equally susceptible to MERS-CoV infection. Therefore, Tg⁺ and their age-matched transgene-negative (Tg⁻) littermates derived from the line 52 founder mouse were backcrossed one or two times onto either a C57BL/6 or B6C3F1/J background. For virus challenge studies, anesthetized 5-7 weeks old Tg⁺ and Tg⁻ littermates were inoculated via

the i.n. route with 10^6 TCID₅₀ of MERS-CoV in a total volume of 80 μ l. Animals were weighed and monitored daily for clinical signs of disease and abnormalities, including appearance, stereotypical behavior/abnormal movements, decreased responsiveness or activity, and weight loss. The clinical scoring system used was as follows: 0, no apparent illness; 1, mildly sick; 2, ruffled fur or hunching; 3, ruffled fur and hunching, with or without additional signs; 4, moribund; and 5, found dead. Some infected mice were sacrificed at indicated times p.i. to obtain tissue specimens for assessing the distribution of virus and associated histopathology using standard protocols, such as a Vero E6 cell-based infectivity assay, quantitative reverse transcription-PCR (RT-qPCR) assay, and immunohistochemical (IHC) staining.

Determination of LD₅₀ and ID₅₀ studies

To determine the LD₅₀ and ID₅₀, we initially administered (i.n.) serial doses of MERS-CoV, decreasing 10-fold from 10^6 to 10^1 TCID₅₀ in a volume of 60 μ l, to groups of four or eight naive Tg⁺ mice and monitored them daily for clinical manifestations (weight loss) and mortality for at least 21 dpi (Experiment 1; Table 2).

To further assess the LD₅₀ and ID₅₀ of the MERS-CoV stock, we challenged (i.n.) another four groups of four Tg⁺ mice with 2-fold decrements of MERS-CoV doses, starting from 10 TCID₅₀; dosages were 10, 5, 2.5, and 1.25 TCID₅₀ of the virus. Mice were followed daily for morbidity (weight loss) and mortality for at least 3 weeks (Experiment 2; Table 2).

Finally, a third experiment was performed as the experiments described above except that mice were given decreasing 10-fold doses of MERS-CoV, from 10^1 to 10^{-3} TCID₅₀.

Immune responses, and immunity of hCD26/DPP4 transgenic mice to MERS-CoV infection studies.

To analyze the infection-induced immune response and immunity to MERS-CoV re-infection, we used the blood collected from the survivor mice (Experiment #2, Table 2) to perform serological assays, which included the determination of MERS-CoV-specific neutralizing antibody and S1 protein-specific IgG antibody responses by Vero E6 cell-based microneutralization assay and ELISA, respectively.

Subsequently, we challenged (i.n.) the low-dose challenge survivors, along with two naive Tg⁺ mice, with 10³ TCID₅₀ (100 LD₅₀) of MERS-CoV at 35 dpi to determine if they had developed immunity to a lethal challenge.

Kinetics and tissue distribution studies - viral infection in hCD26/DPP4 Tg⁺ mice challenged with 10 LD₅₀ of MERS-CoV.

For determining the tissue distribution of viral infection and histopathology over time with a potential working dose of virus, 18 age-matched (10-to-14-week-old) Tg⁺ mice were challenged (i.n.) with 10² TCID₅₀ (10 LD₅₀) of MERS-CoV. Three mice each were sacrificed at 2, 4, 6, 8, 10, and 12 dpi for assessing viral infection in the lungs, brain, heart, liver, kidney, spleen, and intestine by quantifying infectious virus and viral RNA expression using Vero E6 cell-based infectivity and RT-qPCR assays, respectively. Standard IHC with a rabbit anti-MERS-CoV hyperimmune serum was also performed for the detection of viral antigens in tissues.

Efficacy of the S377-588-Fc as a subunit vaccine

Groups of age-matched Tg⁺ mice were immunized intramuscularly (i.m.) twice (once and then again three weeks later) with 10 µg of S377-588-Fc in 50 µl of PBS formulated

with an equal amount of MF59 adjuvant (AddaVax [catalog no. vac-adx-10]; InvivoGen) or with MF59 alone, designated S377-588-Fc/MF59 or PBS/MF59, respectively. Sera from immunized mice after the second immunization were subjected to serological assays for quantifying neutralizing and MERS-CoV S1 protein-specific IgG antibodies. Immunized mice were subsequently challenged (i.n.) at day 10 after the second immunization with 10^3 TCID₅₀ of MERS-CoV in a volume of 60 μ l. Three mice in each group were sacrificed at 2 dpi for quantifying infectious virus and viral RNA expression, whereas the remaining five in each group were monitored daily for morbidity (weight loss) and mortality.

Preventive and therapeutic efficacy of a fusion inhibitor peptide.

Both the preventive and therapeutic efficacies of a fusion inhibitor peptide recently proven effective, HR2M6 (Channappanavar, Lu et al. 2015) were evaluated. For measuring the prophylactic potential, groups of Tg⁺ mice were treated (i.n.) with 200 μ g of HR2M6 in 50 μ l of PBS or PBS alone at 1 and/or 4 h prior to challenge (i.n.) with 100 TCID₅₀ of MERS-CoV in 60 μ l. For assessing the therapeutic effect, groups of Tg⁺ mice previously infected (i.n.) with 100 TCID₅₀ of MERS-CoV were treated with 50 μ l of PBS or 200 μ g of HR2M6 in 50 μ l of PBS at 1, 12, and 24 h after infection and then once daily until 7 dpi. Three mice in each group were sacrificed at 2 dpi for assessing yields of infectious virus or viral RNA in lungs, whereas the remaining five animals in each group were monitored daily for morbidity and mortality.

CHAPTER III: GENERATION OF A TRANSGENIC MOUSE MODEL OF MIDDLE EAST RESPIRATORY SYNDROME

Introduction

Although significant information has been obtained about MERS and MERS-CoV since its emergence, vast deficiencies in basic and translational research exist. They largely stem from the lack of suitable small-animal models for studies of pathogenesis and for the development of vaccines and antivirals. Unfortunately, standard small animals used in research such as mice, hamsters, and ferrets, all lack the MERS-CoV receptor, human CD26 (hCD26), or dipeptidyl peptidase-4 (DPP4) and are not susceptible to MERS-CoV infection (Scobey, Yount et al. 2013, Coleman, Matthews et al. 2014). Although studies with nonhuman primates (NHPs) such as rhesus macaques and marmosets have demonstrated their susceptibility to various degrees to MERS-CoV infection, NHPs are expensive models with limited availability (de Wit, Rasmussen et al. 2013, Falzarano, de Wit et al. 2014). Hence, mice are the most desirable small animals for this purpose because of availability and the existence of a vast knowledge base, particularly of genetics and immunology. Even though a mouse lung infection model was described wherein an adenovirus vector was used to transduce the viral receptor gene (Zhao, Li et al. 2014), it is generally agreed that a transgenic mouse model expressing the hCD26/DPP4 receptor is needed for research on MERS-CoV infection and disease. In contrast to the adenovirus transduced mice, by using transgenic mice it is possible to develop a model that will permit to have a consistent expression of the hDPP4 in the lungs. Also, it is possible to achieve a stable (not transient) expression of the hDPP4, in contrast with the transduced model in which the expression was observed only for approximately 3 weeks. To derive such models, we used constitutive global promoter, the CAG promoter, which is a composite promoter consisting of the

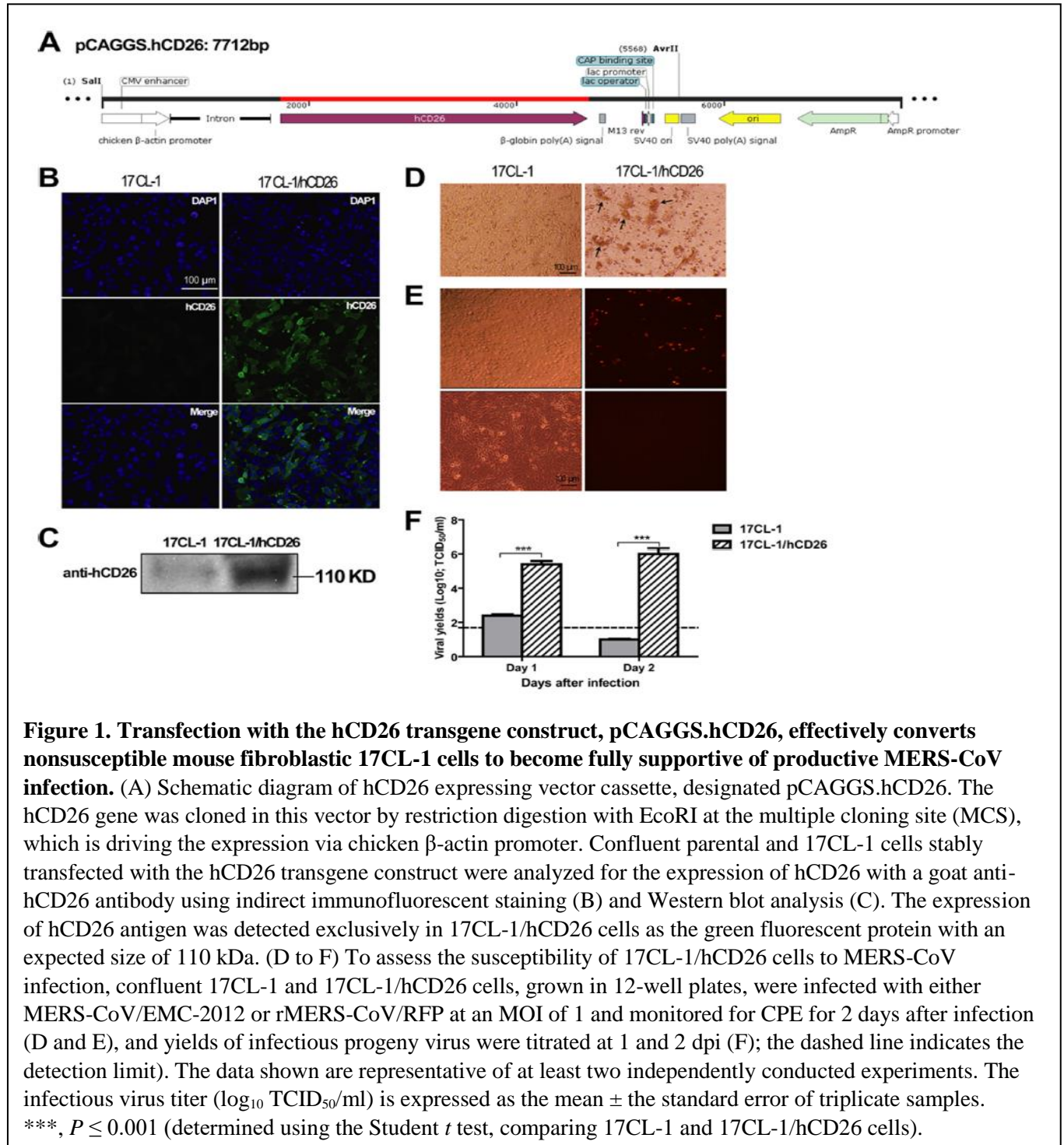
cytomegalovirus (CMV)/ immediate-early enhancer and the chicken β -actin promoter, containing rabbit globin splicing and polyadenylation sites. We describe here the first transgenic mouse lineage globally expressing hCD26/DPP4 receptor and show that these transgene-positive (Tg^+), but not transgene-negative (Tg^-) mice are highly susceptible to MERS-CoV infection and disease.

Results

Characterization of the hCD26 transgene construct in tissue culture

To validate the potential of the hCD26 transgene cassette (**Fig. 1A**) in expressing the transgene, 17 CL-1 cells were cotransfected with the hCD26 expression plasmid, pCAGGS-CD26, and a plasmid encoding puromycin resistance. After selection with puromycin (2 μ g/ml), the transfectants were assessed for level of transgene expression at the protein level by both immunofluorescence (IF) staining and Western blotting analyses. As shown in **Fig. 1B and C**, an intense green fluorescence staining and a distinct band of \sim 110 kDa in Western blots, the estimated size of hCD26, were seen almost exclusively in 17CL-1 cells transfected with the hCD26 expressing plasmid, indicating the effectiveness of the transgene construct in promoting cellular hCD26 expression. The much weaker band seen in wild-type 17CL-1 cells likely represented mouse CD26 as the anti-hCD26 antibody (R&D Systems) used for Western blotting was shown to having \sim 5% cross-reactivity to mouse CD26. To determine whether the expression of hCD26 viral receptor can confer susceptibility to MERS-CoV in otherwise permissive 17CL-1 cells, confluent cultures of 17CL-1/hCD26 cells and parental 17CL-1 cells were infected with either MERS-CoV or a rMERS-CoV expressing red fluorescent protein (RFP) at an MOI of 1, followed by monitoring for morphological changes of infected cells and for the intensity of infection over time. In

contrast to the infection-resistant parental 17CL-1 cells, 17CL-1/hCD26 cells were fully susceptible to MERS-CoV infection, resulting in the development of CPE (Fig. 1D), readily detectable expression of RFP (Fig. 1E), and high yields of infectious progeny virus as early



as 1 dpi (**Fig. 1F**). Based on these results, we conclude that induction of hCD26 expression using this transgene construct effectively converts non-susceptible 17CL-1 cells into susceptible cells, capable of fully support MERS-CoV infection.

Generation and characterization of hCD26 transgenic mice.

Transgenic mice expressing hCD26 were generated by microinjecting the expression cassette, excised from pCAGGS-CD26 by AvrII/Sall digestion, into pronuclei of zygotes from either the C57BL/6J or C57BL/6J × B6C3F1/J background, as described in Materials and Methods, which led to 81 live births. Based on the RT-qPCR and/or Southern blot analyses of genomic DNA, we identified five B6/C3H hybrid and two B6 founders that were then crossed with C57BL/6J and/or B6C3F1/J to propagate the lines. Based on their ability to transmit hCD26 transgene to their offsprings, lines 52, 62, and 72 were selected among the seven Tg⁺ founder lineages to further expand the transgenic colonies and characterize the hCD26 expression. Southern blot analyses revealed that the intensity of hCD26 transgene was highest in line 62, followed by line 72 and line 52, in that order (**Fig. 2A**). However, line 62 had extremely poor transgene transmissibility and had neonatal deaths of the Tg⁺ pups. Moreover, the majority of the Tg⁺ pups of Line 72 died prematurely at ~3 weeks of age (**Table 1**).

To evaluate the expression of hCD26 in lines 72 and 52, total RNA was extracted from tissues of Tg⁺ G₁ pups and subjected to RT-qPCR analysis using the same hCD26-specific primer-probe set used for genotyping. Although both lines expressed hCD26 in all tissues analyzed, the levels of hCD26 expression appeared to be higher in line 72 than in line 52, with the heart and spleen as the only exceptions (**Fig. 2B**).

In contrast to the extreme difficulty that we encountered to propagate lines 62 and 72, the line 52 founder mouse was capable of generating many first-, second-, and third-generation Tg^+ pups that survived to maturity, permitting characterization of hCD26 expression. To investigate the tissue distribution of hCD26 protein expression, cellular lysates and paraffin-embedded sections of various tissues were analyzed by Western blotting and IHC staining using a polyclonal antibody known to recognize hCD26 with <5% cross-reactivity to mouse CD26 (R&D Systems, catalog no. AF1180). Among six tissues analyzed (i.e., heart, lung, spleen, intestine, liver, and kidneys) by Western blotting, the expression of hCD26 was higher in both lungs and kidneys than in the other tissues (**Fig. 2C**). The standard IHC assays also detected the expression of hCD26 antigen in all tissues analyzed, including the lung, brain, heart, liver, kidney, and intestine (**Fig. 2D**). In Tg^+ mice, hCD26 was primarily detected in both types of alveolar pneumocytes in lung as well as the neuronal and endothelial cells in the brain (**Fig. 2Da and b**). Prominent epithelial and/or endothelial hCD26 expression was detected in the liver, kidneys, and the gastrointestinal (GI) tract (**Fig. 2Dd to f**). Hepatic expression of hCD26 extended to the surface of hepatocytes. The expression of hCD26 was focalized within the muscularis layer of the GI tract and cardiomyocytes of the heart. Importantly, this positive staining is specific to hCD26 since no staining could be detected in tissues from Tg^- mice. Taken together, these results indicate that line 52 is a stable transgenic lineage globally expressing the hCD26 receptor for MERS-CoV.

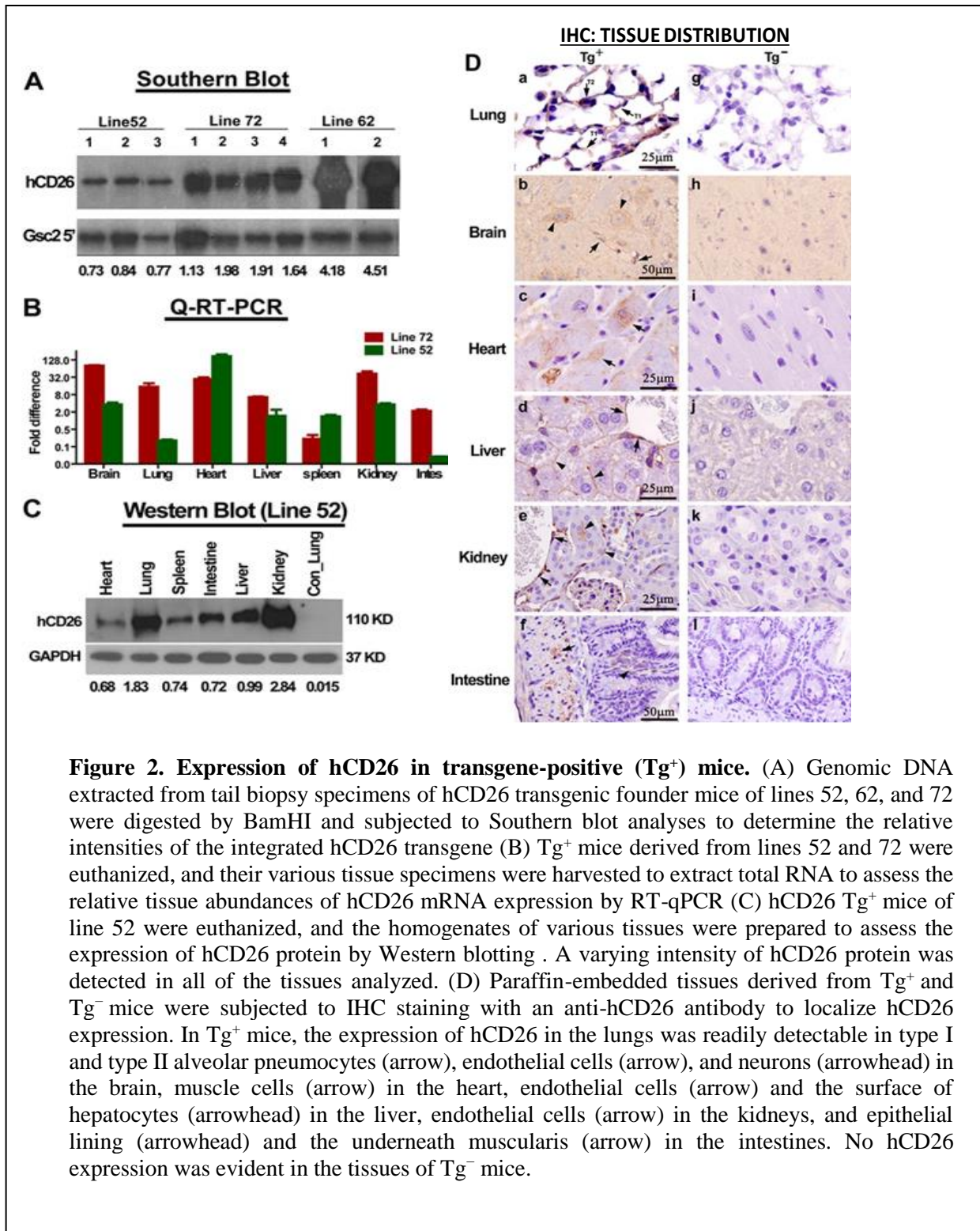


TABLE 1. Founders of hCD26 transgenic lineages

Founder (lineage)	Sex	Background	Transgene confirmation method	Germ line transmission	Notes
7	F	B6/C3 mix	SB/RT-qPCR	No	The mouse was fertile, but produced no transgene-positive pups.
52	F	B6/C3 mix	RT-qPCR	Yes	The mouse was viable and fertile.
54	M	B6/C3 mix	RT-qPCR	ND	The mouse died shortly after weaning.
62	M	B6/C3 mix	SB/RT-qPCR	Yes	The mouse was fertile, but produced small-size litters. A few transgene-positive pups were found but they died within a week after birth.
72	F	B6/C3 mix	SB/RT-qPCR	Yes	The mouse was fertile. The majority of transgene-positive pups died after weaning before sexual maturity.
76	ND	B6	SB/RT-qPCR	ND	The mouse died before weaning.
78	F	B6	SB/RT-qPCR	Yes	The mouse was fertile, but did not take care of the pups. None of the pups survived beyond neonatal periods.

ND, not determined; SB, Southern blotting; B6/C3 mix, cross with B6C3F1/J and C57BL/6J

Transgenic mice expressing hCD26 are susceptible to MERS-CoV infection that results in disease and mortality.

With the characterized expression of hCD26 of the transgenic lineage, we explored whether line 52 hCD26 Tg⁺ mice would be susceptible to MERS-CoV infection. For a pilot study, we infected two Tg⁺ mice of different genetic backgrounds obtained from backcrossing the founder 52 (B6/C3 mix) to either B6 or B6C3F1/J mice, along with two Tg⁻ age-matched littermates, with 10⁶ TCID₅₀ of MERS-CoV intranasally in 80 µl. Mice were sacrificed 2 days after infection to assess the yield of infectious virus in the lungs using Vero E6 cell-based infectivity assays. We found that Tg⁺ mice of different genetic background, but not those of Tg⁻ littermates, were equally susceptible to infection, as

evidenced by high yields of infectious virus of approximately 10^7 TCID₅₀ of MERS-CoV per gram of lung tissue for both mice with different backgrounds.

Encouraged by the results of this pilot study, we subsequently inoculated additional age-matched line 52 Tg⁺ and Tg⁻ mice; nine animals in each Tg group were given 10^6 TCID₅₀ i.n. in 80 μ l for initial assessment of the kinetics of infection and disease. Mice were monitored daily for signs of clinical illness, weight loss, and mortality. Virus replication and disease pathogenesis in different tissues were assessed by sacrificing two mice in each group at 2 and 4 dpi. We noted that challenged Tg⁺, but not Tg⁻, mice developed an acute wasting syndrome, as evidenced by progressive weight loss starting at 2 dpi and leading to 30% and 100% mortality at 5 and 6 dpi, respectively (**Fig. 3A and B**). Other clinical manifestations in infected Tg⁺ mice included ruffled fur, lethargy, inactivity, and rapid and shallow breathing. Despite their immobility, we did not observe any signs of neurological disorder such as seizure or paralysis, in the Tg⁺ mice. The Tg⁻ mice continued to thrive throughout the course of infection without showing any weight loss or signs of clinical illness.

Line 52 transgenic mice expressing hCD26 developed disseminated infection.

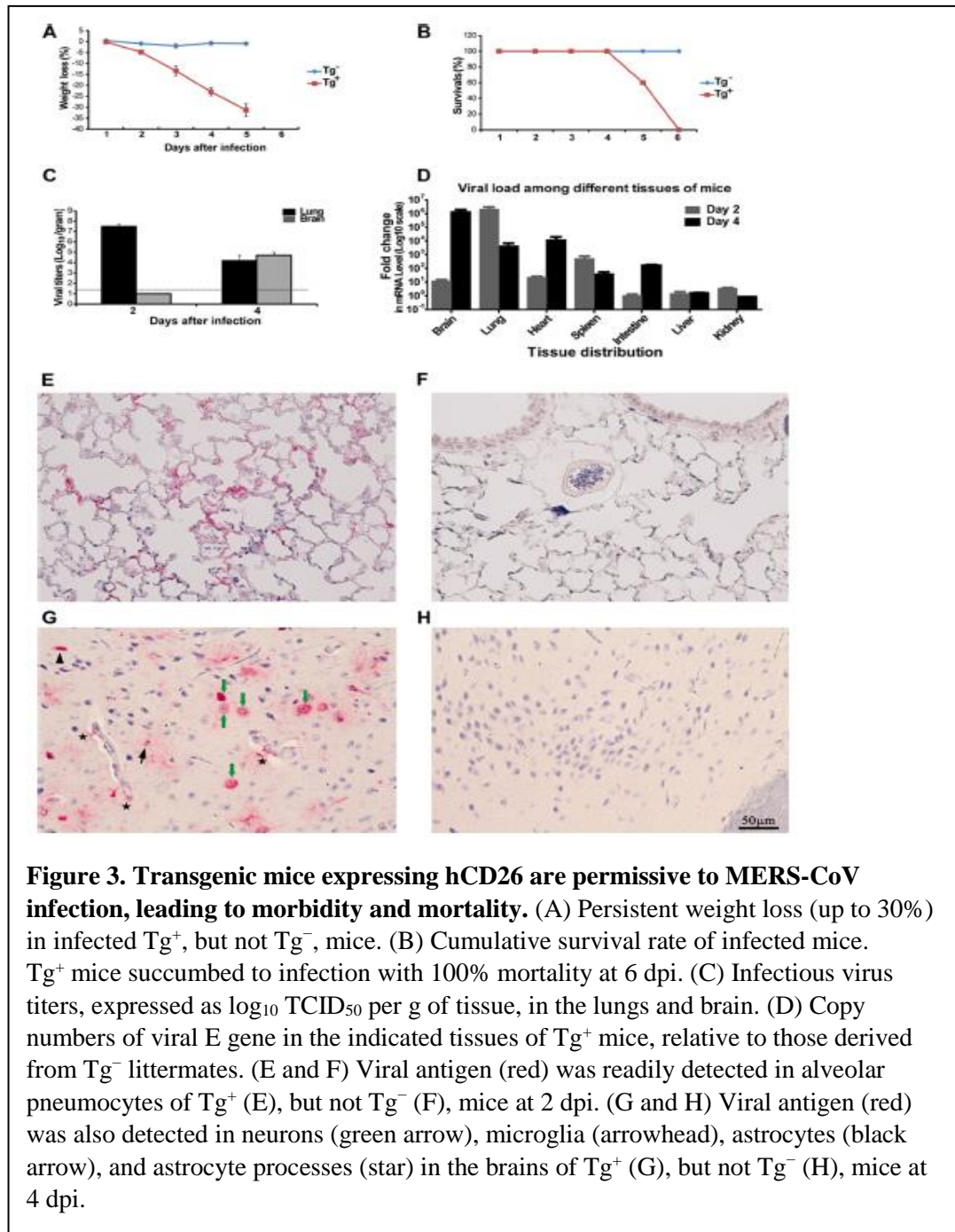
To determine the kinetics and tissue distribution, tissue specimens of Tg⁺ and Tg⁻ mice collected on 2 and 4 dpi were tested for infectious virus in the Vero E6 cell-based infectivity assay. It was clear that lung and brain appeared to be the prime sites of intense viral infection (**Fig. 3C and D**). We detected titers as high as $\sim 10^7$ TICD₅₀ of MERS-CoV per gram of the lung tissue at 2 dpi that dropped at 4 dpi to $\sim 10^4$ TCID₅₀ per gram, a net loss of 3 logs. In contrast to the acute and robust pulmonary infection, we were unable to isolate infectious virus from the brain until 4 dpi when an average of 7×10^4 TCID₅₀/g was detected.

These results indicate that the kinetics of MERS-CoV infection in the lung and brain of Tg⁺ mice were substantially different. Despite the high yields of infectious virus detected in the lung and brain, we were unable to isolate any infectious virus from other tissues, including the liver, heart, spleen, kidneys, and intestines, at either 2 or 4 dpi. To verify the presence or absence of virus in tissues with no infectious virus, we tested for the presence of viral RNA by RT-qPCR targeting the upstream E gene of MERS-CoV in all tissues collected at both 2 and 4 dpi. Consistent with the yields of infectious virus, a 6-log higher viral RNA was detected in the lungs and brains of infected Tg⁺ mice than that in the Tg⁻ mice (**Fig. 3D**). MERS-CoV RNA was also readily detected at either 2 or 4 dpi in the heart, spleen, and intestine, even though we were unable to isolate any infectious virus. Taken together these data suggest a disseminated MERS-CoV infection in the hCD26 Tg⁺ mice.

Interestingly, we were unable to detect any viral RNA in the liver and kidneys, despite the expression of hCD26 in these organs (**Fig. 2B, C, and D**).

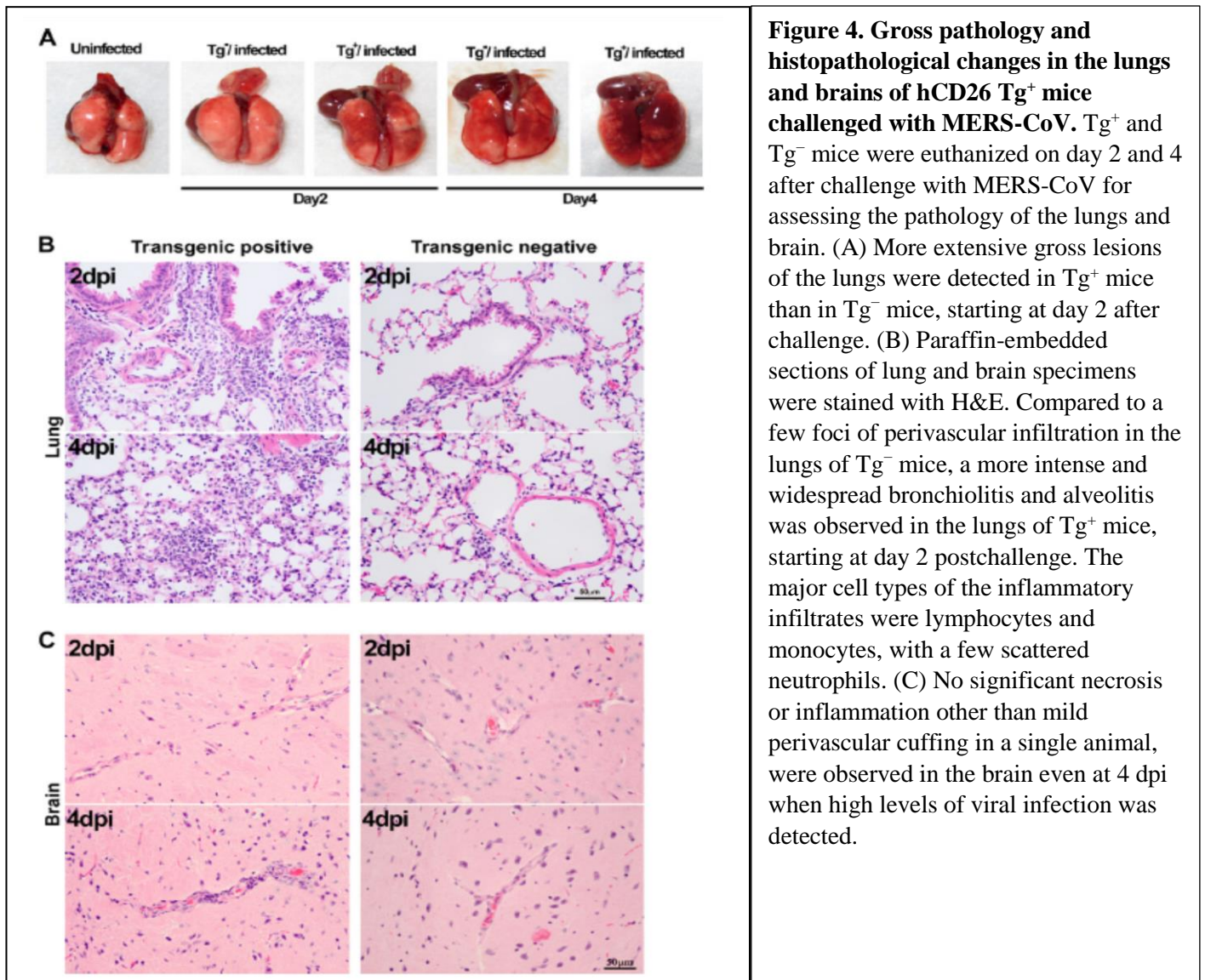
Because high titers of infectious virus could be readily recovered from lungs and brains of challenged Tg⁺ mice, we performed IHC staining with paraffin-embedded tissues and a specific antibody for detecting viral antigen, as described in Materials and Methods, to confirm the cellular tropism of MERS-CoV infection for each tissue. As shown in **Fig. 3E and G**, lung alveolar pneumocytes, both type I and type II, and brain microglia, astrocytes, and neuronal cells expressed abundant viral antigen in Tg⁺ mice at 2 and 4 dpi. While two-color IHC staining was not performed to conclusively prove it, patterns of viral antigen expression correlated with the cellular distribution of the hCD26 receptor (**Fig. 2D**). These findings indicate that transgenic mice expressing hCD26/DPP4 are highly susceptible

to MERS-CoV infection that results in disseminated infection with significant morbidity and mortality.



Histopathology in MERS-CoV-infected hCD26 Tg⁺ mice.

Pathological changes in MERS-CoV-infected Tg⁺ and Tg⁻ mice were assessed at 2 and 4 dpi. Consistent with higher viral infection, discoloration (red to dark red) and multifocal consolidation were observed in the lungs of Tg⁺ but not in Tg⁻ mice at 2 dpi, which became more pronounced at 4 dpi (Fig. 4A). Histological examination of the lung at 2 dpi showed moderate bronchiointerstitial pneumonitis, and multifocal perivascular infiltrates with some changes extending into the terminal bronchioles and adjacent pulmonary parenchyma. At 4 dpi, increased cellular infiltrates, including pulmonary macrophages and lymphocytes, were seen within



alveolar spaces (**Fig. 4B**). Both type I and type II alveolar epithelial cells appeared to be the targets for MERS-CoV infection in hCD26 Tg⁺ mice (**Fig. 2D**). No significant necrosis or inflammation other than mild perivascular cuffing in a single animal, were observed in the brain even at 4 dpi when high levels of viral infection was detected (**Fig. 4C**). Similarly, no pathological findings could be identified in other tissues collected from virus-challenged Tg⁺ or Tg⁻ mice.

Discussion

Small-animal models for studying MERS-CoV pathogenesis and immune responses are key to the development of vaccines and antivirals. The failure of mice, hamsters, and ferrets, the most commonly used small animal models, to support MERS-CoV infection (van Doremalen, Miazgowiec et al. 2014) has impaired scientific progress on these fronts. In contrast, mice, hamsters, and other small animals were susceptible to SARS-CoV infection and disease (Roberts, Lamirande et al. 2008). Moreover, a SARS-CoV virus strain that caused severe respiratory disease and death was developed by serial passaging in mice (Roberts, Deming et al. 2007). This was, at least partly, due to the expression of virus receptor for SARS-CoV (hACE-2) in small animals. Availability of small animal models permitted a relatively fast-paced research on SARS-CoV infection and disease. However, the receptor for MERS-CoV, human CD26/DPP4 is not expressed naturally in tissues of mice, hamsters, and ferrets making them not susceptible to infection. In last few years, two NHP species, rhesus macaques and marmosets, and Ad5-hDPP4-transduced mice have been reported as models for MERS-CoV infection and disease (de Wit, Rasmussen et al. 2013, Falzarano, de Wit et al. 2014, Zhao, Li et al. 2014). In contrast to the transient and self-limited viral infection and mild-to-moderate respiratory disease caused by experimental MERS-CoV infection in rhesus macaques and Ad5-hDPP4-transduced mice, marmosets

developed a more serious infection, predominantly in the respiratory tract, that caused progressive severe pneumonia and death in some animals. Hence, before the studies presented in this Chapter, marmoset appeared to be the best model for MERS-CoV infection and disease.

With considerable effort, we succeeded in establishing a transgenic mouse model for MERS-CoV infection and disease. In contrast to the variable duration and level of hDPP4 expression in Ad5-hDPP4-transduced mice, our transgenic mice expressed hCD26/DPP4 globally. Moreover, as compared to the limited transient infection in the Ad5-hDPP4-transduced mice, the transgenic mice also supported robust MERS-CoV infection, especially in lungs and brain, and developed a severe respiratory and generalized illness that led to death within days after infection. We consistently observed signs of severe disease including relentless weight loss, acute and profound pulmonary viral infection, and death along with characteristic lung pathological changes in MERS-CoV-challenged hCD26/DPP4 transgenic mice. Transgenic mice expressing hCD26/DPP4 were established using the pCAGGS.hCD26 plasmid that was first shown to convert nonsusceptible, but otherwise permissive, mouse 17CL-1 cells to full susceptibility to MERS-CoV infection (**Fig. 1**). Among four identified fertile founders of transgenic lineages capable of transmitting the transgene to offspring (**Table 1**), three founders (lines 62, 72, and 78) either had neonatal mortality or had very small litter sizes. However, the line 52 founder was fertile and gave birth to litters with an average of 8 to 12 healthy pups, thereby allowing the generation of many G₁, G₂, and even G₃ Tg⁺ offsprings. Such a low rate in successfully establishing hCD26/DPP4 transgenic lineages was unexpected, as we had successfully used a similar pCAGGS plasmid-based approach to establish at least five transgenic lineages globally

expressing different levels of hACE-2 receptor for SARS-CoV (Tseng, Huang et al. 2007), suggesting that the expression of hCD26/DPP4 may have negative effect on the well-being of mice.

CD26/DPP4, a type II transmembrane serine peptidase, is unambiguously expressed at various levels in many human tissues and can regulate diverse biological functions, in health and disease, through the cleavage of X-proline dipeptides of many growth factors, chemokines, neuropeptides, vasoactive peptides and other biologically active polypeptides (Lambeir, Durinx et al. 2003, Yu, Yao et al. 2010). In addition, an ill-regulated enzymatic function of CD26/DPP4 could lead to the inactivation of incretin hormones, such as glucagon-like peptide 1 (GLP-1) and glucose-dependent insulinotropic polypeptide (GIP), resulting in decreasing glucose-dependent secretion of insulin, the hallmark of diabetes (Mu, Petrov et al. 2009). Moreover, an increased CD26/DPP4 expression can negatively affect the growth of endothelial cells, especially within the microvasculature network (Takasawa, Ohnuma et al. 2010). Therefore, DPP4 inhibitors have been used successfully as antidiabetic drugs, reversing the detrimental effect imposed by inactivated incretin hormones by increasing insulin secretion and suppressing glucagon secretion (Takasawa, Ohnuma et al. 2010), providing the therapeutic basis for using DPP4 inhibitors for treating vascular complications associated with diabetes. Based on these reports of DPP4 function, we explored whether uncontrolled sugar metabolism could be responsible for neonatal or premature deaths of Tg^+ pups of lines 62 and 72. Preliminary data obtained from a pilot study of line 62 founder and a few G_1 or G_2 pups (~3 to 4 weeks of age) derived from lines 72 and 52 indicated that there were 2- to 3-fold increase in blood sugar levels of the Tg^+ mice of each lineage compared to their Tg^- littermates. Coincidentally, pathological examination also

revealed the existence of irregular vasculature in the kidneys, lungs, and liver of Tg⁺ mice of Line 72 but not line 52. These results led us to speculate that hCD26 is likely catalytically active in Tg⁺ mice, having a negative impact, to a varying extent, on the well-being of mice in a lineage-dependent manner. However, whether such an “add-on” hDPP4 activity in Tg⁺ mice could be responsible for elevated blood sugar levels and abnormal vasculatures and contribute to breeding difficulties and prenatal or postnatal deaths awaits additional studies. Similarly, whether altered glucose metabolism influences the course of infection and disease in line 52 Tg⁺ mice needs to be studied further.

Kinetics and tissue distribution of MERS-CoV replication in MERS-CoV-infected (i.n.) lineage 52 Tg⁺ mice clearly indicated that a robust viral infection took place primarily in the lung and brain, the prime tissues for MERS-CoV infection in these animals. The highest load of infectious virus in the lung was detected at 2 dpi, which was reduced by 3 logs at 4 dpi; whereas infectious virus in the brain could not be detected until 4 dpi, suggesting that the respiratory tract was the initial site of MERS-CoV infection (**Fig. 3C**). While IHC showed that MERS-CoV primarily replicated in type I and II pneumocytes in the lung alveolae many cell types including microglia, astrocytes, and neurons were infected in the brain (**Fig. 3E and G**). Although infectious virus was not recovered from the other tissues collected, viral RNA was readily detected by RT-qPCR in the heart, spleen, and intestines, suggesting a disseminated infection. However, despite confirmed hCD26/hDPP4 expression, no viral RNA was detected in the liver and kidneys (**Fig. 3D and 2D**). In some MERS patients, acute renal failure has been reported (Zaki, van Boheemen et al. 2012). Despite the widespread viral infection in experimentally infected rhesus macaques and marmosets, viral RNA from kidneys could only be detected in marmosets; however, neither

infectious virus nor histopathology was detected in the kidneys of infected marmosets (de Wit, Rasmussen et al. 2013, Falzarano, de Wit et al. 2014). Similar to our findings in the mouse model, respiratory infection with MERS-CoV in marmosets led to viral spread in the central nervous system as evidenced by the detection of viral RNA in the frontal lobe, cerebellum, and brain stem (Falzarano, de Wit et al. 2014). However, virus isolation from the brain was not attempted in the marmosets study.

Consistent with an acute, robust MERS-CoV infection, histopathological examination identified lungs as the main target tissue in MERS-CoV-challenged Tg⁺ mice. In addition to readily recognizable gross changes (**Fig. 4A**), microscopic lesions occurred as early as 2 dpi and it progressed to severe bronchointerstitial pneumonia with prominent inflammatory infiltrates of lymphocytes, macrophages, and neutrophils at 4 dpi (**Fig. 4B**). Although mild thickening of alveolar walls was present at 4 dpi, edema and/or fibrin deposition was not detected in pulmonary interstitium. Other than a mild perivascular cuffing in a single mouse, pathological change was not detected in the brain even at 4 dpi when robust viral replication was detected (**Fig. 4C and Fig. 3**). Similarly, no pathological changes were identified in heart, liver, spleen, kidneys, and intestines.

In summary, the data presented here shows the successful establishment of a transgenic line of mice expressing hCD26/DPP4 and characterization of these mice as a lethal small-animal model for MERS-CoV infection and disease. Not only these Tg⁺ mice support robust MERS-CoV infection, but they also develop clinical manifestations and death within a week after infection. We believe that this newly established transgenic mouse model will be useful as an additional model for studying the pathogenesis of and evaluating the efficacy of preventive and therapeutic agents for MERS-CoV infection and disease.

CHAPTER IV: CHARACTERIZATION AND DEMONSTRATION OF THE VALUE OF A LETHAL MOUSE MODEL OF MIDDLE EAST RESPIRATORY SYNDROME CORONAVIRUS INFECTION AND DISEASE

Introduction

Although our globally expressing hCD26/DPP4 transgenic mice are highly permissive to MERS-CoV infection and disease, the acute onset of severe morbidity and mortality makes it difficult to fully investigate the pathogenesis, host immune responses, and immunity associated with MERS-CoV infection and disease. By mice starting to die at day 5 pi it makes certainly difficult to develop a study design due to the limited number of days they remain alive. As an example to illustrate this, we can mention that in order to study adaptive immune response, it is needed from 4–7 before the initial adaptive immune response takes effect. To further develop this transgenic mouse model for MERS studies, we determined the 50% lethal dose (LD₅₀) and 50% infectious dose (ID₅₀) of MERS-CoV and studied the tissue distribution of viral infection and histopathology in the hCD26/DPP4 Tg⁺ mice challenged with a much lower, dose of MERS-CoV. Additionally, we show that these transgenic mice can be used as a robust preclinical model for evaluating the efficacy of vaccines and antivirals against MERS.

Results

Determination of LD₅₀ and ID₅₀

To characterize our mouse model further, we determined the 50% lethal dose (LD₅₀) and 50% infectious dose (ID₅₀) of MERS-CoV by i.n. inoculation of groups of Tg⁺ mice with 10¹ to 10⁶ TCID₅₀ of MERS-CoV in the first experiment. We observed that mice receiving a

dose from 10^2 to 10^6 TCID₅₀ succumbed to infection (100% mortality), and with an increase in the number of days the mice survived as the inoculum dose was reduced. Weight loss was extreme ($\geq 20\%$) for dosages of 10^3 and higher; all mice that were given a dose of 10^2 died, but weight loss was 8% or less. Only 5 of 8 mice given a dose of 10^1 died; deaths occurred between 8 to 13 dpi, and weight loss was only 4% (**Experiment 1; Table 2**). All of the surviving mice continued to appear healthy up to 21 dpi when the experiment reached the study endpoint.

In a second experiment, we further assessed the LD₅₀ and ID₅₀ of the MERS-CoV. Four groups of four Tg⁺ mice were challenged (i.n.) with 2-fold decrements of MERS-CoV

Table 2. Determining the 50% lethal dose (LD₅₀) and infectious dose (ID₅₀) of MERS-CoV in hCD26/DPP4 transgenic mice

Experiment	Challenge Dose (TCID₅₀/mouse)	No. Deaths / No. Challenged (% Survival)	Day of death post challenge	No. infected / No. tested (% infected)^a
1	10^6	8/8 (100)	4-6	NA ^b
	10^5	4/4 (100)	5-7	NA
	10^4	4/4 (100)	5-8	NA
	10^3	4/4 (100)	6-10	NA
	10^2	8/8 (100)	6-12	NA
	10^1	5/8 (62.5)	8-13	ND ^c
2	10^1	2/4 (50)	9,10	2/2 (100)
	5	1/4 (25)	9	3/3 (100)
	2.5	0/4 (0)	NA ^a	3/4 (75)
	1.25	1/4 (25)	10	3/3 (100)

a. Infection determined by serum antibody response in neutralization a/o ELISA tests.

b. Not applicable (NA)

c. Not determined (ND)

NOTE: Estimated LD₅₀ and ID₅₀ are 10 and < 1 TCID₅₀, respectively.

starting with 10 TCID₅₀ i.e. 10, 5, 2.5, and 1.25 TCID₅₀ of virus. Although none of the infected mice exhibited any significant weight loss; two mice died (one each on days 9 and 10) in group infected with 10 TCID₅₀ and one mouse each died in group infected with 5 or 1.25 TCID₅₀, whereas all mice challenged with 2.5 TCID₅₀ of MERS-CoV survived without

Table 3. Determining infectious dose (ID₅₀) of MERS-CoV in hCD26/DPP4 transgenic mice			
Experiment	Challenge Dose (TCID₅₀/mouse)	Number of mice per group	% of mice positive for ELISA IgG antibody
3	10 ¹	6	4/6 (67%)
	10 ⁰	6	5/6(83%)
	10 ⁻¹	6	6/6(0%)
	10 ⁻²	6	6/6(0%)

any clinical illness (**experiment 2; Table 2**). From the data in **Table 2**, we estimated the LD₅₀ and ID₅₀ of MERS-CoV for our transgenic mouse model to be 10 and <1 TCID₅₀, respectively, further emphasizing the extreme susceptibility of hCD26/DPP4 transgenic mice to MERS-CoV infection and disease. With a third follow-up experiment by using inoculums of 10-fold downward dilutions of 10, 10⁻¹, 10⁻², 10⁻³ TCID₅₀, we were able to further refine the LD₅₀ and ID₅₀ doses determinations as 4.6 TCID₅₀ and 0.32 TCID₅₀, respectively (**Table 3**).

Infection-induced immune response and immunity to re-challenge with MERS-CoV.

From the second experiment described above for the LD₅₀ and ID₅₀ studies (**Experiment 2; Table 2**), all except one surviving mouse developed MERS-CoV S1 protein-specific IgG by 21 days post-infection, with ELISA titers of 1:400 to 1:800, (**Table 4**). We subsequently challenged (i.n.) these survivors at 35 dpi, along with two naive Tg⁺ mice, with 10³ TCID₅₀ (100 LD₅₀) of MERS-CoV to determine if they are immune to a

lethal infection dose. While both the naive mice lost more than 20% body weight and succumbed to infection within 10 dpi, all mice that had survived the prior low-dose challenge, including the one that failed to exhibit a serum antibody response, were immune to the lethal challenge and survived without significant weight loss for more than 3 weeks after the challenge. The rechallenged mouse without serum antibody in the standardized test ELISA antibody results for lower-endpoint criteria, less than 1:100. Thus, previous infection with a nonlethal dose of MERS-CoV is sufficient to induce immune responses that fully protect Tg⁺ mice against lethal infection.

Table 4. Serum Antibody titers to MERS-CoV in survivals of initial challenge and their response to re-challenge				
Initial challenge dose (TCID₅₀)	Number of survivors	Serum antibody responses^a		Death or wt loss on rechallenge^d
		Neutralizing antibody^b	ELISA IgG antibody^c	
10 ¹	2	< 10, 10	800,800	0/2
5	3	10, < 10, 20	800,400,800	0/3
2.5	4	20, 20, < 10, 20	400, 400,<100, 400	0/4
1.25	3	< 10, 10, < 10	400,400,400	0/3

a: Antibody responses were determined at day 21 p.i.

b: The highest dilution of sera that completely inhibited CPE formation in 100% of infected Vero E6 cultures (NT₁₀₀)

c: The highest dilution of sera with MERS-CoV S1-specific antibody with a mean optical density (OD) ≥ 2 standard deviation (SD) greater than the mean for naïve mice

d: Re-challenged with 100 LD₅₀ (10³ TCID₅₀) of MERS-CoV at day 35 after the initial infection. Two out of two simultaneously challenged naïve Tg⁺ mice exhibited severe weight loss (> 20%) and death occurred within 10 days p.i.

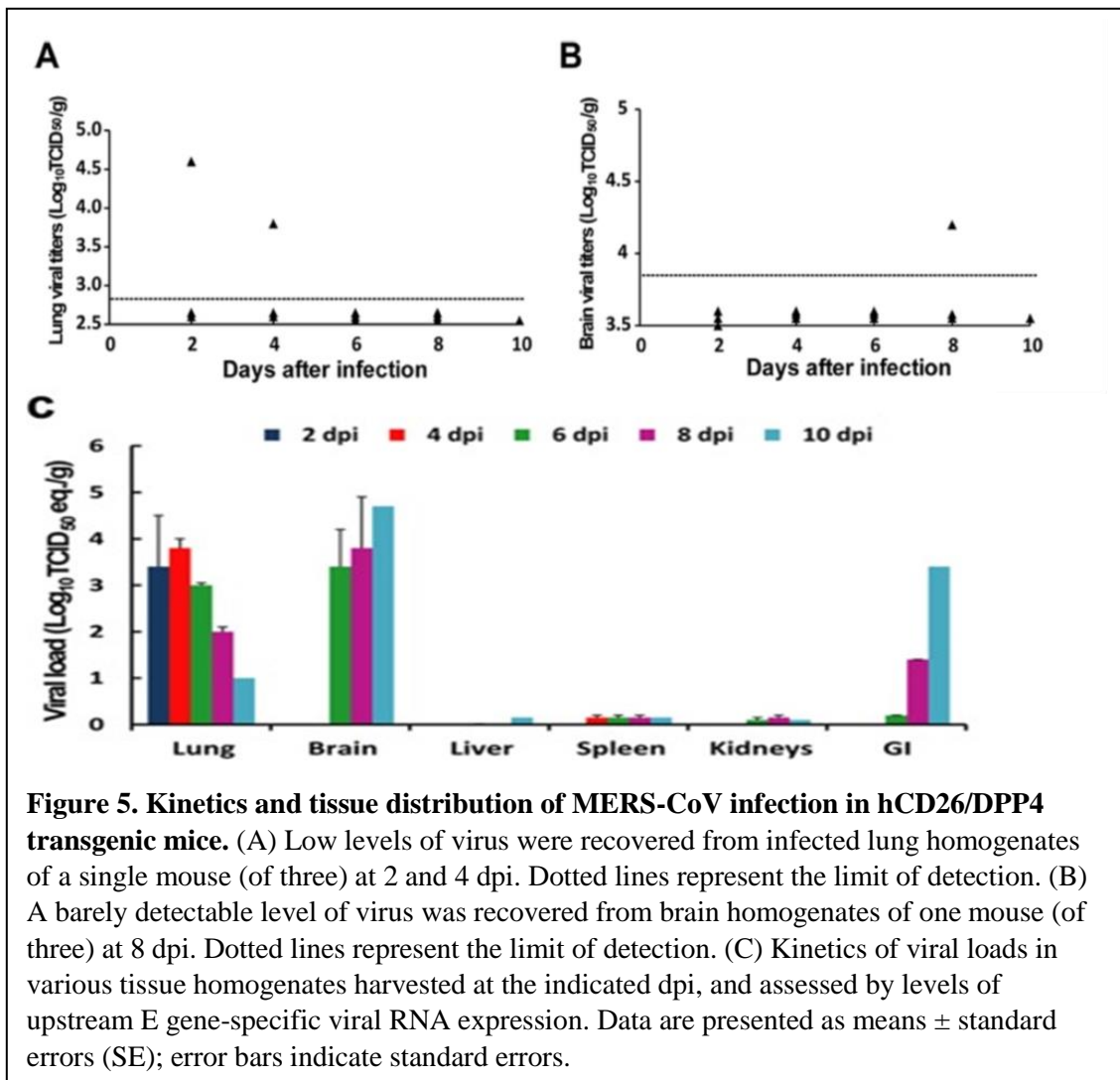
Kinetics of and tissue distribution of viral infection in hCD26/DPP4 Tg⁺ mice challenged with 10 LD₅₀ of MERS-CoV.

To avoid overwhelming the mice with MERS-CoV, we selected 10 LD₅₀ as the potential working dose for future studies of pathogenesis as well as evaluation of antiviral therapies. We have shown that Tg⁺ mice challenged (i.n.) with 10⁶ TCID₅₀ of MERS-CoV suffered profound weight loss of ≥ 20% with 100 % deaths within 6 dpi. While infectious virus could be readily recovered from the lungs and brain and progressive pneumonia with extensive infiltration of inflammatory cells was seen, no histopathological lesions were identified in the brain of infected mice.

In contrast to the acute, extensive weight loss and mortality seen with high dose infection, a lower dose of 10 LD₅₀ (~100 TCID₅₀) MERS-CoV exhibited a maximum of only 8% weight loss before death. In contrast to the consistent recovery of ≥ 10⁷ TCID₅₀/g of infectious virus from the lungs of mice inoculated with 10⁵ LD₅₀ (10⁶ TCID₅₀), a much lower titer of virus (~10^{4.6} TCID₅₀/g) was detected in the lungs of only a single mouse at 2 and 4 dpi (**Fig. 5A**). Moreover, we detected only approximately 10^{4.2} TCID₅₀/g of infectious virus from the brain of a single mouse at 8 dpi (**Fig. 5B**). IHC failed to reveal the expression of viral antigens in lung and brain tissues including those positive for infectious virus. Consistent with those inoculated with 10⁶ TCID₅₀ of MERS-CoV, we were unable to faithfully recover any infectious virus from other tissues, including liver, spleen, kidneys, and intestines from the low-dose challenged mice.

Although infectious virus could be detected only sporadically, RT-qPCR indicated consistent expression of viral RNA, especially in lungs and brains (**Fig. 5C**). All lung specimens collected over time were positive for viral RNA, with the highest level detected

at 4 dpi. In contrast, viral RNA was undetectable in brains until day 6; however, expression increased thereafter, reaching the highest level at 10 dpi. Although attempts to isolate virus from the gastrointestinal (GI) tract were unsuccessful, viral RNA was detected at day 6 and increased thereafter, reaching a level equivalent to $10^{3.4}$ TCID₅₀ eq/g at 10 dpi (Fig. 5C). Viral RNA was detectable in all other tissues over time but at low levels. Taken together, these results indicate that, despite differences in the kinetics and intensities of viral infection,



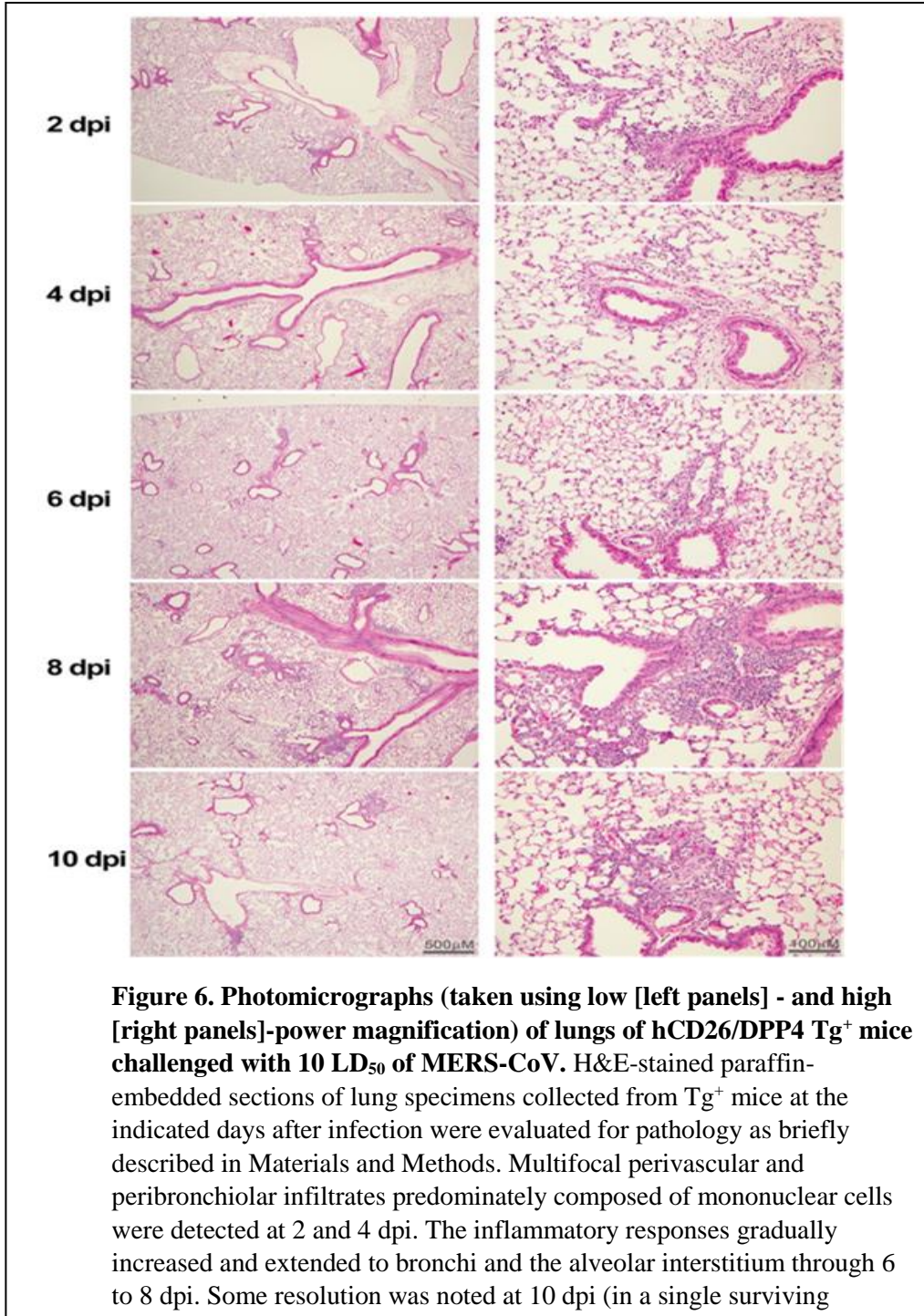
lung, brain, and, possibly GI tracts appear to be the major tissues supporting MERS-CoV infection in Tg⁺ mice.

Histopathology of hCD26/DPP4 transgenic mice infected with 10 LD₅₀ of MERS-CoV.

In contrast to the profound gross lesions detected solely in the lungs of animals challenged with 10⁶ TCID₅₀ of MERS-CoV, no gross organ pathology was noted in the lungs, brain, and other organs of animals sacrificed at 2-day intervals for virological and histological evaluations. However, microscopic lesions were noted on different days after infection in lungs, in brain, and, to a lesser extent, in liver but not in spleens, kidneys, and small intestines, etc.. As shown in **Fig. 6**, lung histopathology of infected mice primarily showed mild and multifocal perivascular, peribronchial, and interstitial infiltrations with mononuclear cells at 2 and 4 dpi. The intensity of these pulmonary infiltrates was slightly increased in 2 of 3 animals and moderately increased in 1 animal at 6 dpi and reached the maximum in all 3 animals sacrificed at 8 dpi. A decreasing trend of the pulmonary inflammatory response was seen in the sole survivor at 10 dpi, suggesting that some resolution was under way.

In contrast to the earlier high-dose viral challenge (10⁶ TCID₅₀/mouse) (**Figure 4**), in which an inconsistent mild perivascular effect was the only pathological change seen in infected brains, mice infected with 10² TCID₅₀/mouse (10 LD₅₀) developed progressive inflammatory responses. As shown in **Figure 7**, no abnormalities could be detected in brain stem tissues at either 2 or 4 dpi. However, pathological changes consisting of perivascular cuffing, microglia activation, and apoptotic bodies that likely represent neuronal death were noted in brain stem tissues from 6 to 10 dpi. While no intracerebral pathology was seen in brain, mild meningitis was noted in cerebral tissues from 8 to 10 dpi. Focal mononuclear

infiltrations were noted in liver specimens collected at 6 to 10 dpi but not in those collected at 2 and 4 dpi; however, we did not detect definite pathology in kidney, small intestine, and spleen.



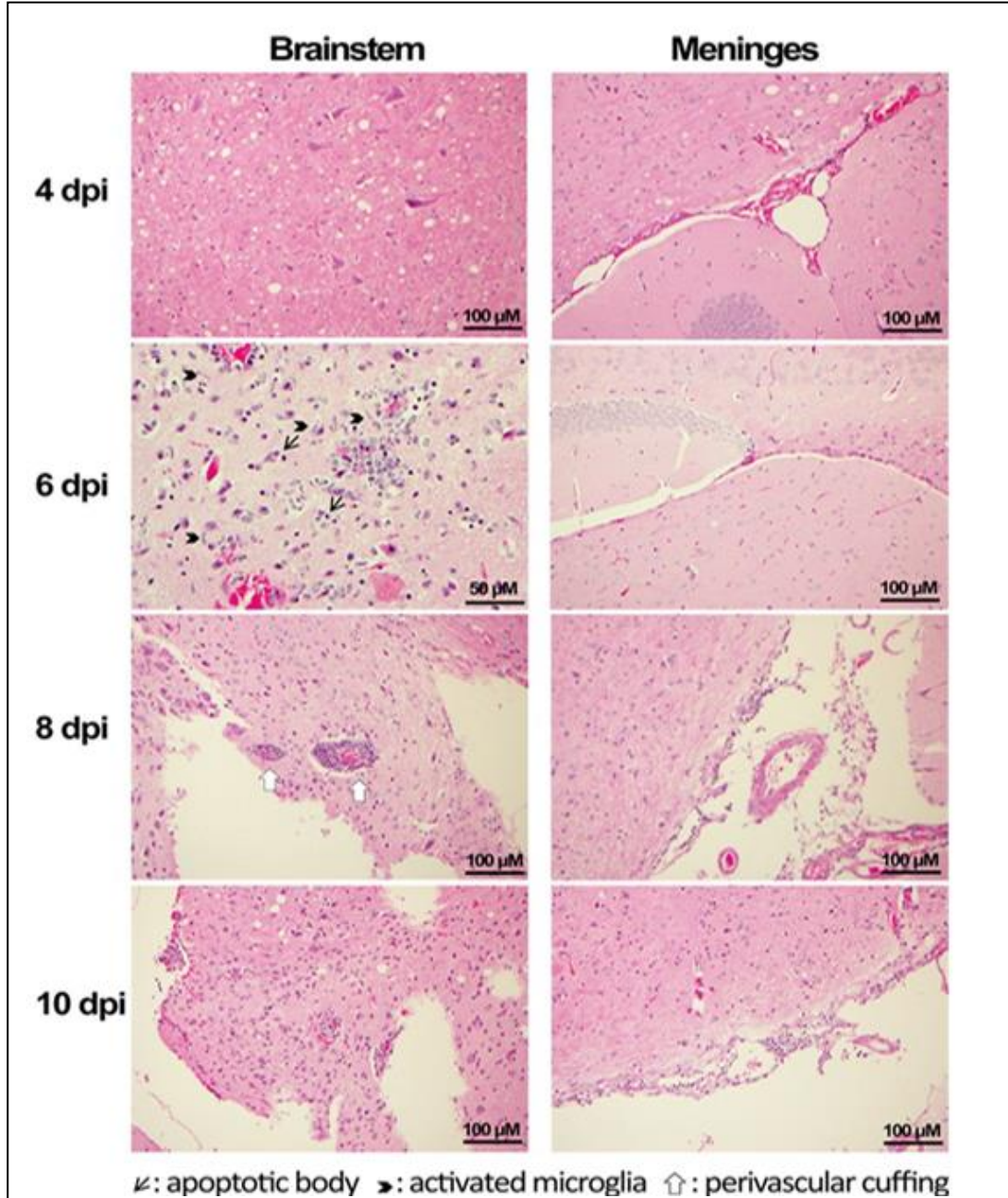


Figure 7. Photomicrographs (taken using high-power magnification) of brain stem and cortex of hCD26/DPP4 Tg⁺ mice challenged with 10 LD₅₀ of MERS-CoV. Brain tissues obtained from the infected mice described in the Fig. 6 legend were processed for assessing histopathology. No pathological lesions were seen at 2 and 4 dpi. However, pathological changes, including the presence of perivascular cuffing, apoptotic bodies, and activated microglia, were seen in the brainstem at 6 to 10 dpi. No intracerebral pathology was seen, but mononuclear cell collections in cortical meninges were seen at 8 and 10 dpi.

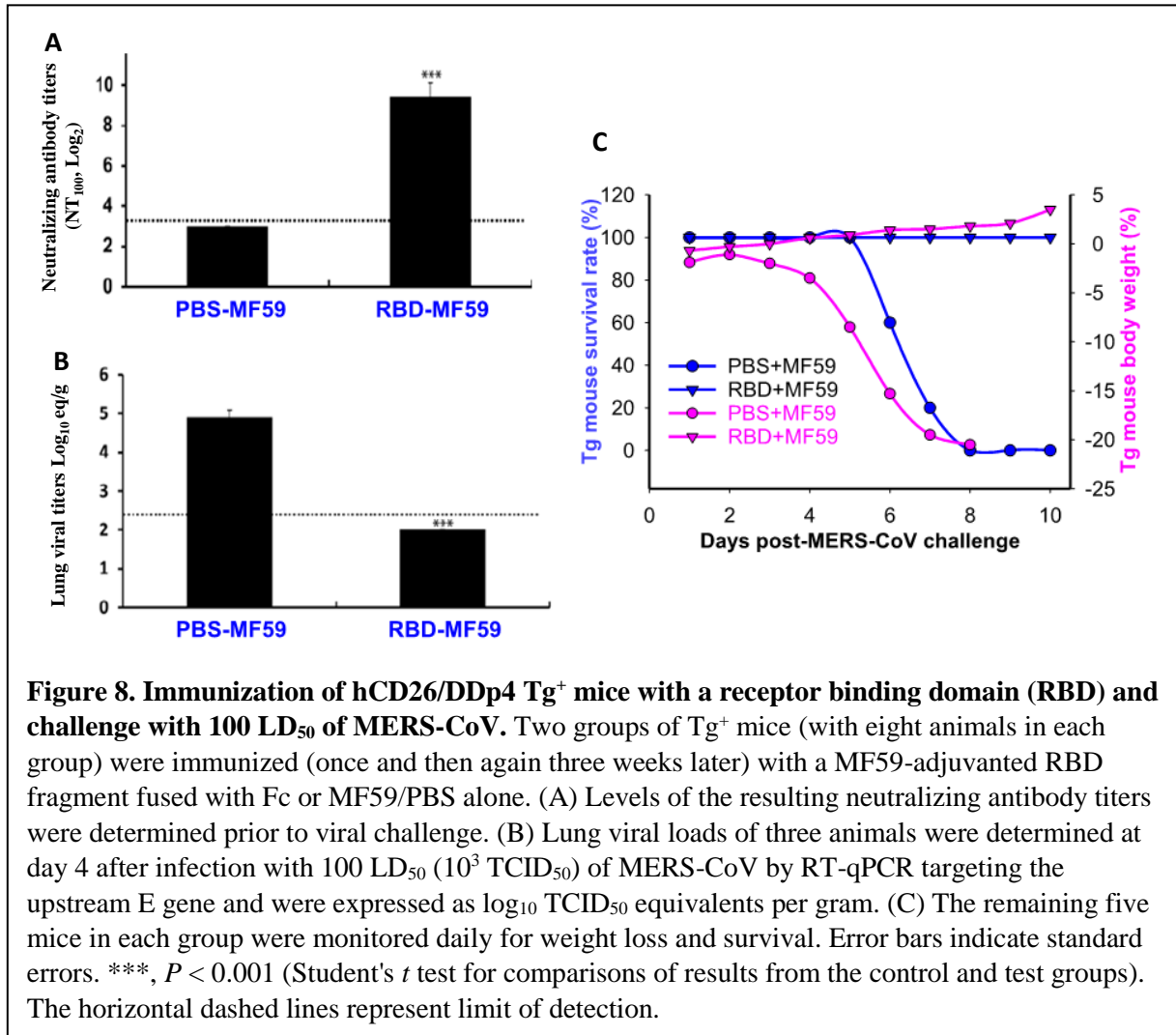
Use of hDPP4/CD26 transgenic mice as preclinical model for the development of vaccines and treatments for MERS.

After establishing LD₅₀ and ID₅₀ for MERS-CoV (**Tables 2**), we explored whether these Tg⁺ mice can be used as a small and economic model for the development of vaccines and treatments for MERS-CoV infection and disease. We evaluated the protective efficacy of a MERS-CoV receptor binding domain (RBD)-based subunit vaccine (S377-588-Fc) (Tang, Zhang et al. 2015, Wang, Shi et al. 2015, Zhang, Channappanavar et al. 2016), and a MERS-CoV-specific fusion inhibitor peptide (HR2M6) (Gao, Lu et al. 2013, Lu, Liu et al. 2014) against MERS-CoV infection in our transgenic mice.

1. Evaluation of the efficacy of S377-588-Fc as a subunit vaccine

As described in the section of methodology, sera of vaccinated mice were collected at day 10 after the second immunization for assessing immunogenicity in neutralizing antibody tests. As shown in **Figure 8**, consistent with the absence of any detectable neutralizing antibody response (< 1:10), mice given PBS/MF59, as controls, harbored ~ 10^{4.9} TCID₅₀ eq/g of MERS-CoV in their lungs harvested at day 2 after challenge (i.n.) with 100 LD₅₀ (10³ TCID₅₀) of MERS CoV. It was also accompanied by profound weight loss (≥ 20%) and uniform death with 100% mortality by 8 dpi. In contrast, those vaccinated with S377-588-Fc/MF59 elicited an average serum neutralizing antibody (NT₁₀₀) titer of ~1:800. None of the three vaccinated and challenged mice tested at 4 dpi had any recoverable infectious virus in lungs, whereas the remaining five vaccinated and challenged mice appeared to be “disease-free” as none suffered any weight loss. Based on these results, we concluded that the receptor binding domain protein vaccine, S377-588-Fc, induced serum neutralizing antibody to MERS-CoV and resulted in full protection against challenge with 100 LD₅₀ of

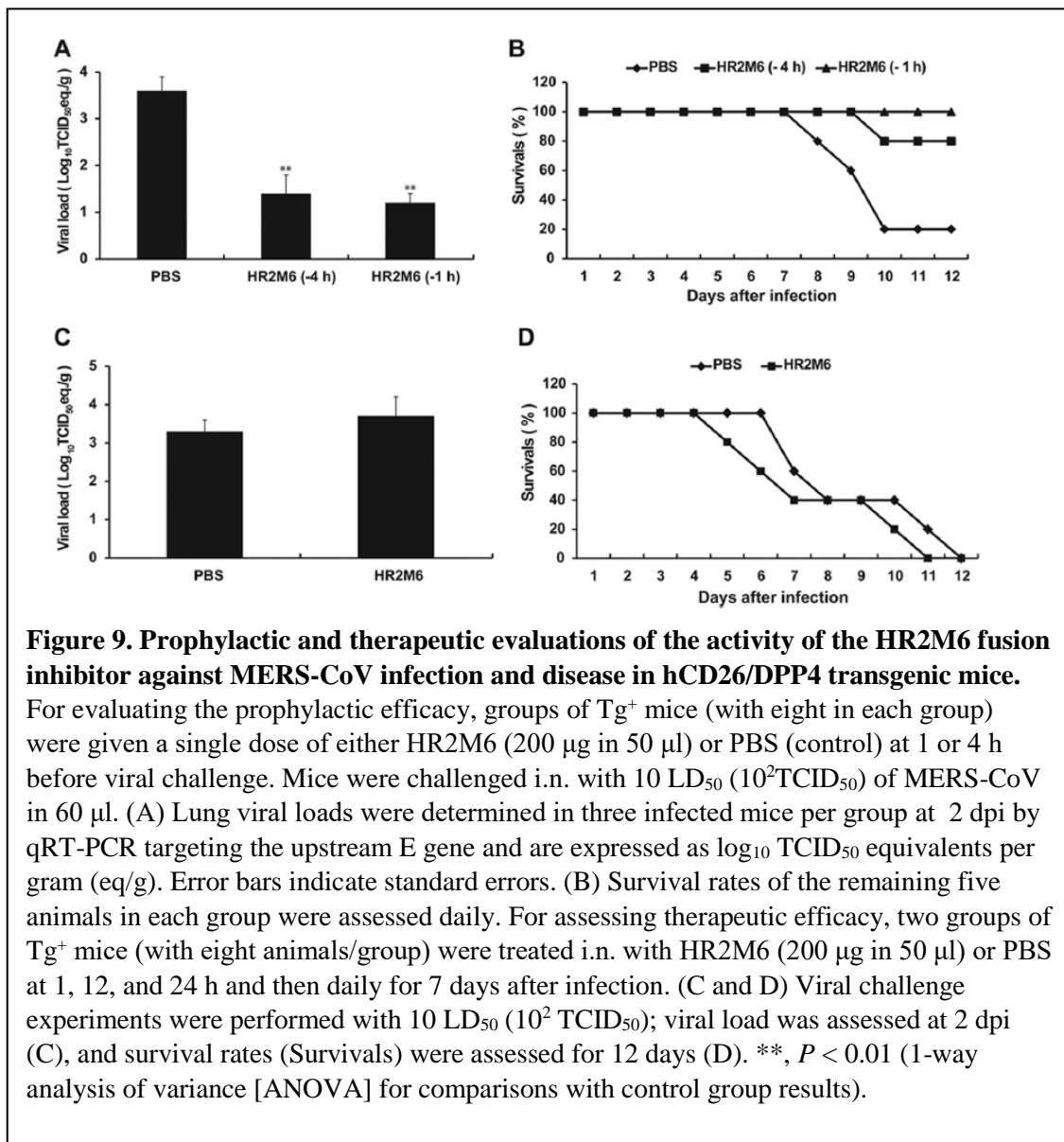
virus (**Fig. 8**). Importantly, these results clearly demonstrate the usefulness of our transgenic mice as a robust preclinical model for evaluating the efficacy of vaccine candidates for MERS.



2. Evaluation of the efficacy of the HR2M6 virus fusion inhibitor for prophylactic and therapeutic treatment.

As mentioned previously S protein is important for the binding and fusion process to the target cell membrane. Therefore, some of the studies intend to target some particular regions of the S protein in order to inhibit viral infection. It has been shown in the case of

some viruses, including MERS-COV that peptides derived from the HR2 domain (such as HR2P) can interact with the HR1 region in the S protein and inhibit the fusion of viral and target cell membranes. One of these peptides is HR2M6 which we decided to test in our model. Although no infectious virus could be recovered from challenged mice regardless of whether they were treated with HR2M6 or not, lung viral RNA titers were significantly reduced from 3.7 log₁₀ TCID₅₀eq/g in PBS-treated mice to 1.2 and 1.4 log₁₀ TCID₅₀ eq/g in those pretreated with HR2M6 at 1 and 4 h, respectively (**Fig. 9A**). All of the remaining five



mice and four of the five mice pretreated with HR2M6 at 1 and 4 h, respectively, were protected from death, whereas four of five PBS-treated mice succumbed to the infection (**Fig. 9B**). When evaluating the therapeutic efficacy of HR2M6, in contrast to the earlier report (Gao, Lu et al. 2013, Lu, Liu et al. 2014), we did not see any therapeutic benefit of HR2M6 as neither the viral loads nor the mortality rates were significantly reduced (**Fig. 9C and D**). Results obtained from additional Tg⁺ mice treated with this fusion inhibitor prior to and/or after exposure to different doses of MERS-CoV consistently indicated that HR2M6 was effective as a prophylactic but not as a therapeutic agent against MERS-CoV infection and disease in the Tg⁺ mouse. Hence, the utility of our mouse model for evaluating the efficacy of antiviral treatments against MERS-CoV has been demonstrated.

Discussion

As indicated in Chapter III, one lineage of the transgenic mice was selected and further evaluated. A 10⁶ TCID₅₀ i.n. dose of MERS-CoV strain EMC/2012 induced severe pneumonia leading to death in 5 to 6 days. Virus titer in lungs was highest on day 2 post-challenge, and was followed by dissemination to many other organs including the brain. Based on RT-qPCR assays, virus titer was highest in lungs on day 2 and brain on day 4 post-challenge. Both extensive gross lung pathology and microscopic lung pathology developed. Major histopathological changes in lungs were seen on day 4 but the brain had minor or no pathological changes despite the detection of high titers of virus and viral antigens in neurons and glial cells. The extensive infection and disease seen with MERS-CoV in our transgenic mouse model were similar to that reported in marmosets challenged with MERS-CoV (Falzarano, de Wit et al. 2014). A concern was that the challenge to our transgenic mice and the challenge to the marmosets might have represented overwhelming doses in very

susceptible animals that caused a very severe acute lung infection with dissemination to numerous organs. Although currently available clinical information is inadequate to exclude dissemination of MERS-CoV as a component of MERS-CoV pneumonia in humans, MERS is considered to be a respiratory infection and disease (Zaki, van Boheemen et al. 2012, Zumla, Hui et al. 2015).

We studied the effect of challenge dose in our transgenic mouse model to further characterize MERS-CoV infection and disease and to optimize conditions for the evaluation of vaccines and antivirals; we conducted studies to estimate ID₅₀ and LD₅₀. These studies yielded an estimated ID₅₀ of <1 TCID₅₀ and an LD₅₀ of 10 TCID₅₀ (**Table 2**). Thus, the initial challenge study with a dose of 10⁶ TCID₅₀ represented a challenge with more than 1 million ID₅₀ and 100,000 LD₅₀ of virus. This might be designated as an “overwhelming” dosage and suggests that this may have also been true for the marmoset study (Falzarano, de Wit et al. 2014).

Current data suggests that virus dissemination and infection of other organs may occur during MERS-CoV infection, particularly in those with severe disease. Virus has been detected in blood and urine of a MERS patient (Drosten, Seilmaier et al. 2013). Moreover, the receptor for MERS-CoV, CD26/DPP4 (Raj, Smits et al. 2014), is ubiquitous in human tissues and, presumably, in primates and humanized mice; its presence has been demonstrated in lung, kidney, GI tract, brain, and most (if not all) other organs (Gorrell 2005). Given access to an organ, virus infection may occur and yield virus and local abnormalities.

Initial reports of SARS emphasized lung disease, its severity, and problems in management (Nicholls, Poon et al. 2003, Denison 2004, Ding, He et al. 2004, Peiris, Guan

et al. 2004). Gastrointestinal infection and disease were reported commonly in early reports for MERS, but disease in other organs was not. However, subsequent reports of autopsies in cases of SARS-related deaths noted dissemination and a high frequency of central nervous system (CNS) disease, particularly in neurons (Ding, He et al. 2004, Gu, Gong et al. 2005, Xu, Zhong et al. 2005). It seems possible that an encephalopathy or an encephalitis type of abnormality might have been missed in patients with severe lung disease. Mouse-adapted MA-15 strain of SARS-CoV in the hACE-2 receptor transgenic mouse models causes severe disease and death and exhibited SARS-CoV dissemination and presence of virus in the brain (McCray, Pewe et al. 2007, Roberts, Deming et al. 2007, Tseng, Huang et al. 2007). Thus, SARS-CoV appears to have a capacity for dissemination with infection and disease in other organs, including brain. In a report of three severe cases of CNS disease in association with MERS, the authors suggested that CNS disease might be missed among cases of severe disease in intensive care units with the use of sedation and neuromuscular blockade (Arabi, Harthi et al. 2015). These findings from SARS-CoV and MERS-CoV infections and diseases in humans suggest a need for caution in drawing conclusions about patterns of human infection and disease until a complete set of data are available. Similarly, data on animal model infections suggest that conclusions about the properties of a model should await a full characterization of the course of infection and disease in the model.

Although further refinement of our transgenic mouse model is desirable, a major value of a small-animal model of infection and disease of humans is in preclinical evaluation of infection and vaccine-induced immunity and of antimicrobials for prevention and treatment. Hence, we conducted a study of immunity induced in surviving mice in the ID₅₀/LD₅₀ determinations (**Table 2 and Table 4**) and a preliminary test of a candidate

vaccine and antiviral for MERS-CoV. Mice surviving infection had developed serum neutralizing antibody, and all were completely immune to challenge with 100 LD₅₀ of MERS-CoV (**Tables 2 and 3**). Similarly, a receptor binding domain protein vaccine, S377-588-Fc, induced serum neutralizing antibody to MERS-CoV and vaccinated animals were significantly protected from challenge with 100 LD₅₀ of virus (**Fig. 8**). Finally, although no benefit was seen with post challenge treatment in our test, we verified (**Fig. 9**) a previous report that i.n. administration of a MERS-CoV fusion inhibitor peptide, HR2M6, before virus challenge prevented disease and death after challenge (Channappanavar, Lu et al. 2015) Thus, the utility of our MERS-CoV model for studies of immunity and for the development of vaccines and antivirals has been demonstrated.

Although we have not yet developed a model of infection not leading to death, the ID₅₀ data available for our virus and test system ensure that an effort would be successful. Variations in the severities and patterns of infection and disease in a MERS-CoV model are potentially important, as human infection and disease apparently span a spectrum from infection with little or no disease to overwhelming disease and death (Al-Tawfiq 2013, Zumla, Hui et al. 2015). Currently available data indicate that our transgenic mouse model can completely span this spectrum of infection and disease. To have both an infection model and a lethal model of MERS-CoV infection is highly desirable.

CHAPTER V: FINAL DISCUSSION

Human MERS-CoV infections

Human MERS-CoV infections show a broad spectrum of disease severity ranging from asymptomatic to progressive, fatal pneumonia and renal or multiorgan failure, in some cases. The asymptomatic cases mostly occur in healthy and immunocompetent individuals,

and are being reported more frequently due to improved surveillance (Centers for Disease and Prevention 2013, Drosten, Meyer et al. 2014). Median incubation period to develop MERS is 5 days. Symptoms include coughing and shortness of breath along with fever, headaches, fatigue, myalgia, arthralgia, vomiting and diarrhea (Birmingham, Chand et al. 2012, Guery, Poissy et al. 2013, Omrani, Matin et al. 2013, Tsiodras, Baka et al. 2014). MERS is usually a lower respiratory tract infection; however, in some cases, sore throat and rhinorrhea (upper respiratory tract) also occur (Cunha and Opal 2014, Oboho, Tomczyk et al. 2015). Patients with comorbidities such as diabetes, renal and cardiovascular diseases are more prone to develop severe disease (Assiri, McGeer et al. 2013, Guery, Poissy et al. 2013, Who Mers-Cov Research 2013). Sputum and bronchoalveolar lavage are the most reliable samples for diagnosis due to their high viral loads (Guery, Poissy et al. 2013, Cunha and Opal 2014). However, MERS-CoV can sometimes be detected in oropharyngeal or nasal swabs, serum, blood, urine, and feces (Guery, Poissy et al. 2013, Hijawi, Abdallat et al. 2013, Memish, Zumla et al. 2013, Drosten, Meyer et al. 2014).

The first autopsy performed on a MERS fatal human case helped us understand the pathogenesis of MERS-CoV infection (Ng, Al Hosani et al. 2016). While not weighing the organs and a delay of 10 days before autopsy was performed (Walker 2016) might have impacted the findings, primary target organ (lung) as well as the cells (pneumocytes, multinucleated epithelial syncytial cells, and bronchial submucosal glands) were successfully identified by using MERS-CoV antigen-specific IHC and EM (electron microscopy). The likely source of viral shed in respiratory secretions that ultimately led to human-to-human transmission could be the bronchial submucosal glands. While lesions in the lungs and submucosal glands were observed, no pathology was seen in CNS or kidneys.

Moreover, no viral antigen was detected in liver, spleen, lymph nodes, small intestine, colon, and kidney. However, IHC is not sensitive enough to detect virus infection if the viral load in that particular organ is less than 10^4 TCID₅₀/g of tissue. While lungs in MERS-CoV patients have high viral loads, loads in other tissues may not be enough to be detected by IHC. A RT-qPCR-based assay would have been a better alternative due to its higher sensitivity.

In contrast to the viral RNA seen in the urine of some human MERS-CoV infections, no renal evidence of MERS-CoV infection and disease was seen in this patient. Therefore, acute renal failure observed in this particular patient was not directly caused by MERS-CoV infection and was probably due to cytokine dysregulation or hypoperfusion. While viral RNA has also been detected in stools of some patients, no evidence of intestinal MERS-CoV infection was seen. Therefore, the gastrointestinal symptoms such as nausea, vomiting, abdominal pain might have not been due to direct effect of GI tract infection. In addition, some of the in vitro studies such as in vitro infection of macrophages and dendritic cells (Chu, Zhou et al. 2016) were not supported by the autopsy report.

Most of the animal models of MERS-CoV infection and disease were developed before the first autopsy report, and apparently, these models do not recapitulate all the features reported from this autopsy. Thus, even though the first autopsy provided a lot of important information, more autopsy studies are required to firmly determine the organ involvement and pathology of human MERS-CoV infection. For more careful studies and delineation of MERS-CoV pathogenesis, in vitro as well as in vivo model systems will continue to be useful.

Animal models for MERS-CoV infection and Disease

Little is known about the pathogenesis of human MERS-CoV infections and no effective vaccines or antivirals against this virus are currently available. Lack of animal models to study this disease has significantly impaired MERS research. Thus, animal models are needed for studying MERS-CoV infection and for the evaluating prophylactic and therapeutic interventions. Various MERS-CoV animal models including mice, rabbits, camels, alpaca and NHPs such as Rhesus macaques and Marmosets have been described below.

Non-human primates (NHP)

Nonhuman primates, such as rhesus macaques and marmosets, are naturally permissive to MERS-CoV infection and disease (de Wit, Rasmussen et al. 2013, Falzarano, de Wit et al. 2014, Chan, Yao et al. 2015). Rhesus macaques can model mild human cases of MERS-CoV infection, as in the cases observed in healthy immunocompetent individuals (de Wit, Rasmussen et al. 2013). However, this model differs from human cases by relatively shorter incubation period, a larger infectious dose and infection of alveolar macrophages (Walker 2016). The main advantage in the use of Rhesus macaques as model for MERS-CoV relays in the fact that they are non-human primates, therefore they highly resemble human immune response. The principal disadvantages would be that they have shown to be models of only mild infection and disease; they are also expensive with limited availability. Additionally, they also have complex husbandry requirements (large ABSL3 facilities) (Table 5).

On the other hand, we have Common marmosets that are considered a better model for the severe MERS-CoV human infections since they develop fatal respiratory disease with

pulmonary damage (Falzarano, de Wit et al. 2014). However, they also have shorter incubation period, require a larger infectious dose, infection of mainly type 1 pneumocytes and alveolar macrophages, and disseminated infection (Walker 2016). Acute renal failure has been reported in some cases of human MERS-CoV infections. In support to this, viral RNA was detected in the kidneys of common marmosets. However, there was no evidence of renal disease suggesting that renal failure is not associated with direct effect of MERS-CoV infection. Also, a study by Chan's group tested the efficacy of Lopinavir/Ritonavir or Interferon- β 1b treatments for MERS-CoV infection and noticed severe disease in Marmosets (Chan, Yao et al. 2015) (**Table 5**).

Contrary to the lethal disease find in the studies mentioned above, Johnson et al. found sub lethal, mild-to-moderate respiratory disease in marmosets infected with 5×10^6 TCID₅₀ of MERS-CoV via i.t. route. They were also not able to recover infectious virus, and detect viral RNA by RT-qPCR or viral antigens by IHC (Johnson, Via et al. 2015). They reported mild radiographic evidence of disease in the lungs, multifocal interstitial pneumonia with a scarce number of syncytial cells. All the reports using marmoset as model for MERS-CoV infection were able to find respiratory disease; however, the severity of it as well as the virology results were different. Therefore, further studies are required to develop a NHP model that is consistently severe (Walker 2016). It can be speculated that the different disease outcome observed by Johnson et al., could be due to some of the following aspects: different age of the Common marmosets as well as the source of them. Different dose of virus used for challenge. And also, it is possible that many number of passages of the strain used by Johnson could have resulted in mutations making it an attenuated strain.

As in the cases of Rhesus macaques, Common marmosets have the advantage of being a NHP, therefore having respiratory and immune systems that are more similar to those of humans. Another advantage in this case is that severe infection/disease has been reported by some, but not others, which turns into a disadvantage since there is a lack of reproducibility of the disease outcome comparing the studies with Marmosets. And of course marmosets have the limitation of being expensive with limited availability, and they are harder to handle in biocontainment (require large ABSL3 facilities) (**Table 5**).

New Zealand white rabbits

New Zealand white rabbits were infected both, intranasally with 1×10^6 TCID₅₀ and intratracheally with 4×10^6 TCID₅₀ of MERS-CoV (Haagmans, van den Brand et al. 2015). No clinical signs or gross lesions were observed; microscopic lesions were observed in the upper and lower respiratory tract at 3 and 4 dpi. MERS-CoV RNA was detected in several upper and lower respiratory tract tissues. Infectious virus was detected in nasal swabs up to 7 dpi (Haagmans, van den Brand et al. 2015). New Zealand white rabbits are models that represent what happens in subclinical MERS-CoV infection in humans. They remain asymptomatic and only mild respiratory lesions were detected. However, they could be of much use for studies of MERS-CoV transmission given the fact that they shed the virus from their upper respiratory tract.

In another study, New Zealand White rabbits were used to test the efficacy of a human monoclonal antibody (hmAb), named m336 (Houser, Gretebeck et al. 2016), which was previously shown to have potent in vitro neutralizing activity against MERS-CoV (Ying, Du et al. 2014). Rabbits were pretreated intravenously (i.v.) and intranasally at 1 day prior and 1 day after challenge with 10^5 TCID₅₀ of MERS-CoV. One day after the antibody

administration and on the day of the necropsy, serum samples were collected. Euthanasia of the rabbits was performed at day 1 and 3 post-infection. A significant decrease in the viral RNA (within 1 day of infection, a 40 to 9000-fold reduction was observed), as well as virus-related pathology in the lungs of the animals, was seen. In the rabbits with low viral RNA, IHC showed almost no viral antigen. Neutralizing antibodies were detected in the serum for several days in rabbits treated via i.v. route, while no antibodies were detected in the serum of rabbits treated via i.n. route. This implies that the antibody administered topically remained in the respiratory tract and accounted for the greater efficacy of the i.n. route as compared to the i.v. route as it was demonstrated previously (Leyva-Grado, Tan et al. 2015). Post-infection therapy was not effective since no reduction in the viral RNA titers was observed.

In conclusion, we can say that the main advantages of the New Zealand white rabbit are that they are readily available and have low cost and. Also, they are easily handled. The disadvantage lies that they only develop mild disease limited to the upper respiratory tract (URT) (**Table 5**)

Dromedary Camels

As mentioned previously dromedary camels play an essential role in the transmission of MERS-CoV (Hemida, Perera et al. 2013, Reusken, Ababneh et al. 2013, Reusken, Haagmans et al. 2013, Alagaili, Briese et al. 2014, Azhar, El-Kafrawy et al. 2014, Haagmans, Al Dhahiry et al. 2014, Hemida, Chu et al. 2014, Memish, Cotten et al. 2014, Meyer, Muller et al. 2014, Nowotny and Kolodziejek 2014). To understand the effects of MERS-CoV infection in camels, some studies have been performed. In one of the studies, three camels were inoculated via i.t.; i.n. and ocular with 10^7 TCID₅₀ of MERS-CoV (Adney,

van Doremalen et al. 2014). The animals developed mild respiratory disease with nasal discharge, which agrees with the field surveillance studies (Hemida, Perera et al. 2013, Azhar, El-Kafrawy et al. 2014, Haagmans, Al Dhahiry et al. 2014, Nowotny and Kolodziejek 2014). Viral RNA was detected in large quantities in the nasal swabs from each of the three animals. Infectious virus was detected until day 7pi, and the viral RNA until day 35 pi in the last animal that was euthanized on day 42 (Adney, van Doremalen et al. 2014). The other two camels were euthanized on day 5 and 28 p.i. Data of naturally infected dromedary camels (Alagaili, Briese et al. 2014, Azhar, El-Kafrawy et al. 2014, Briese, Mishra et al. 2014, Haagmans, Al Dhahiry et al. 2014, Hemida, Chu et al. 2014) has shown the similar route of virus shedding. MERS-CoV was not detected in feces or urine, which also correlates with the field findings (Azhar, El-Kafrawy et al. 2014, Hemida, Chu et al. 2014). This study suggests that both camel-to-camel and camel-to-human transmission likely occur through direct contact or large droplets. Predominant site of MERS-CoV replication in camels is the respiratory epithelium of the nasal turbinates (Upper respiratory tract). Neutralizing antibodies were detected from day 14 until day 42 with a maximum neutralizing titer of 640 at day 35 pi (Adney, van Doremalen et al. 2014).

Dromedary camels have also used to test the efficacy of an orthopoxvirus-based vaccine. The results demonstrated that this vaccine was able to reduce virus excretion after MERS-CoV infection (Haagmans, van den Brand et al. 2016) (**Table 5**).

While dromedary camels are considered natural host for MERS-CoV and seem to be good model for studies of MERS-CoV transmission, they are expensive, and their availability is limited. More importantly, they only developed mild disease limited to URT (**Table 5**). Also, as in the case of NHP there is need of large ABSL-3 facilities for the studies.

Alpaca

Since the use of dromedary camels as animal models for study MERS-CoV can be difficult due to their larger size, higher cost and high-containment requirements, Adney's group proposed the use of alpaca due to their availability in the United States and smaller size. They infected 3 alpacas intranasally with 10^7 PFU of MERS-CoV. Two days later, another group of 3 alpacas were introduced into the same room and housed together with the infected animals. Infectious virus was detected in the 3 experimentally infected and in 2 of the 3 in-contact alpacas. All the 6 alpacas seroconverted and they were rechallenged with the same dose of virus, 70 days later after the first challenge. At the time of the rechallenge, another group of 3 alpacas was used as infection controls and also to evaluate tissue distribution of the virus. The initially infected alpacas were completely (3 out of 3) protected against reinfection; however, in the contact animals, the protection was partial against reinfection. Animals from the control group were necropsied on day 5 after infection and showed presence of the virus in the upper respiratory tract. As in the dromedary camels, none of the alpacas showed any increase in body temperature and their activity level and food intake were unchanged. In contrast to camels, none of the alpacas showed nasal discharge. Thus, alpacas can be a good model for efficient virus replication and animal-to-animal transmission and might be useful surrogates for the dromedary camels (Adney, Bielefeldt-Ohmann et al. 2016).

Cramer's group also used alpacas to conduct a challenge and rechallenge study. They primary were looking to determine if viral shedding was observed after reinfection, and to evaluate the presence of antibodies for protection. They only used 3 alpacas, which were challenged oronasally with 10^6 TCID₅₀ of MERS-CoV. Animals were monitored for

21 days, and then they were re-challenged with the same amount of virus used for the initial infection. After re-exposure to the virus, alpacas were monitored for 14 days. One alpaca was euthanized on day 33 and the other two on day 35 after the primary infection. The alpacas did not show any symptom of the disease, except for one of them that presented with increase temperature on days 17 to 20 pi. However, postmortem examination concluded that this was likely caused by extended abnormalities from the stomach to the umbilicus (Crameri, Durr et al. 2016).

They successfully recovered virus from oral and superficial nasal samples until day 12 pi while deep nasal swabs were positive until day 10 pi. After rechallenge, viral RNA was not detected from any sample. Antibodies were detected by Luminex in all the 3 alpacas starting at day 10 or 12; however, neutralizing antibodies were detected only in 2 out of the 3 alpacas, starting from day 10 (alpaca 2), day 21 (alpaca 1) and no antibodies from alpaca 3. Together these data showed that alpacas shed infectious virus after oronasal infection and that their immune response to the primary infection prevented virus shedding after rechallenge. Therefore, alpaca might be a useful model that could contribute to the development and testing of vaccine candidates and be useful tools for virus transmission studies (Crameri, Durr et al. 2016).

Alpacas have the major advantages that they have shown to be a good model for transmission studies and reagents are readily available; however, the main disadvantage is that they only develop mild disease limited to URT (similar to camels) (**Table 5**). Also, as in the case of NHP and camels there is need of large ABSL-3 facilities for the studies.

Mice models of MERS-CoV infection

Small-animal models are needed to provide the numbers of animals required for controlled and extensive studies of pathogenesis and immunity as well as for the development of vaccines and antivirals. Mice are the most desirable small animal for this because of availability and a thorough knowledge base of their genetics and immunology. Unfortunately, mice and the standard small animals (hamsters, and ferrets) lack the functional MERS-CoV receptor (human CD26 [hCD26]/DPP4) and are not susceptible to infection (de Wit, Prescott et al. 2013, Coleman, Matthews et al. 2014, Raj, Smits et al. 2014). To overcome this problem, different mice models have been developed over time. The first mice model developed was the hDPP4-transduced mouse model (Zhao, Li et al. 2014). The second was our model, which actually is the first humanized model generated for the study of MERS-CoV infection and disease (Agrawal, Garron et al. 2015), which we further characterized as a lethal model and tested its usefulness for the evaluation of vaccine candidates and antiviral therapy (Tao, Garron et al. 2015). The third mouse model, the Regeneron Knock-in (KI) model, (Pascal, Coleman et al. 2015), for MERS, was reported by Pascal et al and was used for studying host immune response (T cell and macrophage) (Coleman, Sisk et al. 2017). These were followed by the Codon-optimized hDPP4 transgenic mice (Zhao, Jiang et al. 2015), the transgenic mouse model (Li Kun's group-IOWA) (Li, Wohlford-Lenane et al. 2016), genomic engineered mice model (288/330+/+) (Cockrell, Yount et al. 2016) and the DPP4 KI model (Li Kun's group-IOWA) was reported (Li, Wohlford-Lenane et al. 2017), in that order.

1. Ad5-hDPP4-transduced mice (IOWA)

The hDPP4-transduced mouse model was made by the transduction with an adenovirus type 5 vector (Ad5) expressing the human DPP4 receptor (Zhao, Li et al. 2014). MERS-CoV infection of these mice induced lung infection with some histopathology, but little to no clinical disease and mortality were seen. Moreover, the lung expression of the hDPP4 in these mice was not stable and weakened by 22 days after transduction. Tests for virus dissemination were apparently not done for the Ad5 model. Despite all the limitations, this model indicated that rapid generation of wild type, as well as knockout mouse strains expressing the hDPP4, was possible and that these mice can be used to study MERS-CoV infection and disease. This mouse model has been shown to be useful for the evaluation of vaccine candidates such as MERS-CoV vaccine based on a recombinant Measles virus vaccine platform (Malczyk, Kupke et al. 2015) and a recombinant modified vaccinia virus Ankara (MVA) vaccine expressing the MERS-CoV spike (S) glycoprotein (Volz, Kupke et al. 2015) (**Table 6**).

On the one hand, the major advantage of the hDPP4-transduced mouse model is that it is possible to rapidly establish in both wild type as well as in knock out mice. On the other hand, the main disadvantages are that only mild disease if any can be observed, and hDPP4 is inconsistently expressed in the lungs (**Table 6**).

2. hDPP4 transgenic mice (UTMB) (Agrawal, Garron et al. 2015, Tao, Garron et al. 2015)

The major advantages of our hDPP4 transgenic mice is that they develop severe infection and disease, they have been fully characterized in terms of LD₅₀ and ID₅₀, and they show consistent morbidity and mortality through generations due to the stable expression of

the hDPP4 expression. The main disadvantage lies in the fact that besides the infection in the lungs we also observe infection of the brain which is likely the cause of death (**Table 6**).

3. Knock-in (KI) model (Regeneron)

For the Regeneron KI model, the approach used to provide the human DPP4 receptor was the replacement of mouse DPP4 (mDPP4) with hDPP4 by using a commercial procedure (VelociGene) in such a way that hDPP4 was expressed under the endogenous mDPP4 promoter. Upon inoculation with 2×10^5 pfu of MERS-CoV, KI mice supported virus replication in the lungs with mild to moderate histologic inflammation without any significant weight loss up to 4 dpi. This model was also used to test the efficacy of a monoclonal antibody (Pascal, Coleman et al. 2015). Follow-up studies using this model (Coleman, Sisk et al. 2017) demonstrated that mice infected with 2.5×10^4 pfu of MERS-CoV, exhibited significant clinical disease with a weight loss of up to 20 % at 5 to 7 dpi thus requiring euthanasia. Increased inflammation and damage in the lungs was also observed. Clinical signs of disease were dose-dependent. At a dose of 2.5×10^3 PFUs/mouse, mice showed some symptoms but recovered, while no clinical symptoms were seen in mice infected with 2.5×10^2 PFUs of MERS-CoV. In this study, they also demonstrated that MERS-CoV replication in the lungs is not affected by the depletion of CD4⁺ T cells, CD8⁺ T cells, or macrophages. Interestingly, CD8⁺ T cells depletion protected while depletion of macrophages aggravated clinical symptoms and MERS-CoV-induced pathology. While some viremia was seen in mice challenged with 2.5×10^4 PFU MERS-CoV, this KI mouse is primarily a lung infection model, since infection did not spread to kidneys or liver (Coleman, Sisk et al. 2017).

The major advantage of this KI model is that upon MERS-CoV infection it develops mild to severe disease. On the other hand, its primary disadvantage is that death was not confirmed, due to the fact that they needed to be euthanized as a result of the development of severe weight loss after upon infection with high infectious viral dose (**Table 6**)

4. Codon-optimized hDPP4 transgenic mice (China)

Zhao's group generated another transgenic mouse model using the same mammalian expression vector as we did. However, they codon-optimized the hDPP4-coding sequence, thus leading to a stronger global expression of the protein (Zhao, Jiang et al. 2015). Mice inoculated i.n. with $10^{4.3}$ TCID₅₀ of MERS-CoV exhibited significant weight loss starting at day 6 and they were dead by day 10. They also developed neurological symptoms (with brain damage) including paralysis at day 9. Damage to other organs such as lungs, spleen, kidney, and liver was also seen. This model seems to closely resemble multiorgan failure seen in some human cases. While, some CNS involvement has been seen in a few human cases (Arabi, Harthi et al. 2015), severe neurological complications such as exaggerated CNS damage leading to paralysis seen in these mice have not been reported in any of the human MERS cases.

The most significant advantage of this model is that it is a lethal model and it resembles the multiorgan failure seen in some patients. However, its limitation lies in the fact that infection of the brain is probably the cause of death (**Table 6**)

5. Transgenic mouse model (IOWA)

Li Kun's group (Li, Wohlford-Lenane et al. 2016) have also developed a transgenic mice model expressing hDPP4 using two different promoters. They used the human surfactant protein C (SPC) promoter (Glasser, Korfhagen et al. 1991) to drive hDPP4

expression in the epithelia of the bronchi and the alveoli, thus generating the SPC-*hDPP4* lines. On the other hand, K18-*hDPP4* line using the cytokeratin 18 (K18) promoter was generated to express hDPP4 in the airway, alveolar, liver kidney and GI tract epithelia, as well as in some cells of the nervous system (Chow, O'Brodovich et al. 1997). Both the transgenic mice lineages were challenged via i.n. inoculation with 1×10^5 pfu of MERS-CoV. While the SPC-*hDPP4* mice did not show any sign of disease (body temperature changes or weight loss) or mortality and, cleared the virus by 14 dpi, the K18-*hDPP4* transgenic mice developed hypothermia and weight loss and died at 6–7 dpi.

K18-*hDPP4* mice had high virus titers in their lung (day 2) and the brain (day 6) tissues and developed disseminated infection as indicated by RT-qPCR. Of particular interest are the high virus titers in the brain. Out of the seven K18-hDPP4 mice infected even with a low infectious dose (10 pfu of MERS-CoV), 3 showed virus titer of approximately 4×10^6 pfu/g of tissue at 9 dpi. suggesting that high mortality was mostly correlated with brain infection. Even though K18-hDPP4 transgenic mice were successfully used for vaccine studies [Immunization with Venezuelan equine encephalitis replicon particles (VRPs) expressing MERS-CoV spike glycoprotein (VRP-MERS-S)] (**Table 6**), the high-titer replication and mortality likely caused by CNS infection might make this model not suitable for evaluating therapeutic agents, that do not cross the blood-brain barrier (Li, Wohlford-Lenane et al. 2016).

The most important advantage of this model is that it develops severe infection and disease after being challenged with MERS-CoV; however, its limitation is that infection of the brain is probably the cause of death (**Table 6**).

6. CRISPR-Cas 9 genomic engineered mice model (UNC)

Recently, the CRISPR/Cas9 genome engineering system was used to generate another mouse model (288/330^{+/+}) in which amino acids at positions 288 and 330 of the mouse DPP4 (mDPP4) were edited to 'human' type sequences. (Crockrell AS et al., 2016). Changes at these two positions in the mDPP4 can confer susceptibility to MERS-CoV infection (Peck, Cockrell et al. 2015). Additionally, Cockrell et al. generated a mouse-adapted virus (MERS-15) by serial passaging of MERS-CoV in their engineered mice. This Mouse-adapted virus was able to replicate efficiently within the lungs of the 288/330^{+/+} mice leading to symptoms of severe acute respiratory distress syndrome (ARDS). Weight loss, decreased pulmonary function, pulmonary hemorrhage, mortality and pathological signs that correlate with end-stage lung disease were observed. Lethality was only observed in homozygous mice 288/330^{+/+} infected with MERS-15, not in the heterozygous mice 288/330^{+/-}. To develop the severe/fatal disease, a high viral infectious dose of the MERS-15 virus was required. Crockrell's group anticipated that accumulation of mutation in MERS-CoV during the mouse adaptation process. They isolated two viral clones from the MERS-15 heterogeneous viral population: MERS-15 clone 1 (MERS-15 C1) and MERS-15 clone 2 (MERS-15 C2). The sequence of the MERS-15 C1 revealed mutations in nsP2 and an extended deletion from orf4b into orf5, while the sequence of MERS-15 C2, showed mutations in the genes encoding the non-structural proteins, nsP2, nsP6 and nsP8, and a large deletion in orf4b.

MERS-15 C2 infection caused higher incidence of hemorrhage and mortality of the mice as compared to MERS-15 C1. However, MERS-15 C2 elicited a lung pathology that resembled the one caused the parental MERS-15 virus and exhibited hyaline membrane

formation, perivascular cuffing, and edema. These mouse adapted MERS-CoV strains might reflect the complexity of the clinical isolates obtained from human cases of MERS, where some deletions in ORF4A and ORF3 have been identified (Lamers, Raj et al. 2016). Mouse line 288/330^{+/+} in combination with MERS-15 C2 constitute a lung infection model that has been used for the evaluation of a vaccine candidate as well as a human monoclonal antibody. Notably, MERS-15 does not cause disease in a classic transgenic mice model.

The authors also demonstrated that this model is useful for the evaluation of a Human monoclonal antibody 3B11 showing that this antibody is able to protect mice from severe respiratory disease, also they showed that vaccination of their mice with a VRP delivering MERS-CoV S protein protects them from challenge with MERS-CoV (**Table 6**).

The principal advantage shown by this model is that the outcome of the infection/disease developed could range from mild to severe. The disadvantages however are that Mouse adapted virus (MERS-15) is needed, thi MERS-15 does not cause disease in classic transgenic mice model, and lethality was only observed in homozygous but not in heterozygous mice (**Table 6**).

7. DPP4 KI model (IOWA)

Another hDPP4 KI mouse model was generated by humanizing exons 10-12 of the mouse DPP4 (Li, Wohlford-Lenane et al. 2017). While these mice support MERS-CoV replication in the lungs, they did not develop disease. They generated a mouse-adapted MERS-CoV (MERS-CoV_{MA}) after 30 passages in their KI model. Using their KI model and the MERS-CoV_{MA}, they were finally able to observe weight loss and fatal disease. However, the mutations identified in MERS-CoV_{MA} have not been reported in isolates from human

cases (Cotten, Watson et al. 2014, Kim, Cheon et al. 2016) and MERS-CoV_{MA} does not cause disease in a classic transgenic mice model.

The advantages of this KI model are that it is a lung infection model and mild to severe infection and disease can be observed. However, as disadvantages it required the use of a Mouse adapted virus (MERS-CoVMA). This mouse adapted virus has shown not to cause disease in classic transgenic mice model (**Table 6**).

As discussed above, there are three KI mouse models. Two of them i.e. the UNC CRISPR-Cas9 genomic engineered mice model, and the IOWA DPP4 KI model require mouse adapted viruses to demonstrate disease. However, the Regeneron KI model does not require any mouse adaptive viral mutations to produce disease. We speculate that these differences could be due to the differences in the promoters that were used to express hDPP4. The Regeneron KI model expresses hDPP4 ORF under the endogenous mDPP4 promoter. Maintaining the pattern of mouse DPP4 expression likely permits a better physiological response to the MERS-CoV infection. The differences between the KI models can also be attributed to the regions/sequences of the mDPP4 ORF that were ‘humanized’. While only amino acids 228 and 230 of mDPP4 were ‘humanized’ the UNC KI mice, exons 10-12 of were changed to hDPP4 in the IOWA KI mice. On the other hand, entire hDPP4 ORF was replaced in the Regeneron model generating a more complete “humanized hDPP4 knock-in”. It is likely that sequences outside the exons 10-12 of DPP4 play a role in mediating efficient virus entry and infection and compensating mutations need to be acquired in the MERS CoV to efficiently replicate in the partially ‘humanized’ KI mice. Studying the molecular basis of these differences can help us better map out the MERS-CoV-hDPP4

interactions and also serve as a starting point to generate a model for MERS-CoV that reproduces human infection better.

Conclusions.

Taken together, current animal models available for MERS reproduce the wide range of disease severity (from asymptomatic to fatal disease) observed in human cases. However, none of them independently completely recapitulates the human infection and disease and also there is still need of more human autopsies to better understand the pathology. While significant progress has been made, further improvements in MERS animal models are also required.

Table 5. Advantages and disadvantages of naturally permissive animal models

Species	Advantages	Disadvantages	Used for testing antivirals and/or vaccines
Rhesus macaques	Non-human primate: highly resembles human immune response.	Mild infection and disease only. Expensive and limited availability.	ND
Common marmosets	Non-human primate. Severe infection/disease has been reported by some, but not other.	Reproducibility of disease. Expensive and limited availability.	Antiviral treatment.
New Zealand white rabbit	Relative low cost and readily available. Easy handling.	Mild disease limited to URT.	ND
Dromedary camels	Natural host for MERS-CoV. Efficient animal-to-animal transmission (field studies).	Mild disease limited to URT. Expensive and limited availability.	Vaccine candidate.
Alpacas	Good model for transmission studies.	Mild disease limited to URT (similar to camels). Reagents readily available.	ND

ND = Not determined

NHP, camels, and alpacas are not ease to handle (they require very large ABSL-3 facilities).

Table 6. Advantages and disadvantages of mice (non-naturally permissive animal models)

Species	Advantages	Disadvantages	Used for testing antivirals and/or vaccines
Ad5-hDPP4-transduced mice (IOWA)	Can be rapidly established in WT and KO mice.	Mild disease if any. hDPP4 inconsistently expressed in the lungs.	Vaccine candidates.
hDPP4-transgenic mice (UTMB)	Severe infection and disease. Fully characterized in terms of LD ₅₀ and ID ₅₀ . Consistent morbidity and mortality through generations.	Infection of the lung and especially brain probably cause of death.	Vaccine candidate and prophylactic efficacy of a fusion inhibitor.
KI model (Regeneron)	Mild and severe infection and disease.	Death was not confirmed (mice infected with high dose developed severe weight loss, therefore they were euthanized)	Monoclonal antibody therapy
Codon-optimized hDPP4 transgenic mice (China)	Lethal model. Resemble multiorgan failure seen in some human cases.	Infection of the brain probably cause of death.	ND
Transgenic mouse model (IOWA)	Severe infection and disease.	Infection of the brain probably cause of death.	Vaccine candidate.
CRISPR-Cas 9 genomic engineered mice model (UNC)	Mild and severe infection/disease. Lung infection model.	Mouse adapted virus (MERS-15) is needed. MERS-15 does not cause disease in classic transgenic mice model. Lethality was only observed in homozygous but not in heterozygous mice.	Vaccine candidate and Human monoclonal antibody 3B11.
DPP4 KI model (IOWA)	Mild and severe infection and disease. Lung infection model.	Mouse adapted virus (MERS-CoV _{MA}) is needed. MERS-CoV _{MA} does not cause disease in classic transgenic mice model.	ND

Mice: easy to handle and house; reagents and assays are widely available

REFERENCES

- Adney, D. R., H. Bielefeldt-Ohmann, A. E. Hartwig and R. A. Bowen (2016). "Infection, Replication, and Transmission of Middle East Respiratory Syndrome Coronavirus in Alpacas." Emerg Infect Dis **22**(6): 1031-1037.
- Adney, D. R., N. van Doremalen, V. R. Brown, T. Bushmaker, D. Scott, E. de Wit, R. A. Bowen and V. J. Munster (2014). "Replication and shedding of MERS-CoV in upper respiratory tract of inoculated dromedary camels." Emerg Infect Dis **20**(12): 1999-2005.
- Agrawal, A. S., T. Garron, X. Tao, B. H. Peng, M. Wakamiya, T. S. Chan, R. B. Couch and C. T. Tseng (2015). "Generation of a transgenic mouse model of Middle East respiratory syndrome coronavirus infection and disease." J Virol **89**(7): 3659-3670.
- Al-Tawfiq, J. A. (2013). "Middle East Respiratory Syndrome-coronavirus infection: an overview." J Infect Public Health **6**(5): 319-322.
- Al-Tawfiq, J. A., K. Hinedi, J. Ghandour, H. Khairalla, S. Musleh, A. Ujayli and Z. A. Memish (2014). "Middle East respiratory syndrome coronavirus: a case-control study of hospitalized patients." Clin Infect Dis **59**(2): 160-165.
- Alagaili, A. N., T. Briese, N. Mishra, V. Kapoor, S. C. Sameroff, P. D. Burbelo, E. de Wit, V. J. Munster, L. E. Hensley, I. S. Zalmout, A. Kapoor, J. H. Epstein, W. B. Karesh, P. Daszak, O. B. Mohammed and W. I. Lipkin (2014). "Middle East respiratory syndrome coronavirus infection in dromedary camels in Saudi Arabia." MBio **5**(2): e00884-00814.
- Almazan, F., M. L. DeDiego, I. Sola, S. Zuniga, J. L. Nieto-Torres, S. Marquez-Jurado, G. Andres and L. Enjuanes (2013). "Engineering a replication-competent, propagation-defective Middle East respiratory syndrome coronavirus as a vaccine candidate." MBio **4**(5): e00650-00613.
- Arabi, Y. M., A. Harthi, J. Hussein, A. Bouchama, S. Johani, A. H. Hajeer, B. T. Saeed, A. Wahbi, A. Saedy, T. AlDabbagh, R. Okaili, M. Sadat and H. Balkhy (2015). "Severe neurologic syndrome associated with Middle East respiratory syndrome corona virus (MERS-CoV)." Infection **43**(4): 495-501.
- Assiri, A., J. A. Al-Tawfiq, A. A. Al-Rabeeah, F. A. Al-Rabiah, S. Al-Hajjar, A. Al-Barrak, H. Flemban, W. N. Al-Nassir, H. H. Balkhy, R. F. Al-Hakeem, H. Q. Makhdoom, A. I. Zumla and Z. A. Memish (2013). "Epidemiological, demographic, and clinical characteristics of 47 cases of Middle East respiratory syndrome coronavirus disease from Saudi Arabia: a descriptive study." Lancet Infect Dis **13**(9): 752-761.
- Assiri, A., A. McGeer, T. M. Perl, C. S. Price, A. A. Al Rabeeah, D. A. Cummings, Z. N. Alabdullatif, M. Assad, A. Almulhim, H. Makhdoom, H. Madani, R. Alhakeem, J. A. Al-Tawfiq, M. Cotten, S. J. Watson, P. Kellam, A. I. Zumla and Z. A. Memish (2013). "Hospital outbreak of Middle East respiratory syndrome coronavirus." N Engl J Med **369**(5): 407-416.

Azhar, E. I., S. A. El-Kafrawy, S. A. Farraj, A. M. Hassan, M. S. Al-Saeed, A. M. Hashem and T. A. Madani (2014). "Evidence for camel-to-human transmission of MERS coronavirus." N Engl J Med **370**(26): 2499-2505.

Bermingham, A., M. A. Chand, C. S. Brown, S. Aarons, C. Tong, C. Langrish, K. Hoschler, K. Brown, M. Galiano, R. Myers, R. G. Pebody, H. K. Green, N. L. Boddington, R. Gopal, N. Price, W. Newsholme, C. Drosten, R. A. Fouchier and M. Zambon (2012). "Severe respiratory illness caused by a novel coronavirus, inpatient transferred to the United Kingdom from the Middle East, September 2012." Eurosurveillance **Volume 17**(Issue 40).

Blander, J. M. and L. E. Sander (2012). "Beyond pattern recognition: five immune checkpoints for scaling the microbial threat." Nat Rev Immunol **12**(3): 215-225.

Briese, T., N. Mishra, K. Jain, I. S. Zalmout, O. J. Jabado, W. B. Karesh, P. Daszak, O. B. Mohammed, A. N. Alagaili and W. I. Lipkin (2014). "Middle East respiratory syndrome coronavirus quasispecies that include homologues of human isolates revealed through whole-genome analysis and virus cultured from dromedary camels in Saudi Arabia." MBio **5**(3): e01146-01114.

Centers for Disease, C. and Prevention (2013). "Updated information on the epidemiology of Middle East respiratory syndrome coronavirus (MERS-CoV) infection and guidance for the public, clinicians, and public health authorities, 2012-2013." MMWR Morb Mortal Wkly Rep **62**(38): 793-796.

Chan, J. F., Y. Yao, M. L. Yeung, W. Deng, L. Bao, L. Jia, F. Li, C. Xiao, H. Gao, P. Yu, J. P. Cai, H. Chu, J. Zhou, H. Chen, C. Qin and K. Y. Yuen (2015). "Treatment With Lopinavir/Ritonavir or Interferon-beta1b Improves Outcome of MERS-CoV Infection in a Nonhuman Primate Model of Common Marmoset." J Infect Dis **212**(12): 1904-1913.

Channappanavar, R., L. Lu, S. Xia, L. Du, D. K. Meyerholz, S. Perlman and S. Jiang (2015). "Protective Effect of Intranasal Regimens Containing Peptidic Middle East Respiratory Syndrome Coronavirus Fusion Inhibitor Against MERS-CoV Infection." J Infect Dis **212**(12): 1894-1903.

Chen, Y., K. R. Rajashankar, Y. Yang, S. S. Agnihothram, C. Liu, Y. L. Lin, R. S. Baric and F. Li (2013). "Crystal structure of the receptor-binding domain from newly emerged Middle East respiratory syndrome coronavirus." J Virol **87**(19): 10777-10783.

Chow, Y. H., H. O'Brodivich, J. Plumb, Y. Wen, K. J. Sohn, Z. Lu, F. Zhang, G. L. Lukacs, A. K. Tanswell, C. C. Hui, M. Buchwald and J. Hu (1997). "Development of an epithelium-specific expression cassette with human DNA regulatory elements for transgene expression in lung airways." Proc Natl Acad Sci U S A **94**(26): 14695-14700.

Chu, H., J. Zhou, B. H. Wong, C. Li, J. F. Chan, Z. S. Cheng, D. Yang, D. Wang, A. C. Lee, C. Li, M. L. Yeung, J. P. Cai, I. H. Chan, W. K. Ho, K. K. To, B. J. Zheng, Y. Yao, C. Qin and K. Y. Yuen (2016). "Middle East Respiratory Syndrome Coronavirus Efficiently Infects Human Primary T Lymphocytes and Activates the Extrinsic and Intrinsic Apoptosis Pathways." J Infect Dis **213**(6): 904-914.

- Cockrell, A. S., B. L. Yount, T. Scobey, K. Jensen, M. Douglas, A. Beall, X. C. Tang, W. A. Marasco, M. T. Heise and R. S. Baric (2016). "A mouse model for MERS coronavirus-induced acute respiratory distress syndrome." Nat Microbiol **2**: 16226.
- Coleman, C. M., K. L. Matthews, L. Goicochea and M. B. Frieman (2014). "Wild-type and innate immune-deficient mice are not susceptible to the Middle East respiratory syndrome coronavirus." J Gen Virol **95**(Pt 2): 408-412.
- Coleman, C. M., J. M. Sisk, G. Halasz, J. Zhong, S. E. Beck, K. L. Matthews, T. Venkataraman, S. Rajagopalan, C. A. Kyratsous and M. B. Frieman (2017). "CD8+ T Cells and Macrophages Regulate Pathogenesis in a Mouse Model of Middle East Respiratory Syndrome." J Virol **91**(1).
- Corman, V. M., N. L. Ithete, L. R. Richards, M. C. Schoeman, W. Preiser, C. Drosten and J. F. Drexler (2014). "Rooting the phylogenetic tree of middle East respiratory syndrome coronavirus by characterization of a conspecific virus from an African bat." J Virol **88**(19): 11297-11303.
- Cotten, M., T. T. Lam, S. J. Watson, A. L. Palser, V. Petrova, P. Grant, O. G. Pybus, A. Rambaut, Y. Guan, D. Pillay, P. Kellam and E. Nastouli (2013). "Full-genome deep sequencing and phylogenetic analysis of novel human betacoronavirus." Emerg Infect Dis **19**(5): 736-742B.
- Cotten, M., S. J. Watson, P. Kellam, A. A. Al-Rabeeah, H. Q. Makhdoom, A. Assiri, J. A. Al-Tawfiq, R. F. Alhakeem, H. Madani, F. A. AlRabiah, S. Al Hajjar, W. N. Al-nassir, A. Albarrak, H. Flemban, H. H. Balkhy, S. Alsubaie, A. L. Palser, A. Gall, R. Bashford-Rogers, A. Rambaut, A. I. Zumla and Z. A. Memish (2013). "Transmission and evolution of the Middle East respiratory syndrome coronavirus in Saudi Arabia: a descriptive genomic study." Lancet **382**(9909): 1993-2002.
- Cotten, M., S. J. Watson, A. I. Zumla, H. Q. Makhdoom, A. L. Palser, S. H. Ong, A. A. Al Rabeeah, R. F. Alhakeem, A. Assiri, J. A. Al-Tawfiq, A. Albarrak, M. Barry, A. Shibl, F. A. Alrabiah, S. Hajjar, H. H. Balkhy, H. Flemban, A. Rambaut, P. Kellam and Z. A. Memish (2014). "Spread, circulation, and evolution of the Middle East respiratory syndrome coronavirus." MBio **5**(1).
- Crameri, G., P. A. Durr, R. Klein, A. Foord, M. Yu, S. Riddell, J. Haining, D. Johnson, M. G. Hemida, J. Barr, M. Peiris, D. Middleton and L. F. Wang (2016). "Experimental Infection and Response to Rechallenge of Alpacas with Middle East Respiratory Syndrome Coronavirus." Emerg Infect Dis **22**(6): 1071-1074.
- Cunha, C. B. and S. M. Opal (2014). "Middle East respiratory syndrome (MERS): a new zoonotic viral pneumonia." Virulence **5**(6): 650-654.
- de Groot, R. J., S. C. Baker, R. S. Baric, C. S. Brown, C. Drosten, L. Enjuanes, R. A. Fouchier, M. Galiano, A. E. Gorbalenya, Z. A. Memish, S. Perlman, L. L. Poon, E. J. Snijder, G. M. Stephens, P. C. Woo, A. M. Zaki, M. Zambon and J. Ziebuhr (2013). "Middle East respiratory syndrome coronavirus (MERS-CoV): announcement of the Coronavirus Study Group." J Virol **87**(14): 7790-7792.

de Wilde, A. H., V. S. Raj, D. Oudshoorn, T. M. Bestebroer, S. van Nieuwkoop, R. W. Limpens, C. C. Posthuma, Y. van der Meer, M. Barcena, B. L. Haagmans, E. J. Snijder and B. G. van den Hoogen (2013). "MERS-coronavirus replication induces severe in vitro cytopathology and is strongly inhibited by cyclosporin A or interferon-alpha treatment." J Gen Virol **94**(Pt 8): 1749-1760.

de Wit, E., J. Prescott, L. Baseler, T. Bushmaker, T. Thomas, M. G. Lackemeyer, C. Martellaro, S. Milne-Price, E. Haddock, B. L. Haagmans, H. Feldmann and V. J. Munster (2013). "The Middle East respiratory syndrome coronavirus (MERS-CoV) does not replicate in Syrian hamsters." PLoS One **8**(7): e69127.

de Wit, E., A. L. Rasmussen, D. Falzarano, T. Bushmaker, F. Feldmann, D. L. Brining, E. R. Fischer, C. Martellaro, A. Okumura, J. Chang, D. Scott, A. G. Benecke, M. G. Katze, H. Feldmann and V. J. Munster (2013). "Middle East respiratory syndrome coronavirus (MERS-CoV) causes transient lower respiratory tract infection in rhesus macaques." Proc Natl Acad Sci U S A **110**(41): 16598-16603.

Denison, M. R. (2004). "Severe acute respiratory syndrome coronavirus pathogenesis, disease and vaccines: an update." Pediatr Infect Dis J **23**(11 Suppl): S207-214.

Ding, Y., L. He, Q. Zhang, Z. Huang, X. Che, J. Hou, H. Wang, H. Shen, L. Qiu, Z. Li, J. Geng, J. Cai, H. Han, X. Li, W. Kang, D. Weng, P. Liang and S. Jiang (2004). "Organ distribution of severe acute respiratory syndrome (SARS) associated coronavirus (SARS-CoV) in SARS patients: implications for pathogenesis and virus transmission pathways." J Pathol **203**(2): 622-630.

Drosten, C., B. Meyer, M. A. Muller, V. M. Corman, M. Al-Masri, R. Hossain, H. Madani, A. Sieberg, B. J. Bosch, E. Lattwein, R. F. Alhakeem, A. M. Assiri, W. Hajomar, A. M. Albarrak, J. A. Al-Tawfiq, A. I. Zumla and Z. A. Memish (2014). "Transmission of MERS-coronavirus in household contacts." N Engl J Med **371**(9): 828-835.

Drosten, C., M. Seilmaier, V. M. Corman, W. Hartmann, G. Scheible, S. Sack, W. Guggemos, R. Kallies, D. Muth, S. Junglen, M. A. Muller, W. Haas, H. Guberina, T. Rohnisch, M. Schmid-Wendtner, S. Aldabbagh, U. Dittmer, H. Gold, P. Graf, F. Bonin, A. Rambaut and C. M. Wendtner (2013). "Clinical features and virological analysis of a case of Middle East respiratory syndrome coronavirus infection." Lancet Infect Dis **13**(9): 745-751.

Du, L., Z. Kou, C. Ma, X. Tao, L. Wang, G. Zhao, Y. Chen, F. Yu, C. T. Tseng, Y. Zhou and S. Jiang (2013). "A truncated receptor-binding domain of MERS-CoV spike protein potently inhibits MERS-CoV infection and induces strong neutralizing antibody responses: implication for developing therapeutics and vaccines." PLoS One **8**(12): e81587.

Du, L., G. Zhao, Z. Kou, C. Ma, S. Sun, V. K. Poon, L. Lu, L. Wang, A. K. Debnath, B. J. Zheng, Y. Zhou and S. Jiang (2013). "Identification of a receptor-binding domain in the S protein of the novel human coronavirus Middle East respiratory syndrome coronavirus as an essential target for vaccine development." J Virol **87**(17): 9939-9942.

ECDC (2015). "Rapid Risk Assessment Severe respiratory disease associated with Middle East respiratory syndrome coronavirus (MERS-CoV) "
<http://ecdc.europa.eu/en/publications/Publications/MERS-rapid-risk-assessment-update-october-2015.pdf> **21st update** (21 October).

Falzarano, D., E. de Wit, F. Feldmann, A. L. Rasmussen, A. Okumura, X. Peng, M. J. Thomas, N. van Doremalen, E. Haddock, L. Nagy, R. LaCasse, T. Liu, J. Zhu, J. S. McLellan, D. P. Scott, M. G. Katze, H. Feldmann and V. J. Munster (2014). "Infection with MERS-CoV causes lethal pneumonia in the common marmoset." *PLoS Pathog* **10**(8): e1004250.

Falzarano, D., E. de Wit, A. L. Rasmussen, F. Feldmann, A. Okumura, D. P. Scott, D. Brining, T. Bushmaker, C. Martellaro, L. Baseler, A. G. Benecke, M. G. Katze, V. J. Munster and H. Feldmann (2013). "Treatment with interferon-alpha2b and ribavirin improves outcome in MERS-CoV-infected rhesus macaques." *Nat Med* **19**(10): 1313-1317.

Faure, E., J. Poissy, A. Goffard, C. Fournier, E. Kipnis, M. Titecat, P. Bortolotti, L. Martinez, S. Dubucquoi, R. Dessein, P. Gosset, D. Mathieu and B. Guery (2014). "Distinct immune response in two MERS-CoV-infected patients: can we go from bench to bedside?" *PLoS One* **9**(2): e88716.

Frey, K. G., C. L. Redden, K. A. Bishop-Lilly, R. Johnson, L. E. Hensley, K. Raviprakash, T. Luke, T. Kochel, V. P. Mokashi and G. N. Defang (2014). "Full-genome sequence of human betacoronavirus 2c jordan-n3/2012 after serial passage in Mammalian cells." *Genome Announc* **2**(3).

Frieman, M., M. Heise and R. Baric (2008). "SARS coronavirus and innate immunity." *Virus Res* **133**(1): 101-112.

Gao, J., G. Lu, J. Qi, Y. Li, Y. Wu, Y. Deng, H. Geng, H. Li, Q. Wang, H. Xiao, W. Tan, J. Yan and G. F. Gao (2013). "Structure of the fusion core and inhibition of fusion by a heptad repeat peptide derived from the S protein of Middle East respiratory syndrome coronavirus." *J Virol* **87**(24): 13134-13140.

Gierer, S., S. Bertram, F. Kaup, F. Wrensch, A. Heurich, A. Kramer-Kuhl, K. Welsch, M. Winkler, B. Meyer, C. Drosten, U. Dittmer, T. von Hahn, G. Simmons, H. Hofmann and S. Pohlmann (2013). "The spike protein of the emerging betacoronavirus EMC uses a novel coronavirus receptor for entry, can be activated by TMPRSS2, and is targeted by neutralizing antibodies." *J Virol* **87**(10): 5502-5511.

Glasser, S. W., T. R. Korfhagen, S. E. Wert, M. D. Bruno, K. M. McWilliams, D. K. Vorbroker and J. A. Whitsett (1991). "Genetic element from human surfactant protein SP-C gene confers bronchiolar-alveolar cell specificity in transgenic mice." *Am J Physiol* **261**(4 Pt 1): L349-356.

Gorrell, M. D. (2005). "Dipeptidyl peptidase IV and related enzymes in cell biology and liver disorders." *Clin Sci (Lond)* **108**(4): 277-292.

Gu, J., E. Gong, B. Zhang, J. Zheng, Z. Gao, Y. Zhong, W. Zou, J. Zhan, S. Wang, Z. Xie, H. Zhuang, B. Wu, H. Zhong, H. Shao, W. Fang, D. Gao, F. Pei, X. Li, Z. He, D. Xu, X. Shi, V. M.

Anderson and A. S. Leong (2005). "Multiple organ infection and the pathogenesis of SARS." J Exp Med **202**(3): 415-424.

Guery, B., J. Poissy, L. el Mansouf, C. Sejourne, N. Ettahar, X. Lemaire, F. Vuotto, A. Goffard, S. Behillil, V. Enouf, V. Caro, A. Mailles, D. Che, J. C. Manuguerra, D. Mathieu, A. Fontanet and S. van der Werf (2013). "Clinical features and viral diagnosis of two cases of infection with Middle East Respiratory Syndrome coronavirus: a report of nosocomial transmission." Lancet **381**(9885): 2265-2272.

Guery, B., J. Poissy, L. el Mansouf, C. Sejourne, N. Ettahar, X. Lemaire, F. Vuotto, A. Goffard, S. Behillil, V. Enouf, V. Caro, A. Mailles, D. Che, J. C. Manuguerra, D. Mathieu, A. Fontanet, S. van der Werf and M. E.-C. s. group (2013). "Clinical features and viral diagnosis of two cases of infection with Middle East Respiratory Syndrome coronavirus: a report of nosocomial transmission." Lancet **381**(9885): 2265-2272.

Haagmans, B. L., S. H. Al Dhahiry, C. B. Reusken, V. S. Raj, M. Galiano, R. Myers, G. J. Godeke, M. Jonges, E. Farag, A. Diab, H. Ghobashy, F. Alhajri, M. Al-Thani, S. A. Al-Marri, H. E. Al Romaihi, A. Al Khal, A. Bermingham, A. D. Osterhaus, M. M. AlHajri and M. P. Koopmans (2014). "Middle East respiratory syndrome coronavirus in dromedary camels: an outbreak investigation." Lancet Infect Dis **14**(2): 140-145.

Haagmans, B. L., J. M. van den Brand, L. B. Provacica, V. S. Raj, K. J. Stittelaar, S. Getu, L. de Waal, T. M. Bestebroer, G. van Amerongen, G. M. Verjans, R. A. Fouchier, S. L. Smits, T. Kuiken and A. D. Osterhaus (2015). "Asymptomatic Middle East respiratory syndrome coronavirus infection in rabbits." J Virol **89**(11): 6131-6135.

Haagmans, B. L., J. M. van den Brand, V. S. Raj, A. Volz, P. Wohlsein, S. L. Smits, D. Schipper, T. M. Bestebroer, N. Okba, R. Fux, A. Bensaid, D. Solanes Foz, T. Kuiken, W. Baumgartner, J. Segales, G. Sutter and A. D. Osterhaus (2016). "An orthopoxvirus-based vaccine reduces virus excretion after MERS-CoV infection in dromedary camels." Science **351**(6268): 77-81.

Health Protection Agency, U. K. N. C. I. t. (2013). "Evidence of person-to-person transmission within a family cluster of novel coronavirus infections, United Kingdom, February 2013." Euro Surveill **18**(11): 20427.

Hemida, M. G., D. K. Chu, L. L. Poon, R. A. Perera, M. A. Alhammadi, H. Y. Ng, L. Y. Siu, Y. Guan, A. Alnaeem and M. Peiris (2014). "MERS coronavirus in dromedary camel herd, Saudi Arabia." Emerg Infect Dis **20**(7): 1231-1234.

Hemida, M. G., R. A. Perera, P. Wang, M. A. Alhammadi, L. Y. Siu, M. Li, L. L. Poon, L. Saif, A. Alnaeem and M. Peiris (2013). "Middle East Respiratory Syndrome (MERS) coronavirus seroprevalence in domestic livestock in Saudi Arabia, 2010 to 2013." Euro Surveill **18**(50): 20659.

Hijawi, B., M. Abdallat, A. Sayaydeh, S. Alqasrawi, A. Haddadin, N. Jaarour, S. Alsheikh and T. Alsanouri (2013). "Novel coronavirus infections in Jordan, April 2012: epidemiological findings from a retrospective investigation." East Mediterr Health J **19 Suppl 1**: S12-18.

Houser, K. V., L. Gretebeck, T. Ying, Y. Wang, L. Vogel, E. W. Lamirande, K. W. Bock, I. N. Moore, D. S. Dimitrov and K. Subbarao (2016). "Prophylaxis With a Middle East Respiratory Syndrome Coronavirus (MERS-CoV)-Specific Human Monoclonal Antibody Protects Rabbits From MERS-CoV Infection." J Infect Dis **213**(10): 1557-1561.

Ithete, N. L., S. Stoffberg, V. M. Corman, V. M. Cottontail, L. R. Richards, M. C. Schoeman, C. Drosten, J. F. Drexler and W. Preiser (2013). "Close relative of human Middle East respiratory syndrome coronavirus in bat, South Africa." Emerg Infect Dis **19**(10): 1697-1699.

Jiang, S., K. Lin, N. Strick and A. R. Neurath (1993). "HIV-1 inhibition by a peptide." Nature **365**(6442): 113.

Johnson, R. F., L. E. Via, M. R. Kumar, J. P. Cornish, S. Yellayi, L. Huzella, E. Postnikova, N. Oberlander, C. Bartos, B. L. Ork, S. Mazur, C. Allan, M. R. Holbrook, J. Solomon, J. C. Johnson, J. Pickel, L. E. Hensley and P. B. Jahrling (2015). "Intratracheal exposure of common marmosets to MERS-CoV Jordan-n3/2012 or MERS-CoV EMC/2012 isolates does not result in lethal disease." Virology **485**: 422-430.

Katze, M. G., Y. He and M. Gale, Jr. (2002). "Viruses and interferon: a fight for supremacy." Nat Rev Immunol **2**(9): 675-687.

Kim, E., K. Okada, T. Kenniston, V. S. Raj, M. M. AlHajri, E. A. Farag, F. AlHajri, A. D. Osterhaus, B. L. Haagmans and A. Gambotto (2014). "Immunogenicity of an adenoviral-based Middle East Respiratory Syndrome coronavirus vaccine in BALB/c mice." Vaccine **32**(45): 5975-5982.

Kim, Y., S. Cheon, C. K. Min, K. M. Sohn, Y. J. Kang, Y. J. Cha, J. I. Kang, S. K. Han, N. Y. Ha, G. Kim, A. Aigerim, H. M. Shin, M. S. Choi, S. Kim, H. S. Cho, Y. S. Kim and N. H. Cho (2016). "Spread of Mutant Middle East Respiratory Syndrome Coronavirus with Reduced Affinity to Human CD26 during the South Korean Outbreak." MBio **7**(2): e00019.

Lambeir, A. M., C. Durinx, S. Scharpe and I. De Meester (2003). "Dipeptidyl-peptidase IV from bench to bedside: an update on structural properties, functions, and clinical aspects of the enzyme DPP IV." Crit Rev Clin Lab Sci **40**(3): 209-294.

Lamers, M. M., V. S. Raj, M. Shafei, S. S. Ali, S. M. Abdallah, M. Gazo, S. Nofal, X. Lu, D. D. Erdman, M. P. Koopmans, M. Abdallat, A. Haddadin and B. L. Haagmans (2016). "Deletion Variants of Middle East Respiratory Syndrome Coronavirus from Humans, Jordan, 2015." Emerg Infect Dis **22**(4): 716-719.

Lei, J., J. R. Mesters, C. Drosten, S. Anemuller, Q. Ma and R. Hilgenfeld (2014). "Crystal structure of the papain-like protease of MERS coronavirus reveals unusual, potentially druggable active-site features." Antiviral Res **109**: 72-82.

Leyva-Grado, V. H., G. S. Tan, P. E. Leon, M. Yondola and P. Palese (2015). "Direct administration in the respiratory tract improves efficacy of broadly neutralizing anti-influenza virus monoclonal antibodies." Antimicrob Agents Chemother **59**(7): 4162-4172.

Li, K., C. Wohlford-Lenane, S. Perlman, J. Zhao, A. K. Jewell, L. R. Reznikov, K. N. Gibson-Corley, D. K. Meyerholz and P. B. McCray, Jr. (2016). "Middle East Respiratory Syndrome Coronavirus Causes Multiple Organ Damage and Lethal Disease in Mice Transgenic for Human Dipeptidyl Peptidase 4." J Infect Dis **213**(5): 712-722.

Li, K., C. L. Wohlford-Lenane, R. Channappanavar, J. E. Park, J. T. Earnest, T. B. Bair, A. M. Bates, K. A. Brogden, H. A. Flaherty, T. Gallagher, D. K. Meyerholz, S. Perlman and P. B. McCray, Jr. (2017). "Mouse-adapted MERS coronavirus causes lethal lung disease in human DPP4 knockin mice." Proc Natl Acad Sci U S A **114**(15): E3119-E3128.

Liu, S., G. Xiao, Y. Chen, Y. He, J. Niu, C. R. Escalante, H. Xiong, J. Farmar, A. K. Debnath, P. Tien and S. Jiang (2004). "Interaction between heptad repeat 1 and 2 regions in spike protein of SARS-associated coronavirus: implications for virus fusogenic mechanism and identification of fusion inhibitors." Lancet **363**(9413): 938-947.

Lu, G., Y. Hu, Q. Wang, J. Qi, F. Gao, Y. Li, Y. Zhang, W. Zhang, Y. Yuan, J. Bao, B. Zhang, Y. Shi, J. Yan and G. F. Gao (2013). "Molecular basis of binding between novel human coronavirus MERS-CoV and its receptor CD26." Nature **500**(7461): 227-231.

Lu, L., Q. Liu, L. Du and S. Jiang (2013). "Middle East respiratory syndrome coronavirus (MERS-CoV): challenges in identifying its source and controlling its spread." Microbes Infect **15**(8-9): 625-629.

Lu, L., Q. Liu, Y. Zhu, K. H. Chan, L. Qin, Y. Li, Q. Wang, J. F. Chan, L. Du, F. Yu, C. Ma, S. Ye, K. Y. Yuen, R. Zhang and S. Jiang (2014). "Structure-based discovery of Middle East respiratory syndrome coronavirus fusion inhibitor." Nat Commun **5**: 3067.

Ma, C., Y. Li, L. Wang, G. Zhao, X. Tao, C. T. Tseng, Y. Zhou, L. Du and S. Jiang (2014). "Intranasal vaccination with recombinant receptor-binding domain of MERS-CoV spike protein induces much stronger local mucosal immune responses than subcutaneous immunization: Implication for designing novel mucosal MERS vaccines." Vaccine **32**(18): 2100-2108.

Ma, C., L. Wang, X. Tao, N. Zhang, Y. Yang, C. T. Tseng, F. Li, Y. Zhou, S. Jiang and L. Du (2014). "Searching for an ideal vaccine candidate among different MERS coronavirus receptor-binding fragments--the importance of immunofocusing in subunit vaccine design." Vaccine **32**(46): 6170-6176.

Malczyk, A. H., A. Kupke, S. Prufer, V. A. Scheuplein, S. Hutzler, D. Kreuz, T. Beissert, S. Bauer, S. Hubich-Rau, C. Tondera, H. S. Eldin, J. Schmidt, J. Vergara-Alert, Y. Suzer, J. Seifried, K. M. Hanschmann, U. Kalinke, S. Herold, U. Sahin, K. Cichutek, Z. Waibler, M. Eickmann, S. Becker and M. D. Muhlebach (2015). "A Highly Immunogenic and Protective Middle East Respiratory Syndrome Coronavirus Vaccine Based on a Recombinant Measles Virus Vaccine Platform." J Virol **89**(22): 11654-11667.

Matthews, K. L., C. M. Coleman, Y. van der Meer, E. J. Snijder and M. B. Frieman (2014). "The ORF4b-encoded accessory proteins of Middle East respiratory syndrome coronavirus and two related bat coronaviruses localize to the nucleus and inhibit innate immune signalling." J Gen Virol **95**(Pt 4): 874-882.

McCray, P. B., Jr., L. Pewe, C. Wohlford-Lenane, M. Hickey, L. Manzel, L. Shi, J. Netland, H. P. Jia, C. Halabi, C. D. Sigmund, D. K. Meyerholz, P. Kirby, D. C. Look and S. Perlman (2007). "Lethal infection of K18-hACE2 mice infected with severe acute respiratory syndrome coronavirus." J Virol **81**(2): 813-821.

Memish, Z. A., M. Cotten, B. Meyer, S. J. Watson, A. J. Alshafi, A. A. Al Rabeeah, V. M. Corman, A. Sieberg, H. Q. Makhdoom, A. Assiri, M. Al Masri, S. Aldabbagh, B. J. Bosch, M. Beer, M. A. Muller, P. Kellam and C. Drosten (2014). "Human infection with MERS coronavirus after exposure to infected camels, Saudi Arabia, 2013." Emerg Infect Dis **20**(6): 1012-1015.

Memish, Z. A., A. I. Zumla and A. Assiri (2013). "Middle East respiratory syndrome coronavirus infections in health care workers." N Engl J Med **369**(9): 884-886.

Meyer, B., M. A. Muller, V. M. Corman, C. B. Reusken, D. Ritz, G. J. Godeke, E. Lattwein, S. Kallies, A. Siemens, J. van Beek, J. F. Drexler, D. Muth, B. J. Bosch, U. Wernery, M. P. Koopmans, R. Wernery and C. Drosten (2014). "Antibodies against MERS coronavirus in dromedary camels, United Arab Emirates, 2003 and 2013." Emerg Infect Dis **20**(4): 552-559.

Mou, H., V. S. Raj, F. J. van Kuppeveld, P. J. Rottier, B. L. Haagmans and B. J. Bosch (2013). "The receptor binding domain of the new Middle East respiratory syndrome coronavirus maps to a 231-residue region in the spike protein that efficiently elicits neutralizing antibodies." J Virol **87**(16): 9379-9383.

Mu, J., A. Petrov, G. J. Eiermann, J. Woods, Y. P. Zhou, Z. Li, E. Zycband, Y. Feng, L. Zhu, R. S. Roy, A. D. Howard, C. Li, N. A. Thornberry and B. B. Zhang (2009). "Inhibition of DPP-4 with sitagliptin improves glycemic control and restores islet cell mass and function in a rodent model of type 2 diabetes." Eur J Pharmacol **623**(1-3): 148-154.

Munster, V. J., E. de Wit and H. Feldmann (2013). "Pneumonia from human coronavirus in a macaque model." N Engl J Med **368**(16): 1560-1562.

Ng, D. L., F. Al Hosani, M. K. Keating, S. I. Gerber, T. L. Jones, M. G. Metcalfe, S. Tong, Y. Tao, N. N. Alami, L. M. Haynes, M. A. Mutei, L. Abdel-Wareth, T. M. Uyeki, D. L. Swerdlow, M. Barakat and S. R. Zaki (2016). "Clinicopathologic, Immunohistochemical, and Ultrastructural Findings of a Fatal Case of Middle East Respiratory Syndrome Coronavirus Infection in the United Arab Emirates, April 2014." Am J Pathol **186**(3): 652-658.

Nicholls, J. M., L. L. Poon, K. C. Lee, W. F. Ng, S. T. Lai, C. Y. Leung, C. M. Chu, P. K. Hui, K. L. Mak, W. Lim, K. W. Yan, K. H. Chan, N. C. Tsang, Y. Guan, K. Y. Yuen and J. S. Peiris (2003). "Lung pathology of fatal severe acute respiratory syndrome." Lancet **361**(9371): 1773-1778.

Niemeyer, D., T. Zillinger, D. Muth, F. Zielecki, G. Horvath, T. Suliman, W. Barchet, F. Weber, C. Drosten and M. A. Muller (2013). "Middle East respiratory syndrome coronavirus accessory protein 4a is a type I interferon antagonist." J Virol **87**(22): 12489-12495.

- Niwa, H., K. Yamamura and J. Miyazaki (1991). "Efficient selection for high-expression transfectants with a novel eukaryotic vector." Gene **108**(2): 193-199.
- Nowotny, N. and J. Kolodziejek (2014). "Middle East respiratory syndrome coronavirus (MERS-CoV) in dromedary camels, Oman, 2013." Euro Surveill **19**(16): 20781.
- Oboho, I. K., S. M. Tomczyk, A. M. Al-Asmari, A. A. Banjar, H. Al-Mugti, M. S. Aloraini, K. Z. Alkhalidi, E. L. Almohammadi, B. M. Alraddadi, S. I. Gerber, D. L. Swerdlow, J. T. Watson and T. A. Madani (2015). "2014 MERS-CoV outbreak in Jeddah--a link to health care facilities." N Engl J Med **372**(9): 846-854.
- Omrani, A. S., M. A. Matin, Q. Haddad, D. Al-Nakhli, Z. A. Memish and A. M. Albarrak (2013). "A family cluster of Middle East Respiratory Syndrome Coronavirus infections related to a likely unrecognized asymptomatic or mild case." Int J Infect Dis **17**(9): e668-672.
- Pascal, K. E., C. M. Coleman, A. O. Mujica, V. Kamat, A. Badithe, J. Fairhurst, C. Hunt, J. Strein, A. Berrebi, J. M. Sisk, K. L. Matthews, R. Babb, G. Chen, K. M. Lai, T. T. Huang, W. Olson, G. D. Yancopoulos, N. Stahl, M. B. Frieman and C. A. Kyratsous (2015). "Pre- and postexposure efficacy of fully human antibodies against Spike protein in a novel humanized mouse model of MERS-CoV infection." Proc Natl Acad Sci U S A **112**(28): 8738-8743.
- Peck, K. M., A. S. Cockrell, B. L. Yount, T. Scobey, R. S. Baric and M. T. Heise (2015). "Glycosylation of mouse DPP4 plays a role in inhibiting Middle East respiratory syndrome coronavirus infection." J Virol **89**(8): 4696-4699.
- Peiris, J. S., Y. Guan and K. Y. Yuen (2004). "Severe acute respiratory syndrome." Nat Med **10**(12 Suppl): S88-97.
- Perlman, S. and J. Netland (2009). "Coronaviruses post-SARS: update on replication and pathogenesis." Nat Rev Microbiol **7**(6): 439-450.
- Pollack, M. P., C. Pringle, L. C. Madoff and Z. A. Memish (2013). "Latest outbreak news from ProMED-mail: novel coronavirus -- Middle East." Int J Infect Dis **17**(2): e143-144.
- Qian, Z., S. R. Dominguez and K. V. Holmes (2013). "Role of the spike glycoprotein of human Middle East respiratory syndrome coronavirus (MERS-CoV) in virus entry and syncytia formation." PLoS One **8**(10): e76469.
- Raj, V. S., H. Mou, S. L. Smits, D. H. Dekkers, M. A. Muller, R. Dijkman, D. Muth, J. A. Demmers, A. Zaki, R. A. Fouchier, V. Thiel, C. Drosten, P. J. Rottier, A. D. Osterhaus, B. J. Bosch and B. L. Haagmans (2013). "Dipeptidyl peptidase 4 is a functional receptor for the emerging human coronavirus-EMC." Nature **495**(7440): 251-254.
- Raj, V. S., S. L. Smits, L. B. Provacica, J. M. van den Brand, L. Wiersma, W. J. Ouwendijk, T. M. Bestebroer, M. I. Spronken, G. van Amerongen, P. J. Rottier, R. A. Fouchier, B. J. Bosch, A. D. Osterhaus and B. L. Haagmans (2014). "Adenosine deaminase acts as a natural antagonist for dipeptidyl peptidase 4-mediated entry of the Middle East respiratory syndrome coronavirus." J Virol **88**(3): 1834-1838.

- Reusken, C. B., M. Ababneh, V. S. Raj, B. Meyer, A. Eljarah, S. Abutarbush, G. J. Godeke, T. M. Bestebroer, I. Zutt, M. A. Muller, B. J. Bosch, P. J. Rottier, A. D. Osterhaus, C. Drosten, B. L. Haagmans and M. P. Koopmans (2013). "Middle East Respiratory Syndrome coronavirus (MERS-CoV) serology in major livestock species in an affected region in Jordan, June to September 2013." Euro Surveill **18**(50): 20662.
- Reusken, C. B., B. L. Haagmans, M. A. Muller, C. Gutierrez, G. J. Godeke, B. Meyer, D. Muth, V. S. Raj, L. Smits-De Vries, V. M. Corman, J. F. Drexler, S. L. Smits, Y. E. El Tahir, R. De Sousa, J. van Beek, N. Nowotny, K. van Maanen, E. Hidalgo-Hermoso, B. J. Bosch, P. Rottier, A. Osterhaus, C. Gortazar-Schmidt, C. Drosten and M. P. Koopmans (2013). "Middle East respiratory syndrome coronavirus neutralising serum antibodies in dromedary camels: a comparative serological study." Lancet Infect Dis **13**(10): 859-866.
- Roberts, A., D. Deming, C. D. Paddock, A. Cheng, B. Yount, L. Vogel, B. D. Herman, T. Sheahan, M. Heise, G. L. Genrich, S. R. Zaki, R. Baric and K. Subbarao (2007). "A mouse-adapted SARS-coronavirus causes disease and mortality in BALB/c mice." PLoS Pathog **3**(1): e5.
- Roberts, A., E. W. Lamirande, L. Vogel, J. P. Jackson, C. D. Paddock, J. Guarner, S. R. Zaki, T. Sheahan, R. Baric and K. Subbarao (2008). "Animal models and vaccines for SARS-CoV infection." Virus Res **133**(1): 20-32.
- Scobey, T., B. L. Yount, A. C. Sims, E. F. Donaldson, S. S. Agnihothram, V. D. Menachery, R. L. Graham, J. Swanstrom, P. F. Bove, J. D. Kim, S. Grego, S. H. Randell and R. S. Baric (2013). "Reverse genetics with a full-length infectious cDNA of the Middle East respiratory syndrome coronavirus." Proc Natl Acad Sci U S A **110**(40): 16157-16162.
- Shirato, K., M. Kawase and S. Matsuyama (2013). "Middle East respiratory syndrome coronavirus infection mediated by the transmembrane serine protease TMPRSS2." J Virol **87**(23): 12552-12561.
- Siu, K. L., M. L. Yeung, K. H. Kok, K. S. Yuen, C. Kew, P. Y. Lui, C. P. Chan, H. Tse, P. C. Woo, K. Y. Yuen and D. Y. Jin (2014). "Middle east respiratory syndrome coronavirus 4a protein is a double-stranded RNA-binding protein that suppresses PACT-induced activation of RIG-I and MDA5 in the innate antiviral response." J Virol **88**(9): 4866-4876.
- Song, F., R. Fux, L. B. Provacia, A. Volz, M. Eickmann, S. Becker, A. D. Osterhaus, B. L. Haagmans and G. Sutter (2013). "Middle East respiratory syndrome coronavirus spike protein delivered by modified vaccinia virus Ankara efficiently induces virus-neutralizing antibodies." J Virol **87**(21): 11950-11954.
- Sorensen, M. D., B. Sorensen, R. Gonzalez-Dosal, C. J. Melchjorsen, J. Weibel, J. Wang, C. W. Jun, Y. Huanming and P. Kristensen (2006). "Severe acute respiratory syndrome (SARS): development of diagnostics and antivirals." Ann N Y Acad Sci **1067**: 500-505.
- Takasawa, W., K. Ohnuma, R. Hatano, Y. Endo, N. H. Dang and C. Morimoto (2010). "Inhibition of dipeptidyl peptidase 4 regulates microvascular endothelial growth induced by inflammatory cytokines." Biochem Biophys Res Commun **401**(1): 7-12.

- Takeuchi, O. and S. Akira (2008). "MDA5/RIG-I and virus recognition." Curr Opin Immunol **20**(1): 17-22.
- Tanaka, T., D. Camerini, B. Seed, Y. Torimoto, N. H. Dang, J. Kameoka, H. N. Dahlberg, S. F. Schlossman and C. Morimoto (1992). "Cloning and functional expression of the T cell activation antigen CD26." J Immunol **149**(2): 481-486.
- Tang, J., N. Zhang, X. Tao, G. Zhao, Y. Guo, C. T. Tseng, S. Jiang, L. Du and Y. Zhou (2015). "Optimization of antigen dose for a receptor-binding domain-based subunit vaccine against MERS coronavirus." Hum Vaccin Immunother **11**(5): 1244-1250.
- Taniguchi, T. and A. Takaoka (2001). "A weak signal for strong responses: interferon-alpha/beta revisited." Nat Rev Mol Cell Biol **2**(5): 378-386.
- Tao, X., T. Garron, A. S. Agrawal, A. Algaissi, B. H. Peng, M. Wakamiya, T. S. Chan, L. Lu, L. Du, S. Jiang, R. B. Couch and C. T. Tseng (2015). "Characterization and Demonstration of the Value of a Lethal Mouse Model of Middle East Respiratory Syndrome Coronavirus Infection and Disease." J Virol **90**(1): 57-67.
- Tseng, C. T., C. Huang, P. Newman, N. Wang, K. Narayanan, D. M. Watts, S. Makino, M. M. Packard, S. R. Zaki, T. S. Chan and C. J. Peters (2007). "Severe acute respiratory syndrome coronavirus infection of mice transgenic for the human Angiotensin-converting enzyme 2 virus receptor." J Virol **81**(3): 1162-1173.
- Tseng, C. T., E. Sbrana, N. Iwata-Yoshikawa, P. C. Newman, T. Garron, R. L. Atmar, C. J. Peters and R. B. Couch (2012). "Immunization with SARS coronavirus vaccines leads to pulmonary immunopathology on challenge with the SARS virus." PLoS One **7**(4): e35421.
- Tseng, C. T., J. Tseng, L. Perrone, M. Worthy, V. Popov and C. J. Peters (2005). "Apical entry and release of severe acute respiratory syndrome-associated coronavirus in polarized Calu-3 lung epithelial cells." J Virol **79**(15): 9470-9479.
- Tsiodras, S., A. Baka, A. Mentis, D. Iliopoulos, X. Dedoukou, G. Papamavrou, S. Karadima, M. Emmanouil, A. Kossyvakis, N. Spanakis, A. Pavli, H. Maltezou, A. Karageorgou, G. Spala, V. Pitiriga, E. Kosmas, S. Tsiagklis, S. Gkatzias, N. Koulouris, A. Koutsoukou, P. Bakakos, E. Markozanhs, G. Dionellis, K. Pontikis, N. Rovina, M. Kyriakopoulou, P. Efstathiou, T. Papadimitriou, J. Kremastinou, A. Tsakris and G. Saroglou (2014). "A case of imported Middle East Respiratory Syndrome coronavirus infection and public health response, Greece, April 2014." Euro Surveill **19**(16): 20782.
- van Boheemen, S., M. de Graaf, C. Lauber, T. M. Bestebroer, V. S. Raj, A. M. Zaki, A. D. Osterhaus, B. L. Haagmans, A. E. Gorbalenya, E. J. Snijder and R. A. Fouchier (2012). "Genomic characterization of a newly discovered coronavirus associated with acute respiratory distress syndrome in humans." MBio **3**(6).
- van Doremalen, N., K. L. Miazgowicz, S. Milne-Price, T. Bushmaker, S. Robertson, D. Scott, J. Kinne, J. S. McLellan, J. Zhu and V. J. Munster (2014). "Host species restriction of Middle East

respiratory syndrome coronavirus through its receptor, dipeptidyl peptidase 4." *J Virol* **88**(16): 9220-9232.

Volz, A., A. Kupke, F. Song, S. Jany, R. Fux, H. Shams-Eldin, J. Schmidt, C. Becker, M. Eickmann, S. Becker and G. Sutter (2015). "Protective Efficacy of Recombinant Modified Vaccinia Virus Ankara Delivering Middle East Respiratory Syndrome Coronavirus Spike Glycoprotein." *J Virol* **89**(16): 8651-8656.

Wakamiya, M., E. A. Lindsay, J. A. Rivera-Perez, A. Baldini and R. R. Behringer (1998). "Functional analysis of Gscl in the pathogenesis of the DiGeorge and velocardiofacial syndromes." *Hum Mol Genet* **7**(12): 1835-1840.

Walker, D. H. (2016). "Value of Autopsy Emphasized in the Case Report of a Single Patient with Middle East Respiratory Syndrome." *Am J Pathol* **186**(3): 507-510.

Wang, L., W. Shi, M. G. Joyce, K. Modjarrad, Y. Zhang, K. Leung, C. R. Lees, T. Zhou, H. M. Yassine, M. Kanekiyo, Z. Y. Yang, X. Chen, M. M. Becker, M. Freeman, L. Vogel, J. C. Johnson, G. Olinger, J. P. Todd, U. Bagci, J. Solomon, D. J. Mollura, L. Hensley, P. Jahrling, M. R. Denison, S. S. Rao, K. Subbarao, P. D. Kwong, J. R. Mascola, W. P. Kong and B. S. Graham (2015). "Evaluation of candidate vaccine approaches for MERS-CoV." *Nat Commun* **6**: 7712.

Wang, N., X. Shi, L. Jiang, S. Zhang, D. Wang, P. Tong, D. Guo, L. Fu, Y. Cui, X. Liu, K. C. Arledge, Y. H. Chen, L. Zhang and X. Wang (2013). "Structure of MERS-CoV spike receptor-binding domain complexed with human receptor DPP4." *Cell Res* **23**(8): 986-993.

Welsh, R. M. and S. N. Waggoner (2013). "NK cells controlling virus-specific T cells: Rheostats for acute vs. persistent infections." *Virology* **435**(1): 37-45.

WHO (2003). "Summary of probable SARS cases with onset of illness from 1 November 2002 to 31 July 2003." http://www.who.int/csr/sars/country/table2004_04_21/en/.

WHO (2017). "Middle East respiratory syndrome coronavirus (MERS-CoV)." <http://www.who.int/emergencies/mers-cov/en/>.

Who Mers-Cov Research, G. (2013). "State of Knowledge and Data Gaps of Middle East Respiratory Syndrome Coronavirus (MERS-CoV) in Humans." *PLoS Curr* **5**.

Wild, C. T., D. C. Shugars, T. K. Greenwell, C. B. McDanal and T. J. Matthews (1994). "Peptides corresponding to a predictive alpha-helical domain of human immunodeficiency virus type 1 gp41 are potent inhibitors of virus infection." *Proc Natl Acad Sci U S A* **91**(21): 9770-9774.

Woo, P. C., S. K. Lau, Y. Huang and K. Y. Yuen (2009). "Coronavirus diversity, phylogeny and interspecies jumping." *Exp Biol Med (Maywood)* **234**(10): 1117-1127.

Woo, P. C., S. K. Lau, K. S. Li, R. W. Poon, B. H. Wong, H. W. Tsoi, B. C. Yip, Y. Huang, K. H. Chan and K. Y. Yuen (2006). "Molecular diversity of coronaviruses in bats." *Virology* **351**(1): 180-187.

- Woo, P. C., S. K. Lau, K. S. Li, A. K. Tsang and K. Y. Yuen (2012). "Genetic relatedness of the novel human group C betacoronavirus to Tylonycteris bat coronavirus HKU4 and Pipistrellus bat coronavirus HKU5." Emerg Microbes Infect **1**(11): e35.
- Woo, P. C., M. Wang, S. K. Lau, H. Xu, R. W. Poon, R. Guo, B. H. Wong, K. Gao, H. W. Tsoi, Y. Huang, K. S. Li, C. S. Lam, K. H. Chan, B. J. Zheng and K. Y. Yuen (2007). "Comparative analysis of twelve genomes of three novel group 2c and group 2d coronaviruses reveals unique group and subgroup features." J Virol **81**(4): 1574-1585.
- Xu, J., S. Zhong, J. Liu, L. Li, Y. Li, X. Wu, Z. Li, P. Deng, J. Zhang, N. Zhong, Y. Ding and Y. Jiang (2005). "Detection of severe acute respiratory syndrome coronavirus in the brain: potential role of the chemokine mig in pathogenesis." Clin Infect Dis **41**(8): 1089-1096.
- Yang, X., X. Chen, G. Bian, J. Tu, Y. Xing, Y. Wang and Z. Chen (2014). "Proteolytic processing, deubiquitinase and interferon antagonist activities of Middle East respiratory syndrome coronavirus papain-like protease." J Gen Virol **95**(Pt 3): 614-626.
- Yang, Y., C. Liu, L. Du, S. Jiang, Z. Shi, R. S. Baric and F. Li (2015). "Two Mutations Were Critical for Bat-to-Human Transmission of Middle East Respiratory Syndrome Coronavirus." J Virol **89**(17): 9119-9123.
- Yang, Y., L. Zhang, H. Geng, Y. Deng, B. Huang, Y. Guo, Z. Zhao and W. Tan (2013). "The structural and accessory proteins M, ORF 4a, ORF 4b, and ORF 5 of Middle East respiratory syndrome coronavirus (MERS-CoV) are potent interferon antagonists." Protein Cell **4**(12): 951-961.
- Yao, Y., L. Bao, W. Deng, L. Xu, F. Li, Q. Lv, P. Yu, T. Chen, Y. Xu, H. Zhu, J. Yuan, S. Gu, Q. Wei, H. Chen, K. Y. Yuen and C. Qin (2014). "An animal model of MERS produced by infection of rhesus macaques with MERS coronavirus." J Infect Dis **209**(2): 236-242.
- Ying, T., L. Du, T. W. Ju, P. Prabakaran, C. C. Lau, L. Lu, Q. Liu, L. Wang, Y. Feng, Y. Wang, B. J. Zheng, K. Y. Yuen, S. Jiang and D. S. Dimitrov (2014). "Exceptionally potent neutralization of Middle East respiratory syndrome coronavirus by human monoclonal antibodies." J Virol **88**(14): 7796-7805.
- Yoneyama, M., M. Kikuchi, T. Natsukawa, N. Shinobu, T. Imaizumi, M. Miyagishi, K. Taira, S. Akira and T. Fujita (2004). "The RNA helicase RIG-I has an essential function in double-stranded RNA-induced innate antiviral responses." Nat Immunol **5**(7): 730-737.
- Yu, D. M., T. W. Yao, S. Chowdhury, N. A. Nadvi, B. Osborne, W. B. Church, G. W. McCaughan and M. D. Gorrell (2010). "The dipeptidyl peptidase IV family in cancer and cell biology." FEBS J **277**(5): 1126-1144.
- Zaki, A. M., S. van Boheemen, T. M. Bestebroer, A. D. Osterhaus and R. A. Fouchier (2012). "Isolation of a novel coronavirus from a man with pneumonia in Saudi Arabia." N Engl J Med **367**(19): 1814-1820.

Zhang, N., R. Channappanavar, C. Ma, L. Wang, J. Tang, T. Garron, X. Tao, S. Tasneem, L. Lu, C. T. Tseng, Y. Zhou, S. Perlman, S. Jiang and L. Du (2016). "Identification of an ideal adjuvant for receptor-binding domain-based subunit vaccines against Middle East respiratory syndrome coronavirus." Cell Mol Immunol **13**(2): 180-190.

Zhang, N., J. Tang, L. Lu, S. Jiang and L. Du (2015). "Receptor-binding domain-based subunit vaccines against MERS-CoV." Virus Res **202**: 151-159.

Zhao, G., Y. Jiang, H. Qiu, T. Gao, Y. Zeng, Y. Guo, H. Yu, J. Li, Z. Kou, L. Du, W. Tan, S. Jiang, S. Sun and Y. Zhou (2015). "Multi-Organ Damage in Human Dipeptidyl Peptidase 4 Transgenic Mice Infected with Middle East Respiratory Syndrome-Coronavirus." PLoS One **10**(12): e0145561.

Zhao, J., K. Li, C. Wohlford-Lenane, S. S. Agnihothram, C. Fett, J. Zhao, M. J. Gale, Jr., R. S. Baric, L. Enjuanes, T. Gallagher, P. B. McCray, Jr. and S. Perlman (2014). "Rapid generation of a mouse model for Middle East respiratory syndrome." Proc Natl Acad Sci U S A **111**(13): 4970-4975.

Zhu, M. (2004). "SARS Immunity and Vaccination." Cell Mol Immunol **1**(3): 193-198.

Zumla, A., D. S. Hui and S. Perlman (2015). "Middle East respiratory syndrome." Lancet **386**(9997): 995-1007.

VITA

TANIA M. GARRON

University of Texas Medical Branch at Galveston
Department of Microbiology and Immunology
Galveston National Laboratory 6.324
301 University Blvd.
Galveston, TX 77555-0610
Email: tmgarron@utmb.edu

100 Market Apt# 41
Galveston, TX 77550
Phone: 409-370-8005
E-mail: taniagarronp@gmail.com

EDUCATION

08/2012 to present Graduate Program
Department of Microbiology and Immunology
The University of Texas Medical Branch, Galveston, TX

October- 2003 "Professional development training in Clinical Diagnostic Microbiology".

Spanish Foundation of Social and Health Studies, Madrid. Santa Cruz, Bolivia

- August- 2003 “Professional development training in Clinical Pharmacology”. Spanish Foundation of Social and Health Studies, Madrid. Santa Cruz, Bolivia.
- January-2002 “Professional license as a Public Health Consultant”. GRECO Consulting Corporation-Bolivian Public Health Medical Society. Santa Cruz, Bolivia.
- April-1997 “Bachelor of Science with a double major in Pharmaceutical Science and Biochemistry”. The San Francisco Xavier Higher, Royal, and Pontifical University of Chuquisaca, Sucre, Bolivia.

PUBLICATIONS

1. Agrawal AS, Tao X, Algaissi A, **Garron T**, Narayanan K, Peng BH, Couch RB, Tseng CK. Immunization with inactivated Middle East Respiratory Syndrome coronavirus vaccine leads to lung immunopathology on challenge with live virus. *Hum Vaccin Immunother.* 2016 Jun 7:1-6.
2. Xinrong Tao*, **Tania Garron***, Anurodh Agrawal*, Abdullah Algaissi, Bi-Hung Peng, Maki Wakamiya, Teh-Sheng Chan, Lu Lu, Lanying Du, Shibo Jiang, Robert Couch, and Chien-Te Tseng. "Characterization and Demonstration of value of a Lethal Mouse Model of Middle East Respiratory Syndrome Coronavirus Infection and Disease" by *Journal of virology* 2015 Oct 7;90(1):57-67. doi: 10.1128/JVI.02009-15.
* **Equal contributors**
3. Agrawal AS*, **Garron T ***, Tao X, Peng BH, Wakamiya M, Chan TS, Couch RB, Tseng CT. 2015. Generation of a transgenic mouse model of middle East respiratory syndrome coronavirus infection and disease. *Journal of virology* 89:3659-3670.
* **Equal contributors**
4. Meyer M, **Garron T**, Lubaki NM, Mire CE, Fenton KA, Klages C, Olinger GG, Geisbert TW, Collins PL, Bukreyev A. 2015. Aerosolized Ebola vaccine protects primates and elicits lung-resident T cell responses. *J Clin Invest* 125:3241-3255.
5. Zhang N, Channappanavar R, Ma C, Wang L, Tang J, **Garron T**, Tao X, Tasneem S, Lu L, Tseng CT, Zhou Y, Perlman S, Jiang S, Du L. 2015. Identification of an ideal adjuvant for receptor-binding domain-based subunit vaccines against Middle East respiratory syndrome coronavirus. *Cellular & molecular immunology.*
6. Flyak AI, Ilinykh PA, Murin CD, **Garron T**, Shen X, Fusco ML, Hashiguchi T, Bornholdt ZA, Slaughter JC, Sapparapu G, Klages C, Ksiazek TG, Ward AB, Saphire

EO, Bukreyev A, Crowe JE, Jr. 2015. Mechanism of human antibody-mediated neutralization of Marburg virus. *Cell* 160:893-903.

7. Ilinykh PA, Tigabu B, Ivanov A, Ammosova T, Obukhov Y, **Garron T**, Kumari N, Kovalskyy D, Platonov MO, Naumchik VS, Freiberg AN, Nekhai S, Bukreyev A. 2014. Role of protein phosphatase 1 in dephosphorylation of Ebola virus VP30 protein and its targeting for the inhibition of viral transcription. *The Journal of biological chemistry* 289:22723-22738.
8. Tseng CT, Sbrana E, Iwata-Yoshikawa N, Newman PC, **Garron T**, Atmar RL, Peters CJ, Couch RB. 2012. Immunization with SARS coronavirus vaccines leads to pulmonary immunopathology on challenge with the SARS virus. *PLoS one* 7:e35421.
9. Zhang Z, **Garron TM**, Li XJ, Liu Y, Zhang X, Li YY, Xu WS. 2009. Recombinant human decorin inhibits TGF-beta1-induced contraction of collagen lattice by hypertrophic scar fibroblasts. *Burns : journal of the International Society for Burn Injuries* 35:527-537.
10. Peredo C, **Garron T**, Pelegrino JL, Harris E, Gianella A. 1999. Detection and identification of dengue-2 virus from Santa Cruz-Bolivia by a single tube RT-PCR method. *Revista do Instituto de Medicina Tropical de Sao Paulo* 41:207-208.
11. Gianella A HA, Lora J, Céspedes JL, **Garron T**, Velásquez N. 1999. Brote de Fiebre Amarilla Selvática en el Departamento de Santa Cruz-Bolivia, año 1999. . *Boletín Científico del CENETROP*. 17:10-17.